1-1-2016

An Analysis Of The Interaction Between Sin3 And Methionine Metabolism In Drosophila

Mengying Liu
Wayne State University,

AN ANALYSIS OF THE INTERACTION BETWEEN SIN3 AND METHIONINE METABOLISM IN *DROSOPHILA*

by

MENGYING LIU

DISSERTATION

Submitted to the Graduate School

of Wayne State University,

Detroit, Michigan

in partial fulfillment of the requirements

for the degree of

DOCTOR OF PHILOSOPHY

2016

MAJOR: BIOLOGICAL SCIENCES

Approved By:

_____

Advisor Date

_____

_____

_____

DEDICATION

献给我的丈夫, 父母, 外祖父母和祖父母

你们的爱和支持造就了现在的我

To my beloved husband, my parents and my grandparents:

Thanks for your support through this long journey!

ACKNOWLEDGEMENTS

I would like to thank many individuals who assisted me with my PhD study. Without their help, this cannot be achieved.

First and foremost, I wish to express my deepest gratitude to my PhD advisor, Dr. Lori A. Pile, for her continued support of my PhD study. She provided me with interesting projects, taught me biological knowledge, and trained me for scientific skills. All of her guidance makes me feel closer to be a professional biologist. Thank you for being a great mentor.

My appreciation also extends to my committee members, Dr. Victoria Meller, Dr. Joy Alcedo and Dr. Douglas Ruden for their insightful suggestions and encouragement throughout my research, but also for the hard questions that widen my view of my work from various inspections.

My thankfulness also goes to our joint lab meeting, chromatin and fly club members, as well as the faculty members who taught the classes I enrolled in during my PhD study. They enhance my professional growth as a scientist.

I also thank all of the staff members of the Department of Biology and my friends at Wayne State University for helping me in many ways during my time here.

My sincere thanks also goes to all the past and present members of the Pile laboratory for their support of my PhD study and personal life in the past several years.

Last but not the least, I want to thank the most important persons in my life, my family members. My parents encouraged me to study abroad, therefore I can pursue a further education degree here. My family members in the United States have helped me a lot and never let me feel lonely in a foreign country. My dearest husband, Hongen

(Owen) Tu, always supports me. Every moment, when I suffered from problems with my research, he stayed with me, encouraged me to keep working. I thank my family members so much for your love and support.

TABLE OF CONTENTS

LIST OF TABLES

LIST OF FIGURES

CHAPTER 1 INTRODUCTION

Epigenetics

Epigenetics is generally defined as the sum of chromatin-based events (Dawson and Kouzarides, 2012), which contain regulatory information beyond nucleotide sequences (Kaelin and McKnight, 2013). This information can be dynamic and be passed to daughter cells. The earliest evidence of transgenerational epigenetic inheritance is from studies in plants, which show that several phenotypes are associated with DNA methylation and that this modification can be inherited (Bender and Fink, 1995; Jacobsen and Meyerowitz, 1997).

The nucleosome, the basic unit of chromatin, is composed of DNA and a core of structural proteins that are called histones (Kornberg, 1974). Biochemical and X-ray results show that the histone core is an octamer containing a histone H3/H4 tetramer and two histone H2A/H2B dimers (Finch et al., 1977; Kornberg, 1974). Additional X-ray studies confirmed the structure of the histone core and demonstrated that approximately 147 base pairs of DNA sequence are wrapped around a histone octamer (Davey et al., 2002; Luger et al., 1997).

Chemical groups can be added on or removed from DNA or the tails of histones by chromatin modifying enzymes. So far, a large number of chromatin modifying enzymes have been identified. For example, yeast HAT1 is the first identified histone acetyltransferase (HAT) to add acetyl groups to histones (Kleff et al., 1995), while RPD3 is the first discovered histone deacetylase (HDAC) to remove acetyl groups from histones (Taunton et al., 1996). To date, many types of DNA modifications and histone modifications, such as DNA methylation, histone acetylation, methylation,

phosphorylation, ubiquitylation, sumoylation and the like, have been discovered (Dawson and Kouzarides, 2012).

The positions of nucleosomes along DNA sequences can be altered by chromatin remodeling enzymes. SWI/SNF is the first identified enzyme that disrupts nucleosomal structure (Cote et al., 1994; Kwon et al., 1994). A year later, another chromatin remodeling enzyme, associated with protein complex NURD, was found (Tsukiyama and Wu, 1995). To date, there are four major groups of chromatin remodeling enzymes: SWI/SNF family, ISWI family, NURD family and INO80 family (Dawson and Kouzarides, 2012).

Epigenetic information, such as chromatin modifications and nucleosome position, plays an important role in transcription. Loss of nucleosomes increases gene expression (Han and Grunstein, 1988). Chromatin modifications regulate transcription through two major mechanisms (Bannister and Kouzarides, 2011). First, chromatin modifications can influence chromatin structure. For instance, histone acetylation and histone phosphorylation reduce the positive net charge of histones, which in turn decreases the interaction between histones and DNA (Dou and Gorovsky, 2000; Hong et al., 1993). As a consequence of this weakened interaction, the chromatin becomes more accessible (Gorisch et al., 2005; Krajewski and Becker, 1998). Second, chromatin modifications can serve as the docking sites to recruit specialized proteins, such as regulatory proteins, that recognize specific modifications. For example, acetylated histone lysine residues can be recognized by the bromodomain motif, which is contained in many transcriptional co-activators (Dhalluin et al., 1999). Another example is heterochromatin protein-1 (HP1), which is a repressor interacting with methylated

H3K9 (Bannister et al., 2001; Lachner et al., 2001; Nakayama et al., 2001).

Alteration of epigenetic control results in abnormal gene expression patterns, which in turn affects many critical biological processes and can lead to disease. For instance, the H3K9 histone methyltransferase G9a promotes lung cancer invasion and metastasis by silencing the cell adhesion molecule Ep-CAM (Chen et al., 2010).

Metabolism

Metabolism is most commonly used to describe all biochemical processes in living organisms (DeBerardinis and Thompson, 2012). Living beings utilize nutrients, such as carbohydrates, fatty acids and amino acids, to produce or consume energy as well as to grow through metabolism. The metabolic pathways can be separated into two classes: catabolism and anabolism. Catabolism breaks down molecules into smaller units and releases energy. In contrast, anabolism builds up larger molecules and stores energy. Many diseases are associated with abnormal metabolic status (DeBerardinis and Thompson, 2012). The Warburg effect is one of the most well studied examples. The Warburg effect is the term used to describe the observations that cancer cells produce energy through a high rate of glycolysis relative to normal cells (Warburg, 1956).

Connection between epigenetics and metabolism

Chromatin modification and cellular metabolism are tightly connected. Epigenetic modification affects metabolism through regulating expression of genes encoding metabolic enzymes (Martinez-Pastor et al., 2013). In opposition, given that chromatin modifying enzymes consume key metabolites, metabolism can then feedback and influence epigenetic information (Katada et al., 2012).

Histone acetylation and acetyl coenzyme A (acetyl-CoA)

The N^{ε}-acetylation of lysine residues in histones was the first discovered histone posttranslational modification (PTM) (Allfrey et al., 1964; Phillips, 1963). Acetylation neutralizes the positive charge on lysine residues, which in turn weakens the electrostatic interaction between histones and negatively charged DNA (Hong et al., 1993). For this reason, chromatin with high levels of histone acetylation is typically considered as more accessible chromatin (Gorisch et al., 2005; Krajewski and Becker, 1998). Consistent with this idea, genome-wide data from many groups have revealed that histone acetylation is often associated with active genes (Kurdistani et al., 2004; Schubeler et al., 2004).

Histone acetylation is a highly dynamic process, which can be tightly regulated by the histone lysine acetyltransferases (HATs), such as GCN5 (Brownell et al., 1996), and the histone deacetylases (HDACs), such as RPD3 (Taunton et al., 1996). Changed levels of HATs or HDACs affect cellular metabolism. Reduction of the histone deacetylase HDAC1 leads to increased histone acetylation and metabolic changes associated with the ATP energy source, oxidative stress and mitochondrial biogenesis in intestinal epithelial cells (Gonneaud et al., 2015). Loss of the H3K9/H3K56 deacetylase SIRT6 results in increased histone acetylation at the promoters of glycolytic genes, up-regulated expression of glycolytic genes and increased glucose uptake with up-regulation of glycolysis in mammalian cells (Zhong et al., 2010).

Acetyl coenzyme A (acetyl-CoA), the only known substrate for acetylation in most eukaryotes, was first isolated in 1951 (Lynen et al., 1951). Although acetyl-CoA can be generated through many different metabolic pathways, the majority of acetyl-CoA is

produced from pyruvate through the mitochondrial pyruvate dehydrogenase complex (Korkes et al., 1951).

There is a link between cellular acetyl-CoA concentration and histone acetylation levels. Increased histone acetylation is observed when the acetyl-CoA donor citrate or acetate is added into the media in intestinal epithelial cells (Gonneaud et al., 2015). Decreased H3K9/27 acetylation in differentiating mammalian cells is blocked by adding acetate in the media (Moussaieff et al., 2015). Depletion of glucose, which can generate the acetyl-CoA donor pyruvate through glycolysis, results in reduced levels of acetylated H3 and H4 in mammalian cells (Gonneaud et al., 2015; Wellen et al., 2009). This decrease in the absence of glucose is eliminated by reduction of HDAC1 (Gonneaud et al., 2015). Acetyl-CoA synthetase, the enzyme generating acetyl-CoA from acetate, is required for histone acetylation in yeast (Takahashi et al., 2006). Reduction of ATP-citrate lyase (ACL), the enzyme converting glucose-derived citrate into acetyl-CoA, results in decreased histone acetylation (Wellen et al., 2009). Disruption of glycolysis leads to decreased acetyl-CoA levels and reduced histone acetylation in mammalian cells (Cluntun et al., 2015). Taken together, results from multiple research groups indicate that histone acetylation levels are responsive to changes in the amount of metabolites that produce acetyl-CoA, alterations in the levels of enzymes that impact the cellular concentration of acetyl-CoA and to glycolysis inhibition.

Histone methylation and S-adenosylmethionine (SAM)

Histone methylation is another major histone modification (Allfrey et al., 1964). Histone methylation occurs on lysine and arginine residues (Allfrey et al., 1964; Kakimoto and Akazawa, 1970). Lysine residues can be modified by one, two or three

methyl groups, while arginine residues can be symmetrically or asymmetrically methylated (Kakimoto and Akazawa, 1970). Histone lysine methylation, as the best-characterized histone methylation mark, will be the main focus in this dissertation. Unlike histone acetylation, histone methylation does not alter the overall charge of the chromatin (Dawson and Kouzarides, 2012). Unlike histone acetylation, which is associated with transcription activation, histone methylation is linked to both repressive and active transcription (Teperino et al., 2010). The specific effect of histone methylation on gene expression is dependent on specifically methylated residues and the number of methyl groups added (Teperino et al., 2010). For example, genome-wide data show that active genes are hypermethylated at H3K4 and H3K79 sites, while H3K27 methylation is enriched at silent genes (Bernstein et al., 2002; Roh et al., 2006; Schubeler et al., 2004).

Histone methylation is highly dynamic and tightly regulated by the competing activities of two enzymatic families: the histone methyltransferases (HMTs), such as SUV39H1 (Rea et al., 2000), which add methyl groups, and the histone demethylases (HDMs), such as LSD1/KDM1A (Shi et al., 2004), which remove methyl groups. Cellular metabolic status can be impacted by altered levels of HMTs or HDMs. Loss of the H3K9 demethylase Jhdm2a leads to changes in metabolic gene expression and metabolic processes associated with energy balance, oxygen consumption and fat oxidation in mouse (Tateishi et al., 2009).

S-adenosylmethionine (SAM), as the only known methyl donor in cells, was discovered in 1952 (Cantoni, 1952). SAM is generated from methionine through SAM synthetase (SAM-S) (Mudd and Cantoni, 1958).

The cellular concentration of SAM impacts histone methylation. Depletion of threonine leads to decreased SAM accumulation and reduced H3K4me3 levels in mouse embryonic stem cells (Shyh-Chang et al., 2013). Disruption of the folate pathway by deleting a gene encoding dihydrofolate synthetase results in decreased H3K4me3 levels in yeast (Sadhu et al., 2013). Deficiency of genes that encode enzymes involved in methionine metabolism leads to decreased H3K4me3 levels in yeast and *Drosophila* cells (Liu et al., 2015; Sadhu et al., 2013). Decreased H3K4me3 levels are observed in human cells when folate and methionine are deficient in the media (Sadhu et al., 2013). Methionine restriction in the media is sufficient to decrease the cellular SAM concentration and reduce H3K4me3 levels (Mentch et al., 2015; Shiraki et al., 2014). Collectively, these previously published studies indicate that changes in the concentration of folate and methionine, which are utilized to generate SAM, or in expression of genes encoding enzymes involved in folate and methionine metabolism, lead to alteration of histone methylation levels.

The SIN3 histone modifying complex

The SIN3 complex is one of multiple histone modifying complexes present in cells. SIN3 is a conserved transcriptional scaffold protein, recruiting the histone deacetylase RPD3 and other associated proteins, from yeast to mammals (Grzenda et al., 2009; Silverstein and Ekwall, 2005). In *Drosophila* and mammals, a histone demethylase is a subunit of a SIN3/RPD3 histone deacetylase (HDAC) complex (Gajan et al., 2016; Hayakawa et al., 2007; Moshkin et al., 2009; Spain et al., 2010). These proteomic data suggest that SIN3 may regulate histone methylation in addition to histone acetylation.

SIN3 impacts development. *Sin3A* is essential in *Drosophila* and mammals (Cowley et al., 2005; Dannenberg et al., 2005; David et al., 2008; Neufeld et al., 1998; Pennetta and Pauli, 1998). In *Drosophila*, one *Sin3A* gene encodes multiple isoforms (Neufeld et al., 1998; Pennetta and Pauli, 1998). The expression of these isoforms are developmental stage specific and tissue specific, suggesting SIN3 is involved in development (Barnes et al., 2014; Sharma et al., 2008). SIN3 is also reported to enhance the rough eye phenotype caused by the mutation of *sina* in *Drosophila*, indicating SIN3 contributes to eye development (Neufeld et al., 1998). The finding that reduction of SIN3 in *Drosophila* wing imaginal discs leads to a curved wing phenotype indicates that SIN3 influences wing development (Swaminathan and Pile, 2010). In mammals, there are two *Sin3* genes: *mSin3A* and *mSin3B* (Ayer et al., 1995). mSin3A is required for T-cell development (Cowley et al., 2005). mSin3B controls the development of multiple hematopoietic lineages in the early embryonic development stage (David et al., 2008).

SIN3 affects cell proliferation. Decreased cell density and a G2/M phase arrest are observed when SIN3 is reduced in *Drosophila* cultured cells (Pile et al., 2002). In mammals, loss of mSin3A leads to decreased cell proliferation through increased apoptosis and leads to cell cycle arrest (Cowley et al., 2005; Dannenberg et al., 2005). In contrast, although *mSin3B* is not cell-essential, the ability of the cells to exit the cell cycle is under the control of *mSin3B* (David et al., 2008; van Oevelen et al., 2008).

SIN3 regulates transcription. A combined microarray analysis from embryonic S2 and Kc cultured cells shows that SIN3 affects 3% of the *Drosophila* genome (Pile et al., 2003). A recently published genome-wide RNA-seq study reveals that reduction of SIN3

affects expression of more than 600 genes in S2 cells (Gajan et al., 2016). Transcriptome analyses of mammalian SIN3 identify a large number of SIN3 targets (Dannenberg et al., 2005; van Oevelen et al., 2008).

SIN3 has been linked to several metabolic pathways. Based on the gene ontology analysis of SIN3 targets in *Drosophila* and mammals, SIN3 affects expression of genes involved in glycolysis, gluconeogenesis and the citric acid cycle (Dannenberg et al., 2005; Gajan et al., 2016; Pile et al., 2003). Deficiency of SIN3 in S2 cells changes mitochondrial gene transcription, ATP levels and the respiration rate (Barnes et al., 2010). Compared to wild type, adult flies with reduced SIN3 are more sensitive to oxidative stress (Barnes et al., 2014). This phenotype can be partially suppressed by glutathione supplementation (Barnes et al., 2014). Reduction in the levels of SIN3 in the adult stage of *Drosophila* decreases longevity and impairs locomotor function, which are each associated with metabolic status (Barnes et al., 2014).

Project outline

Cellular function relies on the ability of the cell to sense nutritional status, as well as environmental changes, and respond accordingly. How the enzymes that control metabolic responses are regulated at the gene expression level is not understood. The major objective of the research described in this dissertation is to elucidate the role of the SIN3 histone modifying complex in regulating this response. I have focused on the mechanism of how SIN3 regulates cellular metabolism, especially methionine metabolic pathway. To address this question, I have carried out the following studies:

We examined the role of methionine metabolic enzymes in regulating biological processes such as viability, wing development and cell proliferation as well as the

interaction between methionine metabolism and histone methylation in Chapter 2. Our findings indicate that disruption of methionine metabolism leads to lethality and abnormal wing morphology and influences histone methylation.

We also determined that SIN3 regulates methionine metabolism and further explored the mechanism and the effect of this regulation in Chapter 3. Our results suggest that SIN3 directly affects H3K4me3 and H3K9ac, which are associated with active genes, at the promoters of methionine metabolic genes to regulate their expression, which in turn controls the SAM level to impact histone methylation.

We identified the genes and metabolites regulated by SIN3 and/or SAM synthetase (SAM-S) in Chapter 4. Moreover, we used the metabolic profiles along with the relative global histone H3K4me3 levels described in Chapter 3 to perform Pearson correlation analysis. Our data reveal that glycolysis is influenced by SIN3 and/or SAM-S. The concentrations of glycolytic metabolites change significantly with the alterations in H3K4me3 mediated by SIN3 and/or SAM-S.

This study has enhanced our understanding of the role of SIN3 in regulating cellular metabolism. The mechanism of this regulation, however, is still not fully understood. Many interesting questions that arise from this work remain for future research. These potential projects are discussed in Chapter 5.

CHAPTER 2 DISRUPTION OF METHIONINE METABOLISM IN *DROSOPHILA MELANOGASTER* IMPACTS HISTONE METHYLATION AND RESULTS IN LOSS OF VIABILITY

The work described in this chapter has been published:

Liu, M., Barnes, V.L., and Pile, L.A. (2015). Disruption of Methionine Metabolism in *Drosophila melanogaster* Impacts Histone Methylation and Results in Loss of Viability. G3 *6*, 121-132.

INTRODUCTION

Methionine is the initiating amino acid in the synthesis of virtually all eukaryotic proteins while methionine metabolism provides many metabolites important for a number of other pathways and biological processes (Brosnan and Brosnan, 2006). Methionine metabolism generates the primary methyl donor *S*-adenosylmethionine (SAM) from methionine through SAM synthetase (SAM-S) (Fig. 2.1). SAM is converted to *S*-adenosylhomocysteine (SAH) via methyltransferases by donating a methyl group to a receptor, such as DNA, RNA, histones, other proteins and smaller metabolites. SAH is hydrolyzed to homocysteine and adenosine by adenosylhomocysteinase (AHCY). Homocysteine is converted to cystathionine via cystathionine-β-synthase (CBS), or it is remethylated to methionine through methionine synthase (MS).

The metabolism of methionine is critical for the development of living organisms. *Sam-S* is an essential gene in *Drosophila* (Larsson and Rasmuson-Lestander, 1998) and fungi (Gerke et al., 2012). Decreased level of SAM-S results in late flowering in rice *Oryza sativa* (Li et al., 2011). Depletion of AHCY or MS leads to lethality in mice (Miller et al., 1994; Swanson et al., 2001). Knockdown of *Cbs* leads to death in *Drosophila* (Kabil et al., 2011). Mice with CBS deficiency suffer from growth retardation and die within 5 weeks after birth (Watanabe et al., 1995). The metabolism of methionine is also

important for cell proliferation. An *Escherichia coli Sam-S* mutant (*metK84*) shows slow growth and filamentation (Newman et al., 1998). Stable overexpression of AHCY induces cell death by apoptosis in human cells (Hermes et al., 2008). Reduction of CBS induces premature senescence in human endothelial cells (Albertini et al., 2012).

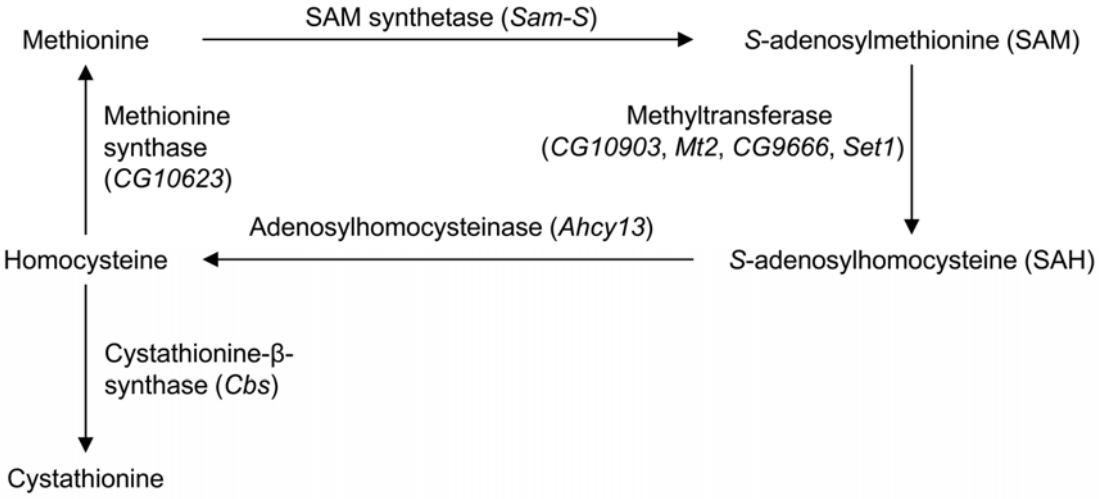

Fig. 2.1: Methionine metabolism in *Drosophila.*

Given that SAM is the universal methyl donor, enzymes that control the levels of SAM play a critical role in determining the extent of histone methylation. RNA interference (RNAi) induced knockdown of *Sam-S* results in a reduction of global histone methylation in rice *Oryza sativa* (Li et al., 2011) and *Caenorhabditis elegans* (Towbin et al., 2012). AHCY deficiency in yeast inhibits histone methylation through increased SAH (Tehlivets et al., 2013). CBS deficient mice have decreased asymmetric dimethylation of arginine 3 on histone H4 (H4R3me2a) relative to wild type in liver cells (Esse et al., 2014). Because histone methylation is related to gene transcription (Black and Whetstine, 2011), it is possible that methionine metabolic enzymes regulate biological processes such as cell proliferation, development and the like through

controlling genes involved in these processes, whose expression is affected by histone methylation (Teperino et al., 2010).

The levels of histone methylation are determined by the activities of histone methyltransferases and demethylases. Histone methylation affects gene expression, which in turn affects cell proliferation and development. H3K4 methylation is associated with active genes (Black et al., 2012; Black and Whetstine, 2011). SET1 is a H3K4 methyltransferase conserved from yeast to human (Shilatifard, 2012). Loss of SET1 leads to decreased H3K4 methylation and slow cell growth rate in yeast (Briggs et al., 2001). Reduced SET1 results in a decrease of global H3K4me2 and H3K4me3 levels and lethality in *Drosophila* (Ardehali et al., 2011; Hallson et al., 2012; Mohan et al., 2011). There are two orthologs of *Set1*, *Setd1a* and *Setd1b*, in mammals (Shilatifard, 2012). Both *Setd1a* and *Setd1b* are essential for development in mice, but only *Setd1a* is required for cell proliferation and H3K4 methylation in mouse ESCs (Bledau et al., 2014). To date, little imaginal discs (LID) and lysine-specific demethylase 2 (KDM2) are the only two *Drosophila* histone demethylases reported to target H3K4me3. *lid* and *Kdm2* genetically interact in *Drosophila* (Li et al., 2010). LID specifically removes H3K4me3 (Eissenberg et al., 2007; Lee et al., 2007; Lloret-Llinares et al., 2008; Secombe et al., 2007). LID is critical for *Drosophila* viability and development (Gildea et al., 2000; Li et al., 2010). Functions of KDM2 are controversial. KDM2 has been shown to influence H3K36me2 demethylation and H2A ubiquitylation in *Drosophila* S2 cells (Lagarou et al., 2008). KDM2 is also reported to target H3K4me3, but not H3K36me2, in *Drosophila* larvae (Kavi and Birchler, 2009). Another group, however, determined that there is no change in H3K4me3 and H3K36me2 in wing imaginal discs from *Kdm2*

mutants (Li et al., 2010). The differences between cells and larvae may result from different KDM2 complexes at different developmental stages or in different tissues (Zheng et al., 2014). Recently, KDM2 has been found to have weak effects on H3K4me3 and H3K36me1/2/3 in *Drosophila* larvae, but does not affect H3K4me1/2/3 and H3K36me1/2/3 in *Drosophila* S2 cells (Zheng et al., 2014). The contradictory results in S2 cells may be due to different *Kdm2* knockdown levels by using different dsRNA or differences between cells (Zheng et al., 2014). An initial report indicated that the strongest *Kdm2* mutant is lethal in flies (Lagarou et al., 2008). Two years later, another group, using a different set of alleles, reported that the strongest *Kdm2* mutant is semi-lethal (Li et al., 2010). Recent results from Ji's group testing a number of alleles, including those tested in the first report, however, suggested that KDM2 is not required for *Drosophila* viability (Zheng et al., 2014). Analysis from Ji's group demonstrated that the lethality observed in the *Kdm2* mutants is very likely due to second-site lethal mutations.

Taken together, research from multiple model organisms suggests that methionine metabolic enzymes, histone methyltransferases as well as demethylases are associated with histone methylation, cell proliferation and development. Whether methionine metabolic enzymes have similar effects on these biological processes in *Drosophila,* however, is understudied. The relationship among these enzymes in regulation of these processes is still not fully understood. Here, we have found that enzymes involved in methionine metabolism and histone demethylases play a role in development and cell proliferation in *Drosophila*. We also observed an interaction among these proteins in regulation of histone methylation. Together, our data provide

insights into the connection between metabolism and epigenetics.

MATERIALS AND METHODS

Cell culture

Drosophila Schneider cell line 2 (S2) cells were cultured at 27ºC in Schneider's *Drosophila* medium (1x) with L-glutamine (Life Technologies), 10% heat-inactivated fetal bovine serum (Invitrogen) and 50 mg/ml gentamycin.

Fly stocks

Drosophila melanogaster stocks were maintained and crosses were performed according to standard laboratory procedures. *Ser-Gal4* (#6791), *Act5C-Gal4* (#4414), *Engrailed-Gal4* (#30564), *UAS-GFP^{RNAi}* (#9331), *UAS-mCherry$^{RNAi-TRiP}$* (35785), *UAS-Sam-S$^{RNAi-TRiP-1}$* (#36306), *UAS-Sam-S$^{RNAi-TRiP-2}$* (#29415), *UAS-Ahcy13$^{RNAi-TRiP}$* (#51477), *UAS-Cbs$^{RNAi-TRiP}$* (#36767), *UAS-CG10623$^{RNAi-TRiP}$* (#51748), *UAS-CG10903$^{RNAi-TRiP}$* (#57481) , *UAS-Mt2$^{RNAi-TRiP}$* (#38224), *UAS-Set1$^{RNAi-TRiP-1}$* (#33704), *UAS-Set1$^{RNAi-TRiP-2}$* (#38368), *UAS-lid$^{RNAi-TRiP}$* (#28944), *UAS-Kdm2$^{RNAi-TRiP-1}$* (#31360) and *UAS-Kdm2$^{RNAi-TRiP-2}$* (#33699) were obtained from the Bloomington *Drosophila* Stock Center. *UAS-Cbs$^{RNAi-KK}$* (#107325KK), *UAS-CG10623$^{RNAi-KK}$* (#109718KK), *UAS-CG10903$^{RNAi-KK}$* (#109610KK), *UAS-Mt2$^{RNAi-GD-1}$* (#37815GD), *UAS-Mt2$^{RNAi-GD-2}$* (#37816GD), *UAS-CG9666$^{RNAi-GD}$* (#45658GD), *UAS-lid$^{RNAi-KK}$* (#103830KK) and *UAS-Kdm2$^{RNAi-KK}$* (#109295KK) were obtained from the Vienna *Drosophila* Research Center. *hsFLP;Act5C > CD2 > GAL4,UAS-EGFP* was kindly provided by Dr. Dirk Bohmann (University of Rochester Medical Center).

dsRNA production

The protocols to generate constructs containing targeting sequences in pCRII-Topo vector and to produce dsRNA are described previously (Pile et al., 2002). The sequences in the pCRII-Topo vector were generated using specific primer pairs (Table 2.1). *Set1* primers were found on DRSC FlyPrimerBank (http://www.flyrnai.org/FlyPrimerBank) (Hu et al., 2013). Primers for *lid* were found on Genome RNAi (http://www.genomernai.org) (Schmidt et al., 2013). The rest of the primers were taken from *Drosophila* RNAi Library 1.0 and *Drosophila* RNAi Library 2.0 on Open Biosystems. dsRNA against GFP prepared from a PCR product was used as a control. GFP template DNA (from Dr. Russell L. Finley, Jr.) was amplified using a T7-containing primer pair (Table 2.1).

RNA interference

The RNA interference (RNAi) procedure is described previously (Pile et al., 2002). In brief, 3 x 10^6 cells with 4 ml Schneider's *Drosophila* medium were plated in a 60-mm-diameter dish. After 3 hr, Schneider's *Drosophila* medium was removed and replaced with 2 ml serum-free medium. 50 µg dsRNA was added into the dish and mixed by swirling. After 30 min, 4 ml Schneider's *Drosophila* medium was added. Cells were assayed four days following addition of dsRNA. dsRNA against GFP was used as the control. Real-time quantitative reverse transcription PCR (qRT-PCR) analysis was routinely carried out for both single- and double-RNAi-treated cells to verify efficient knockdown of targets.

Table 2.1: Primers used for dsRNA production.

Gene	Primer orientation	Primer sequence (oriented 5' to 3')
Sam-S	Forward	TTC CAA AAC ACA AGT AAC CTG C
	Reverse	TTG TGA CTT GTG AGA AGT TCC G
Ahcy13	Forward	GAG GGC TAT GAG GTT ACC ACC
	Reverse	ACG TGA GAT GGG TTT TTA TTG G
Cbs	Forward	GAG AAG ATG TCC AAC GAG AAG G
	Reverse	ACG AAC TTG GTC ATG TAG TTG C
CG10623	Forward	TTT TGT CGT ATC GCA TTG TAC G
	Reverse	AAT CTC AAT TCT TGT CTT GTG CC
CG10903	Forward	AGA TCC AAG TAG AAA TGG CCG
	Reverse	GAT AGT CGA CAA CCA ATC CTC C
Mt2	Forward	GGC AGT AAT TTG GTG AAA ACT AGG
	Reverse	GTC AAT TTC CTT GAC CAA CTC G
CG9666	Forward	AGC CAC AGT ATC AGC AAA TAG C
	Reverse	AGG GAG TAA ACT GCT CTG TTG G
Set1	Forward	GCA GGA CGT TCG GAA TAT C
	Reverse	TCC CAT TAC AGA CTT TTG ATT G
lid	Forward	CGA CAT GGC CGA AAT GGT
	Reverse	GAT ACC CAG TTG CTG TAT GAC
Kdm2	Forward	ATC ATA TTT CGT TAC CTT CCG C
	Reverse	CAG ATT AAG CTC CGT GAG ACG
GFP	Forward	GAA TTA ATA CGA CTC ACT ATA GGG AGA TGC CAT CTT CCT TGA AGT CA
	Reverse	GAA TTA ATA CGA CTC ACT ATA GGG AGA TGA TGT TAA CGG CCA CAA GTT

Real-time quantitative reverse transcription PCR assay

Total RNA was extracted from whole flies or wing imaginal discs using Trizol (Invitrogen) and purified using the RNeasy Mini Kit (Qiagen). Total RNA was extracted from RNAi treated cells using the RNeasy Mini Kit (Qiagen). cDNA was generated from total RNA using the ImProm-II Reverse Transcription System (Promega) with random hexamers. The cDNA was used as a template in a real-time quantitative PCR assay. The analysis was performed using ABsolute Blue SYBR Green ROX master mix (Fisher Scientific) and carried out in a Stratagene Mx3005P real-time thermocycler. *Taf1*,

encoding TBP-associated factor 1, was used to normalize RNA levels. The mRNA levels were quantified using real-time quantitative PCR with specific primers for each gene (Table 2.2). Primers for *Mt2* were found on DRSC FlyPrimerBank (http://www.flyrnai.org/FlyPrimerBank) (Hu et al., 2013). Primers for *Set1* were taken from a previously published report (Ardehali et al., 2011). The gene expression changes are represented as the mean (± SEM) of the fold changes observed in the fly lines or RNAi treated cells. In the whole flies, fold differences were calculated by relative comparison of flies *Act5C-Gal4/UAS-GOI (gene of interest)*^{RNAi} to *Act5C-Gal4/UAS-GFP*^{RNAi} flies. In lines where ubiquitous knockdown was lethal, fold differences were calculated by relative comparison of *Ser-Gal4/UAS-GOI*^{RNAi} wing imaginal discs to *Ser-Gal4/UAS-GFP*^{RNAi} wing imaginal discs. In cells, fold differences were calculated by relative comparison of GOI RNAi cells to GFP RNAi cells. This experiment utilized a minimum of three sets of RNA for each cell type or fly line.

Table 2.2: Primers used for gene expression analysis.

Gene	Primer orientation	Primer sequence (oriented 5' to 3')
Sam-S	Forward	AAA CTT TGA CCT CAG GCC C
	Reverse	CGC TGG TAT ATC GGC TGG
Ahcy13	Forward	AGA CCT TGG TCT TCC CCG
	Reverse	GAC ACC GGT GGT CGT CTC
Cbs	Forward	TGC AAC TGT TGG TGA GGC
	Reverse	CAT CCT GAT CCA CGA CGG
CG10623	Forward	TCC AAA GTC GGA AGG CTG
	Reverse	GGC CAC TTT GGT AAG CGA
CG10903	Forward	AGG ATC TGC TGA GCT GCC
	Reverse	CGA CGT TCC TCT TCA GGT G
Mt2	Forward	AGC CTG AGT GTA AAG GAA GTC A
	Reverse	ACA GAT GAG TAA GTG CAT CCG A
CG9666	Forward	GGG CGG GAT CAT AAA CCT
	Reverse	GGA TTC ACT GTC GTC GGC
Set1	Forward	CAA AAG GCA TTG ATG CCG AAG
	Reverse	GGT CAG TTG TGC AGT GAT CCA CC
lid	Forward	CGA CAT GGC CGA AAT GGT
	Reverse	GAT ACC CAG TTG CTG TAT GAC
Kdm2	Forward	GAG AGG AAG CAG CGC AAG
	Reverse	GAT TCG AGC TTC TCG GCA
Sesn	Forward	GAG GAG CTC CAC CGG ACT
	Reverse	ATG CGC TCC ATT AGC GTC
CG14696	Forward	TGA AGC ACA ACA AGG CCA
	Reverse	GCT TGA AGG TCT TGG CGA
Mlf	Forward	GAG GAG GGA GAA GCC GAG
	Reverse	CAA CGT CGA GGT GTG TGC
Gale	Forward	AAG GCG TTG GAC AAG CTG
	Reverse	TTG ACC TTC TTG CCG GAG
Taf1	Forward	CTG GTC CTG GTG AGG TGA
	Reverse	CCG GAT TCT GGG ATT TGA

Fly viability

Viability of flies with ubiquitous knockdown of each gene was measured by crossing *Act5C-Gal4/CyO* flies to RNAi lines of each gene of interest. The percent

viability was calculated by dividing the number of *Act5C-Gal4;RNAi* progeny by the number of *CyO;RNAi* progeny. Three biological replicates were performed.

Fly wing phenotype

The effect of knockdown of each gene in the wing imaginal discs of knockdown fly lines was examined by crossing *Ser-Gal4* flies to RNAi lines of each gene of interest. Wings of *Ser-Gal4;RNAi* progeny were scored for shape, vein defects and curvature. Three biological replicates were conducted.

Clonal analysis

hsFLP;Act5C > CD2 > GAL4,UAS-EGFP flies were crossed to $mCherry^{RNAi\text{-}TRiP}$ or to the RNAi lines of each gene of interest to generate random GFP positive clones. 0-4 hr embryos were collected and heat shocked for 2 hr at 37°C, 48-52 hour after egg laying (AEL). Wing discs from wandering third instar larvae were dissected after approximately 96 hr AEL and immunostained with monoclonal antibody against GFP.

Immunostaining

For clonal analysis, wing discs from wandering third instar larvae were dissected in 1 X PBS. Roughly 70 wing discs per cross (obtained from three biological replicates) were fixed in 4% formaldehyde in 1 X PBS and stained as previously described (Swaminathan and Pile, 2010). Antibody against GFP (1:1000; Abcam, ab1218) followed by sheep anti-mouse Alexa 488 (1:2000; Life Technologies, A11001) was used for staining. GFP positive clone pixel count was quantified using Photoshop CS. For H3K4me2 staining, wing discs from wandering third instar larvae were dissected in 1 X PBS. Roughly 60 wing discs per cross (obtained from three biological replicates) were fixed in 4% formaldehyde in 1 X PBS and stained as previously described

(Swaminathan and Pile, 2010). Antibody against dimethyl-histone H3 (Lys4) (1:1000; Millipore 07-030) followed by donkey anti-rabbit Alexa 594 (1:2000; Life Technologies, A11001) was used for staining. Discs for both clonal analysis and H3K4me2 staining were mounted in Vectashield medium plus DAPI (Vector Laboratories; H-1200). Visualization and imaging (200X) were done using a Zeiss Axioscope 2 fitted with an Axiophot photography system.

Imaging

Wing images (63X and 115X) and adult fly images (30X) were taken with an Olympus DP72 camera coupled to an Olympus SZX16 microscope.

S2 cell proliferation assay

Four days after RNAi treatment, RNAi-treated cells were stained with Trypan Blue. The number of cells per ml in each sample was calculated by following hemacytometer standard protocol. The experiments were repeated with three biological trials.

Western blotting analysis

Western blotting analysis of whole cell protein extract was performed in accordance with standard protocols as described previously (Pile et al., 2002). 12 µg whole cell protein extracts were separated on a 15% SDS-polyacrylamide gel and transferred to a polyvinylidene difluoride (PVDF) membrane (Pall). Membranes were probed with various rabbit primary antibodies followed by incubation with donkey anti-rabbit HRP-conjugated IgG (1:3000; GE Healthcare) secondary antibody. The antibody signals were detected using the clarity western ECL substrate (Bio-Rad) for H3K4me2 and H3K4me3 or ECL prime western blotting detection system (GE Healthcare) for

H3K9me2 and H4. Primary antibodies included: H3K4me2 (1:5000; Millipore), H3K4me3 (1:2500; Active Motif), H3K9me2 (1:500; Millipore) and H4 (1:15,000; Abcam) as a loading control. At least three biological replicates were performed.

Chromatin immunoprecipitation and real-time quantitative PCR

To prepare chromatin, 4 x 10^7 cells were subjected to cross-linking with 1% formaldehyde for 10 min and quenched with 125 mM glycine at room temperature. Cells were then washed 3 times with 1 X PBS at 4^{o}C for 5 min and were resuspended in 15 ml resuspension buffer (10 mM Tris (pH 8), 10 mM KCl, 3 mM $CaCl_2$, 0.34 M Sucrose, 1 mM DTT, 0.1% Triton X-100, 0.2 mM EGTA, 1.5 Roche complete protease inhibitor tablet). The resuspended cells were incubated on ice for 15 min and then homogenized by a dounce homogenizer using a loose pestle 10 times and a tight pestle 15 times followed by low speed centrifugation at 4^{o}C for 10 min. The loose pellet was resuspended in 200 µl 10X micrococcal nuclease (MNase) digest buffer (15 mM Tris (pH 8), 60 mM KCl, 15 mM NaCl, 1mM $CaCl_2$, 0.25 M sucrose, 1 mM DTT) and subjected to MNase digestion using 20 units of MNase for 30 min at room temperature. 10 mM EDTA was added to stop the reaction. Samples were diluted with 950 µl Ten140 buffer (140 mM NaCl, 10 mM Tris (pH 7.6), 2 mM EDTA). The samples were then subjected to sonication for 7 times of 30 sec pulses with 1 min intervals at 20% amplitude using an Ultrasonic dismembrator (Model 500 (Fisher Scientific)) sonicator. Sonicated samples were centrifuged for 15 min at 4^{o}C and the chromatin was in the supernatant.

To prepare input DNA, 18.75 µg sonicated chromatin diluted to a final volume of 250 µl Ten140 buffer was used. Chromatin was treated with 0.05 µg/µl RNase A at

37°C for 15 min and then incubated overnight at 65°C after adding 200 mM NaCl. Samples were then treated with 0.04 µM Proteinase K (Fisher Scientific), 10 µM EDTA, 20 µM Tris (pH 8.0) at 45°C for 1.5 hr and subjected to phenol chloroform extraction and ethanol precipitation. Precipitated DNA was resuspended in 25 µl 0.1 mM Tris (pH 8.0).

For immunoprecipitation, 75 µg prepared chromatin was diluted to a final volume of 500 µl Ten140 buffer. IgG was used as a non-specific control and H3 acted as a loading control. Chromatin was incubated overnight with 2.5 µl IgG, 3 µl H3K4me3 (Active Motif) or 4 µl H3 (Abcam) antibody on a nutator at 4°C. Samples were then mixed with 30 µl anti-IgG beads (Protein A agarose (Pierce)), which were pre-washed 6 times with lysis buffer (50 mM Tris (pH 7.6), 280 mM NaCl, 2 mM EDTA, 0.3% sodium dodecyl sulfate). The samples with beads were placed on a nutator at 4°C for 4 hr. Anti-IgG beads were then washed with 1 ml lysis buffer for 5 min, 1 ml IP 1 buffer (25 mM Tris (pH 7.6), 500 mM NaCl, 1 mM EDTA, 0.1% sodium deoxycholate, 1% Triton X-100) for 10 min and 1 ml IP 2 buffer (10 mM Tris (pH 7.6), 250 mM LiCl, 1 mM EDTA, 0.5% sodium deoxycholate, 0.5% Triton X-100) for 5 min at 4°C. The beads were then rinsed with 1 ml Tris-EDTA (pH 8.0) and incubated with 500 µl elution buffer (1% sodium dodecyl sulfate, 0.1 M $NaHCO_3$) at 65°C for 1 hr. Eluted samples were subject to reverse cross-linking in the same way as described above for input preparation. Precipitated DNA was resuspended in 50 µl 0.1 mM Tris (pH 8.0).

Input DNA (diluted 1:100) and immunoprecipitated samples (diluted 1:4) were used as the template in a real-time quantitative PCR assay. The analysis was performed using ABsolute Blue SYBR Green ROX master mix (Fisher Scientific) and

carried out in a Stratagene Mx3005P real-time thermocycler. Primers are listed in Table 2.3.

Table 2.3: Primers used for ChIP-qPCR analysis.

Gene	Primer orientation	Primer sequence (oriented 5' to 3')
Sesn	Forward	GAA AAC GGA CGA AAA TCG AG
	Reverse	CAC GAA AAC TGT GGA TAA AAT G
CG14696	Forward	TGG ACA GGA TGA GCA GCA
	Reverse	CGT AAT CAG TTC CGC CGT
Mlf	Forward	TCG AGC AAC AGA AAG CCA
	Reverse	CCG AGA TCG TCG TCG AAA
Gale	Forward	GAA TCG GGA GCC AAA GGT
	Reverse	AGC AGG CTG ACT TGG TCG

Statistical analyses

All significance values were calculated by the unpaired two sample Student‘s *t*-test from GraphPad Software (http://www.graphpad.com/quickcalcs/ttest1/).

Data availability

The primers used to generate dsRNA can be found in Table 2.1. The primers used for gene expression and ChIP-qPCR analysis can be found in Table 2.2 and Table 2.3, respectively.

RESULTS

Functions of genes involved in methionine metabolism and histone demethylase genes in *Drosophila* viability and wing morphology

To address the role of enzymes in methionine metabolism and histone demethylases in regulating developmental processes, we utilized RNAi to ubiquitously knock down the genes of interest through the GAL4-UAS system (Duffy, 2002; Lee and Carthew, 2003). To date, according to the information on Flybase (http://flybase.org) (St Pierre et al., 2014), *Sam-S* is the only known SAM synthetase gene (Larsson and

Rasmuson-Lestander, 1994), *Ahcy13* is the major adenosylhomocysteinase gene (Caggese et al., 1997), and *Cbs* is the only known cystathionine-β-synthase gene in *Drosophila*. *CG10623* may encode a putative methionine synthase. CG10903 is predicted to have SAM-dependent methyltransferase activity and is reported to positively affect cell proliferation in *Drosophila* neural stem cells (Neumuller et al., 2011). CG9666 is a predicted N6-adenine specific DNA methyltransferase based on sequence and structural analysis. *Mt2* is a candidate CpG DNA methyltransferase gene in *Drosophila*, but this type of DNA methyltransferase activity is controversial (Dunwell and Pfeifer, 2014; Raddatz et al., 2013; Tang et al., 2003). In addition, MT2 is reported to have tRNA methyltransferase activity (Schaefer et al., 2010). We chose these seven genes, as well as a known histone methyltransferase gene *Set1* and two histone demethylase genes *lid* and *Kdm2* to investigate their role in development.

To knock down the genes of interest, we crossed *UAS-RNAi* fly lines to the *Act5C-Gal4* driver line. Progeny will ubiquitously express dsRNA recognizing the target, so the expression of the gene will be knocked down in all tissues. We refer to these offspring as deficient flies. To rule out the possibility that phenotypes observed in the RNAi knockdown fly lines are the result of an off target effect, we utilized more than one *UAS-RNAi* line for each gene whenever possible. We utilized multiple targeting lines for all genes with exception of *Ahcy13* and *CG9666*. The efficiency of knockdown was validated by qRT-PCR analysis (Fig. 2.2). Individual ubiquitous knockdown of methionine metabolic genes *Sam-S, Ahcy13, Cbs,* but not *CG10623*, resulted in lethality (Table 2.4). These data are consistent with previous studies demonstrating that *Sam-S* and *Cbs* are essential genes (Kabil et al., 2011; Larsson and Rasmuson-

Lestander, 1998) and indicate that the majority of enzymes in the methionine pathway are critical for fly viability. For three genes annotated to have methyltransferase activity, deficiency of *CG10903*, but not *Mt2* and *CG9666*, affected viability (Table 2.4). *Mt2* was previously demonstrated to be non-essential for viability (Lin et al., 2005). Reduction of histone methyltransferase Set1 or demethylase LID impaired viability in our hands (Table 2.4), which is consistent with previously published work (Gildea et al., 2000; Hallson et al., 2012). The effect of KDM2 in *Drosophila* viability is controversial (Lagarou et al., 2008; Li et al., 2010; Zheng et al., 2014), but our results support the idea that *Kdm2* is not essential (Table 2.4). Similar results were obtained from the different RNAi fly lines targeting the same gene. Thus, it is very likely that the observed lethality is due to the reduction of the specific gene tested, and not the result of an off target effect. The viability data demonstrate that some but not all tested methyltransferases and demethylases are essential. Although the genes selected have been shown or predicted to be a methyltransferase or demethylase, some may be redundant with other enzymes or may affect specific methylation or demethylation reactions that are not essential. These viability tests, consistent with published work, indicate that enzymes involved in methionine metabolism, histone methylation and demethylation are necessary for development in *Drosophila*.

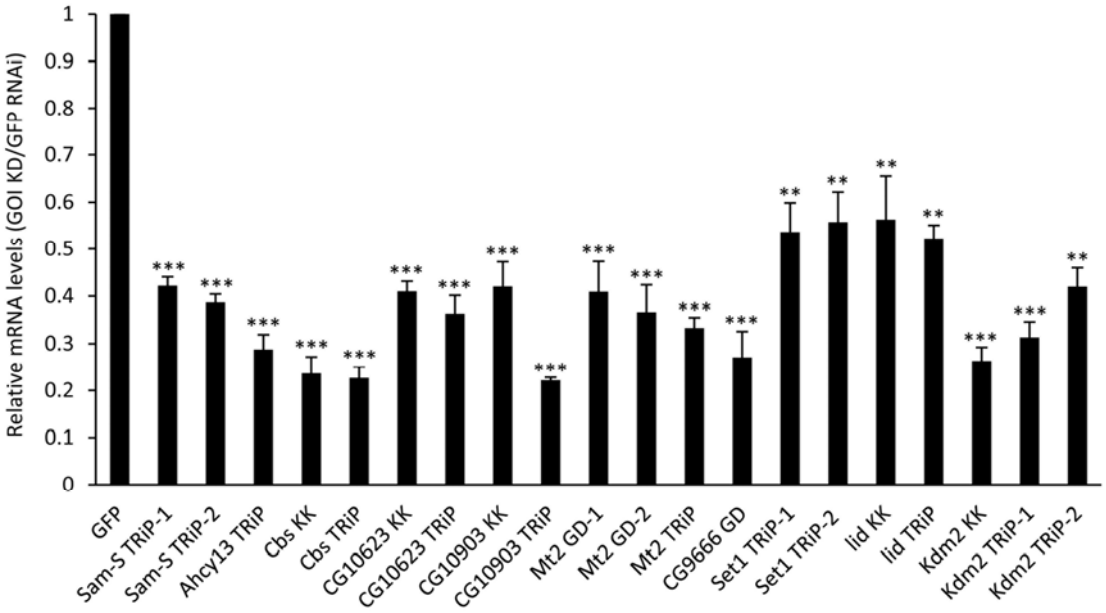

Fig. 2.2: Quantification of mRNA levels in the gene of interest knockdown flies. Real-time quantitative reverse transcription-PCR (qRT-PCR) analysis was performed using cDNA prepared from RNA isolated from either whole flies (*CG10623*, *Mt2*, *CG9666* or *Kdm2*) or from wing imaginal disc tissue (*Sam-S*, *Ahcy13*, *Cbs*, *CG10903*, *Set1* or *lid*). Results are the average of three biological replicates. Error bars represent standard error of the mean. The statistical analysis results comparing each individual knockdown sample to the control GFP RNAi sample are indicated on each knockdown sample. (**) $P < 0.01$, (***) $P < 0.001$. GFP, control flies expressing dsRNA against GFP. GOI KD, flies expressing dsRNA against the gene of interest.

Table 2.4: Ubiquitous knockdown of *Sam-S*, *Ahcy13*, *Cbs*, *CG10903*, *Set1* or *lid* results in a loss of viability.

		♂			♀		
			Flies Scored			Flies Scored	
Gene	**Stock Name (*UAS-GOI*)**	**% Viable**	***Act5C-Gal4/UAS-GOI***	***CyO/UAS-GOI***	**% Viable**	***Act5C-Gal4/UAS-GOI***	***CyO/UAS-GOI***
Sam-S	*Sam-S$^{RNAi-TRiP-1}$*	0	0	180	0	0	222
	Sam-S$^{RNAi-TRiP-2}$	0	0	178	0	0	190
Ahcy13	*Ahcy13$^{RNAi-TRiP}$*	0	0	137	0	0	188
Cbs	*Cbs$^{RNAi-KK}$*	0	0	146	0	0	183
	Cbs$^{RNAi-TRiP}$	0	0	146	0	0	183
CG10623	*CG10623$^{RNAi-KK}$*	98.7±24.1	231	273	98±12.5	229	249
	CG10623$^{RNAi-TRiP}$	96±21.5	195	203	99±7.2	217	222
CG10903	*CG10903$^{RNAi-KK}$*	0	0	144	0	0	187
	CG10903$^{RNAi-TRiP}$	0	0	113	0	0	157
Mt2	*Mt2$^{RNAi-GD-2}$*	93.3±11.6	144	159	123±20	195	163
	Mt2$^{RNAi-TRiP}$	102.3±11.3	187	184	99.7±3	187	188
CG9666	*CG9666$^{RNAi-GD}$*	139±10.4	146	110	85.7±7.6	125	154
Set1	*Set1$^{RNAi-TRiP-1}$*	0	0	194	0	0	192
	Set1$^{RNAi-TRiP-2}$	0	0	133	0	0	169
lid	*lid$^{RNAi-KK}$*	0	0	122	0	0	237
	lid$^{RNAi-TRiP}$	0	0	231	0	0	334
Kdm2	*Kdm2$^{RNAi-KK}$*	98±19.7	138	148	90.4±13	147	167
	Kdm2$^{RNAi-TRiP-1}$	98.3±10.2	137	143	106.3±2.4	176	165
	Kdm2$^{RNAi-TRiP-2}$	103±29.4	191	185	99.1±8.9	180	182

GOI, gene of interest.
TRiP, Transgenic RNAi Project at Harvard Medical School; KK, ΦC31 Transgenic RNAi Library; GD, P-element Transgenic RNAi Library.
The percent viability is calculated by dividing the number of *Act5C-Gal4/UAS-GOI* progeny by the number of *CyO/UAS-GOI* progeny. Standard error of the mean is indicated. Three trials were performed.

The lethality caused by ubiquitous reduction of methionine metabolic enzymes and histone modifiers led us to further investigate their role in development using a conditional knockdown system. Wing tissue is non-essential and has been used by us and others to explore developmental functions of individual factors. We conditionally knocked down each tested gene in wing imaginal disc cells by activating expression of specific dsRNA targeting sequences with the wing specific driver *Ser-Gal4*. Knockdown of *CG10903* in wing imaginal disc cells using the *UAS-CG10903$^{RNAi-KK}$* line resulted in

severely wrinkled, blistered adult wings in all progeny (Fig. 2.3). The use of the *UAS-CG10903*$^{RNAi\text{-}TRiP}$ line led to lethality in the pupal stage of development. The different results are possibly due to the measured differences in RNAi efficiency of the dsRNA constructs utilized (Fig. 2.2). While we do not have a definitive explanation for the lethality caused by reduced CG10903 in wing tissue, it may be related to a "molting checkpoint" (Cherbas et al., 2003). As proposed in Chebas *et al.* (2003), due to the presence of a molting checkpoint, tissue specific reduced expression of a particular gene may block development of the entire animal, leading to lethality. Reduction of SET1 in wing precursor cells led to a curved rather than straight adult wing in all offspring (Fig. 2.3A) and a ruffled wing between veins L5 and L6 (Fig. 2.3B). In accord with previous work indicating that *lid* can genetically interact with *Notch* or *Snf5-related 1* (*snr1*) to affect wing vein development (Curtis et al., 2011; Moshkin et al., 2009), we found decreased LID resulted in a curved wing in all progeny (Fig. 2.3A). The multiple RNAi lines tested each yielded very similar results indicating that the wing defects are specific for SET1 or LID and are not due to off target effects. All flies with reduced SAM-S, AHCY13, CBS, CG10623, MT2, CG9666 or KDM2 showed normal adult wings (data not shown). Taken together, these observations indicate that while the methionine metabolic pathway is not critical for wing development, direct regulation of histone methylation and demethylation plays an important role in the development of normal wing morphology in *Drosophila*.

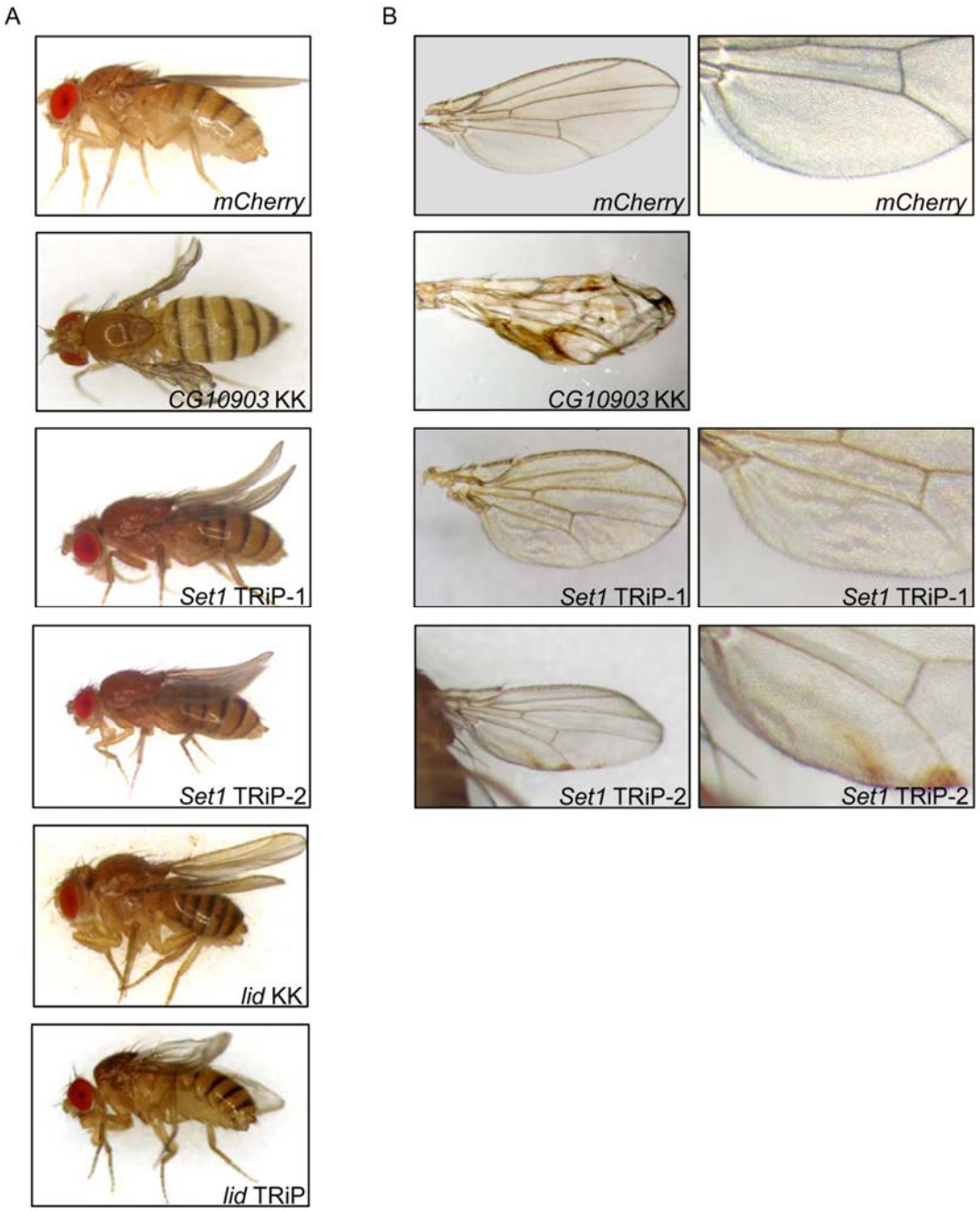

Fig. 2.3: *CG10903*, *Set1* and *lid* affect wing morphology. Micrographs of flies (A) or wings (B) carrying the *Ser-Gal4* driver and the indicated *UAS-RNAi* constructs. *mCherry*: control flies expressing *mCherry* dsRNA. Flies with knockdown of *Sam-S, Ahcy13, Cbs, CG10623, Mt2, CG9666* and *Kdm2* had straight wings, similar to the control. For each knockdown sample, at least 174 flies from three biological replicates were scored. All progeny in the same knockdown sample showed the same phenotype.

Cell proliferation is modulated by altering the levels of enzymes involved in methionine metabolism and a histone demethylase

Abnormal wing development has been found to occur when normal cell proliferation pathways are mutated (Herranz and Milan, 2008). Additionally, altered levels of enzymes controlling methionine metabolism can affect cell proliferation in human cells (Albertini et al., 2012; Hermes et al., 2008). For these reasons, we decided to determine whether methionine metabolic enzymes, histone methyltransferases and demethylases contribute to regulation of cell proliferation in *Drosophila*. We first checked for defects in cell proliferation by measuring cell number in *Drosophila* S2 cells upon RNAi-mediated depletion of genes of interest. For these experiments, the level of gene knocked down was determined by qRT-PCR analysis (Fig. 2.4). Compared to control cells treated with GFP dsRNA, individual knockdown of all tested genes, except *Kdm2*, led to lower cell counts with a range of 10% - 30% decrease (Fig. 2.5).

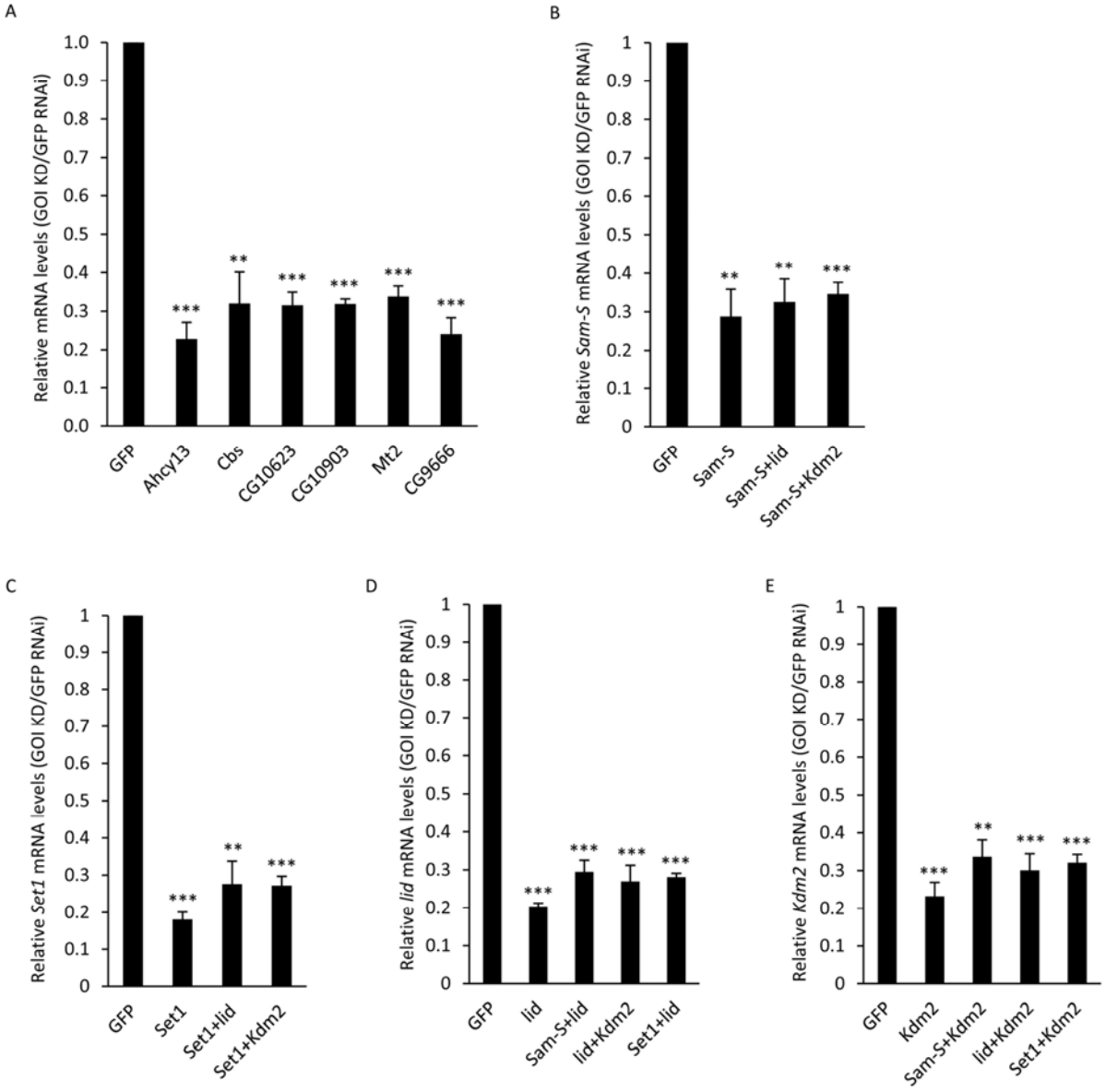

Fig 2.4: Quantification of mRNA levels in RNAi-treated S2 cells. Real-time quantitative reverse transcription-PCR (qRT-PCR) analysis was performed using cDNA prepared from RNA isolated from S2 cells incubated with dsRNA against either GFP or indicated gene. Results are the average of three biological replicates. Error bars represent standard error of the mean. The statistical analysis results comparing individual knockdown sample to the control GFP RNAi cells are indicated on knockdown samples. (**) $P < 0.01$, (***) $P < 0.001$. GFP, control cells treated with dsRNA against GFP. GOI KD, cells treated with dsRNA against the gene(s) of interest.

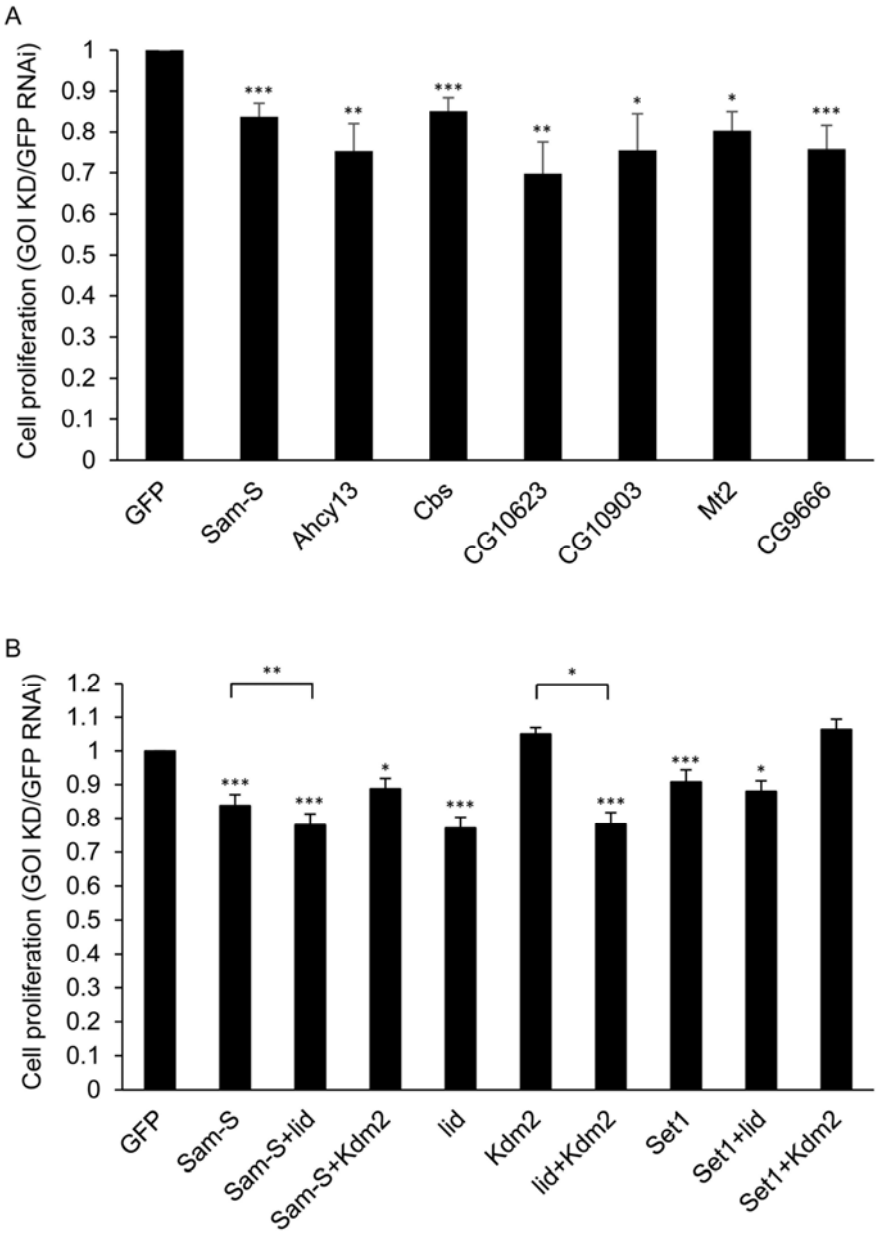

Fig. 2.5: Cell proliferation in S2 cells is affected by methionine metabolic enzymes and histone methyltransferases and demethylases. (A, B) Quantification of cell density by cell counts from RNAi-treated cells. Results are the average of three biological replicates. Error bars represent standard error of the mean. Statistically significant results comparing the individual knockdown samples to the GFP RNAi control are indicated on knockdown samples. P-values were also calculated between the double knockdown samples and each single knockdown sample for the two tested genes, e.g. *Sam-S+lid* to *Sam-S* and *Sam-S+lid* to *lid*. Statistically significant results are indicated with bars. (*) P <0.05, (**) P < 0.01, (***) P < 0.001. GFP, control cells treated with dsRNA against GFP. GOI KD, cells treated with dsRNA against the gene(s) of interest.

To further investigate the relationship among these enzymes in affecting cell proliferation, we measured cell counts in S2 cells having different combinations of knockdown factors. Because we observed a connection between SAM-S and histone demethylases as well as between SET1 and histone demethylases in regulation of histone methylation (described in detail below), we focused on the same combinations to determine their role in cell growth. Double knockdown cells did not show an additive effect on cell proliferation relative to the single knockdown cells (Fig. 2.5B). The double knockdown cells showed cell numbers comparable to the single knockdown cells that had the larger effect between two tested genes (Fig. 2.5B). These results imply that methionine metabolism, histone methylation and demethylation probably influence the same pathway(s) to regulate cell proliferation in this cell type.

All tested genes, except *Kdm2*, affected cell proliferation in S2 cells, which prompted us to analyze the role of these genes in cell growth during fly development. To address this question, we performed clonal analysis in *Drosophil*a wing imaginal discs. We utilized the heat shock flip-out system to randomly generate clones expressing GFP in RNAi knockdown cells. Reduction of all tested enzymes, except KDM2, resulted in small GFP positive clones that were fewer in number relative to the *mCherry* RNAi control (Fig. 2.6). The defects of cell proliferation in wing imaginal discs are specific for the targeted genes as they could be confirmed using a second RNAi line, except *Ahcy13* and *CG9666* as mentioned (Fig. 2.6). Collectively, data from cultured cells and developing flies demonstrate that the methionine pathway, histone methylation and demethylation have a critical role in the regulation of cell proliferation.

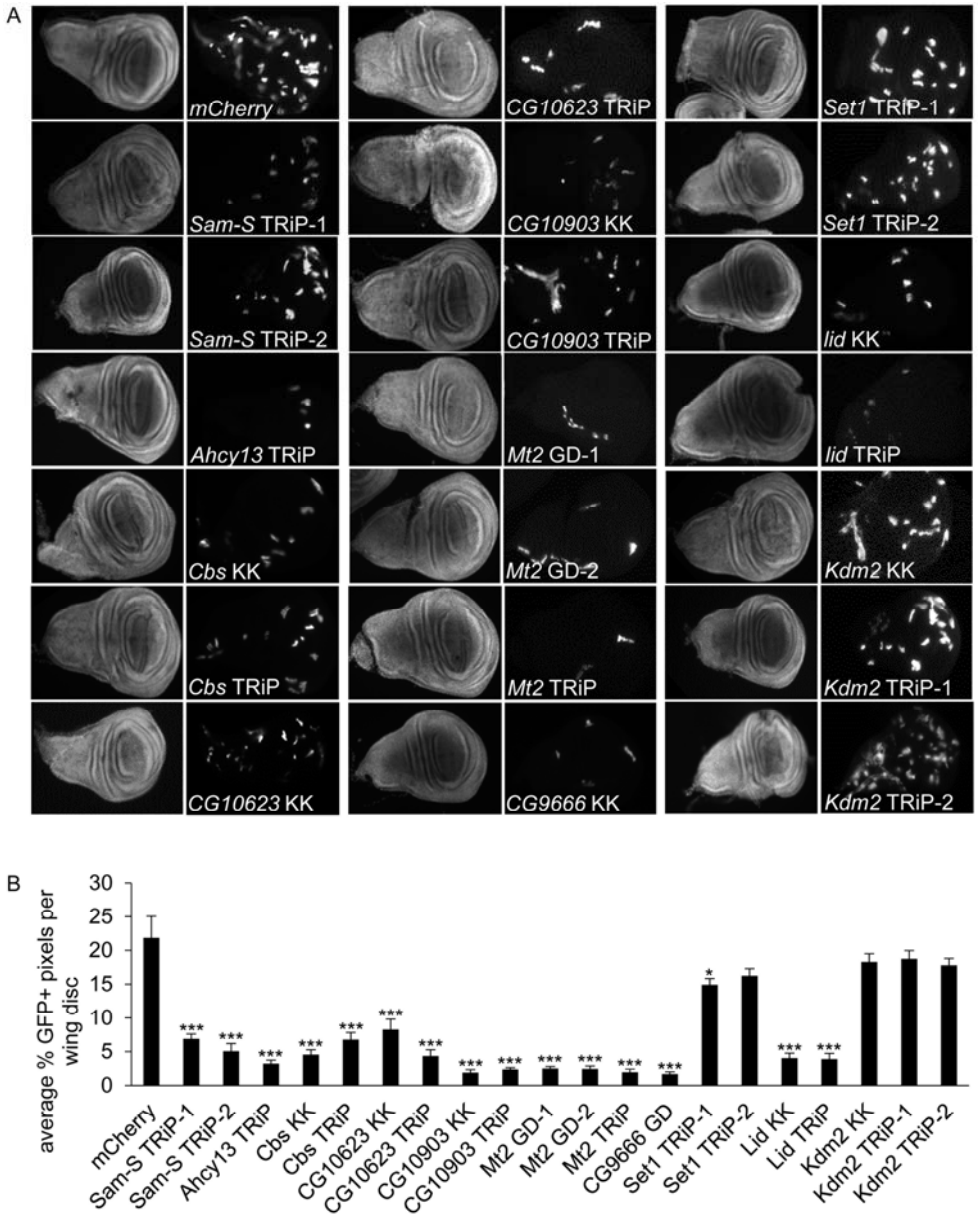

Fig. 2.6: Cell proliferation in wing imaginal discs is affected by methionine metabolic enzymes and histone methyltransferases and demethylases. (A) *mCherry* RNAi control and knockdown wing disc clones were generated using the flip-out GAL4 system and immunostained with antibody to GFP. GFP signal is shown in the right panel of paired images for each fly line. DAPI staining is in the left panel. (B) Quantification of GFP signal in wing imaginal discs. Results are the average of GFP positive pixel counts from three biological replicates with at least 70 wing imaginal discs in total for each knockdown sample. Error bars represent standard error of the mean. P-values were calculated by comparing the GFP positive pixel count measured in the individual knockdown fly to the GFP positive pixel count in the *mCherry* RNAi control. Statistically significant results are indicated on knockdown samples. (*) P <0.05, (***) P < 0.001. *mCherry*, control fly carrying dsRNA against *mCherry*.

Disruption of methionine metabolism affects histone methylation

Given that methionine metabolism generates the major methyl donor SAM, we wanted to characterize the functions of genes involved in methionine metabolism in the possible modulation of histone methylation levels. It is known that H3K4 methylation is associated with active transcription, whereas H3K9 methylation is associated with repressive transcription (Black et al., 2012). We performed western blotting analysis of whole cell protein extracts from *Drosophila* S2 cells with RNAi-mediated depletion of genes of interest. The blots were probed with antibodies specific for H3K4me2, H3K4me3, H3K9me2 as well as histone H4 as the loading control (Fig. 2.7A). Global histone methylation levels normalized with histone H4 in each condition were quantified (Fig. 2.7B). Knockdown of *Sam-S* resulted in decreased global H3K4me3 and H3K9me2 levels. Reduction of *Mt2* led to increased global H3K9me2 levels. Global H3K4me2 levels were reduced upon decreased expression of *CG10623* or *CG9666* relative to control GFP dsRNA treated cells. The decrease in the level of H3K4me2 in S2 cells, while small, was reproducible. To further analyze the possible function of CG10623 or CG9666, we looked at global H3K4me2 levels during fly development. We crossed the *UAS-RNAi* fly lines to the *Engrailed-Gal4* driver line. Targeted genes are knocked down in the posterior region of wing imaginal discs in the progeny. No obvious changes of H3K4me2 levels were found between posterior and anterior compartments of wing imaginal discs when CG10623 or CG9666 was reduced (Fig. 2.8). The impact of these enzymes on downstream processes in S2 cells or on H3K4me2 in other cell types remains open for further study.

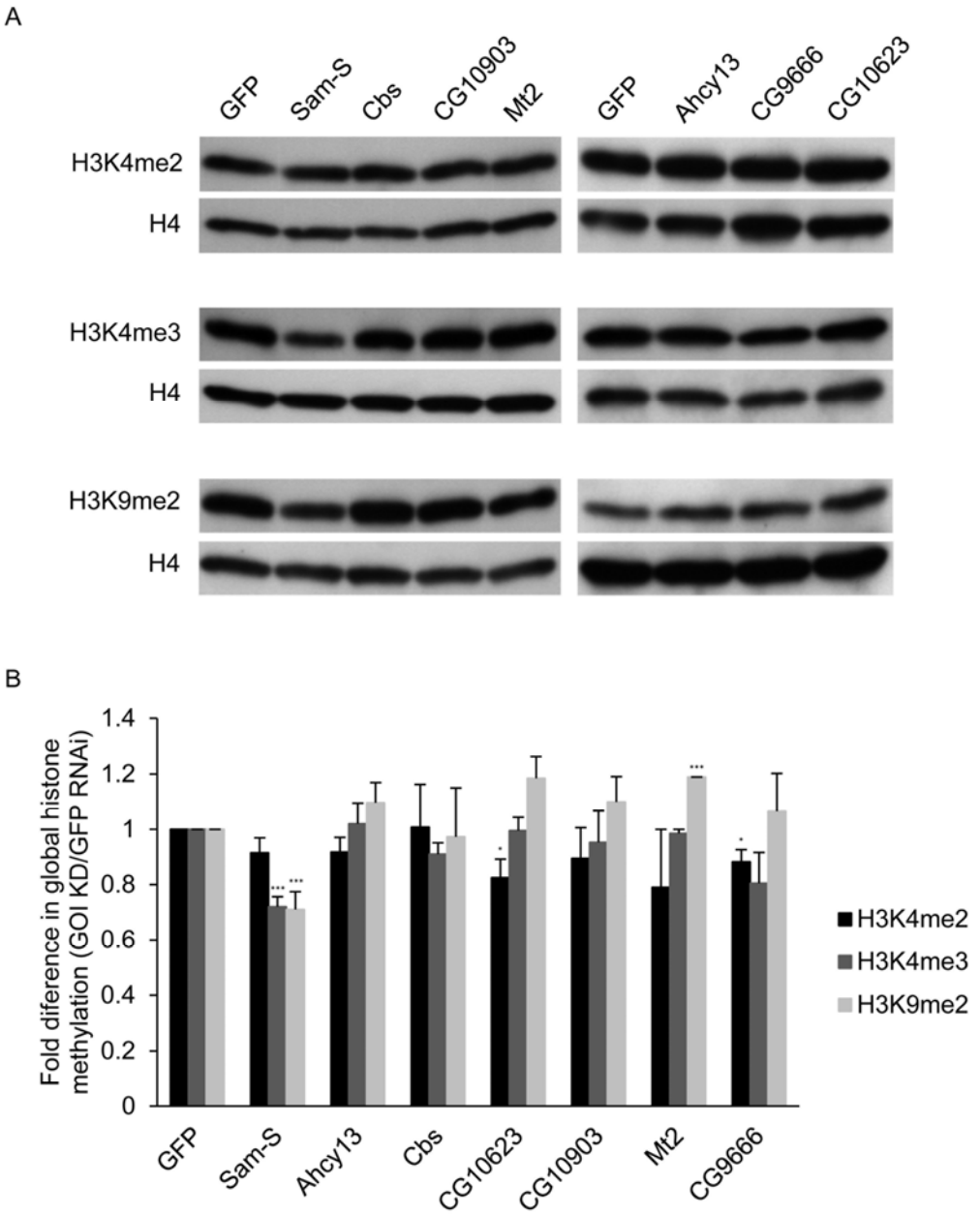

Fig. 2.7: Global histone methylation levels in S2 cells are regulated by enzymes involved in methionine metabolism. (A) Whole cell extracts from RNAi-treated cells were subjected to western blotting analysis for H3K4me2, H3K4me3, H3K9me2 or H4. (B) Western blots as shown in A were repeated with protein extracts prepared from at least three independent cultures and the results were quantified after normalization to histone H4. Error bars represent standard error of the mean. P-values were calculated between the individual knockdown sample and the GFP RNAi control. Statistically significant results are indicated. (*) P <0.05, (***) P < 0.001. GFP, control cells treated with dsRNA against GFP. GOI KD, cells treated with dsRNA against the gene of interest.

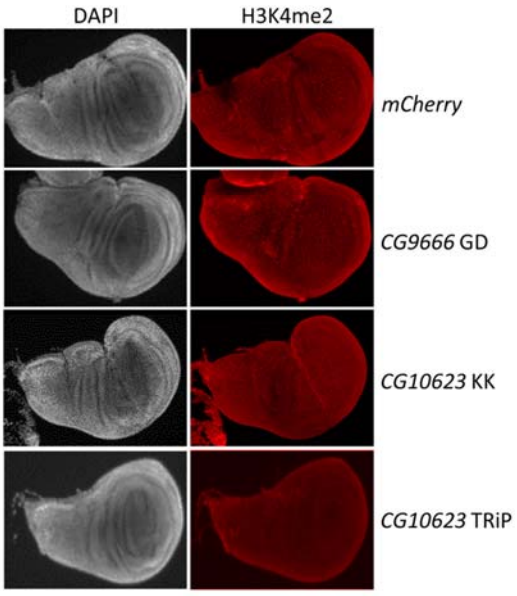

Fig. 2.8: Knockdown of *CG9666* and *CG10623* does not affect H3K4me2 levels in wing imaginal discs. *mCherry*: control flies expressing *mCherry* dsRNA. *mCherry* RNAi control and gene of interest knockdown wing imaginal discs were generated using the *Engrailed-Gal4* driver and immunostained with antibody to H3K4me2. H3K4me2 signal is shown in the right panel of paired images for each fly line. DAPI staining is in the left panel.

The finding that *Sam-S* affects global histone methylation led us to further investigate the activity of this key enzyme in regulation of gene specific histone methylation marks. Because H3K4me3 is an important histone mark associated with active genes (Black et al., 2012; Black and Whetstine, 2011), we focused on this histone modification for further study. We selected four genes, *Sestrin* (*Sesn)*, *CG14696*, *Myelodysplasia/myeloid leukemia factor* (*Mlf)* and *UDP-galactose 4'-epimerase* (*Gale*), based on the published ChIP-seq analysis of H3K4me3 levels in S2 cells (Gan et al., 2010). *Sesn* and *Mlf* are implicated in cell proliferation (Jasper et al., 2002; Lee et al., 2010). *Gale* is involved in the galactose metabolic process (Sanders et al., 2010). The function of *CG14696* is unknown. Gan *et al.* (2010) determined that the promoter regions of *Mlf* and *Gale* have the highest H3K4me3 levels in the whole

genome, *sesn* has middle H3K4me3 levels, *CG14696* has the lowest, yet still observable, H3K4me3 levels of these four genes. To examine if SAM-S affects the enrichment of H3K4me3 at these four genes, we performed ChIP-qPCR analysis using chromatin prepared from GFP RNAi control and *Sam-S* deficient S2 cells and immunoprecipitated with antibody to IgG, H3K4me3 or H3 (Fig. 2.9). IgG was used as a non-specific control. Histone H3 signal was used to normalize H3K4me3 levels. Typically, a more than 100-fold enrichment of H3K4me3 or H3 compared to IgG was observed at all regions sampled (Fig. 2.9). Knockdown of *Sam-S* led to a significant decrease of H3K4me3 levels at *Sesn*, a non-significant decrease at *CG14696* and *Gale*, and no change at *Mlf* (Fig. 2.10A). Given that H3K4me3 is associated with active genes (Black et al., 2012; Black and Whetstine, 2011), we predicted that decreased H3K4me3 would result in a decline in gene expression. To test this hypothesis, we measured expression of these four genes in GFP RNAi control and *Sam-S* deficient S2 cells by qRT-PCR analysis. A significant decrease of *Sesn* expression was observed when SAM-S was reduced, while expression of the other three genes was not significantly changed (Fig. 2.10B). Taken together, these data reveal that SAM-S regulates global and gene specific histone methylation, which is associated with gene expression.

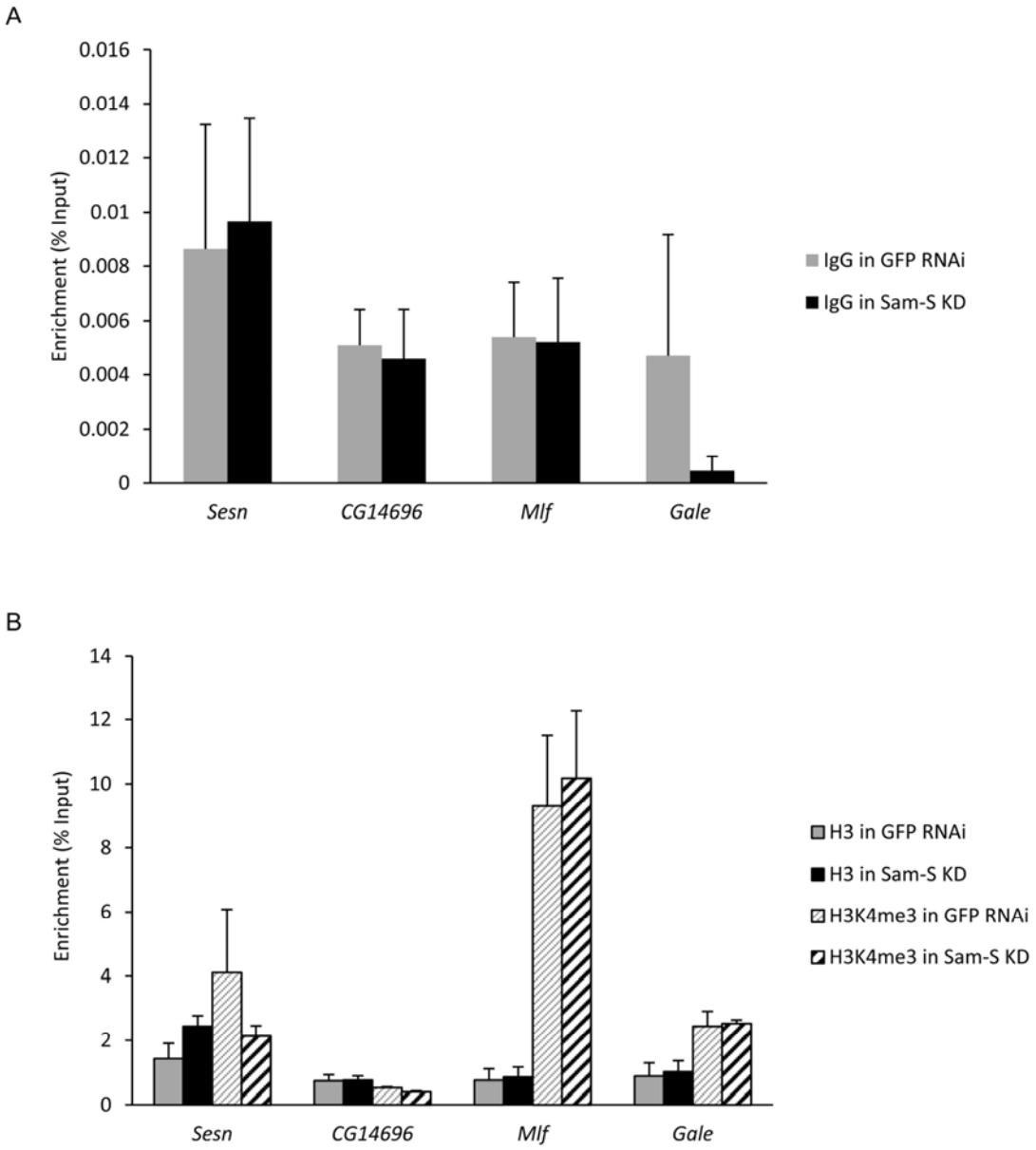

Fig. 2.9: ChIP-qPCR analysis. ChIP-qPCR was performed using DNA prepared from chromatin pulled down by IgG, H3 or H3K4me3 antibody in GFP RNAi control and *Sam-S* deficient S2 cells. Results are the average of three biological replicates. Error bars represent standard error of the mean.

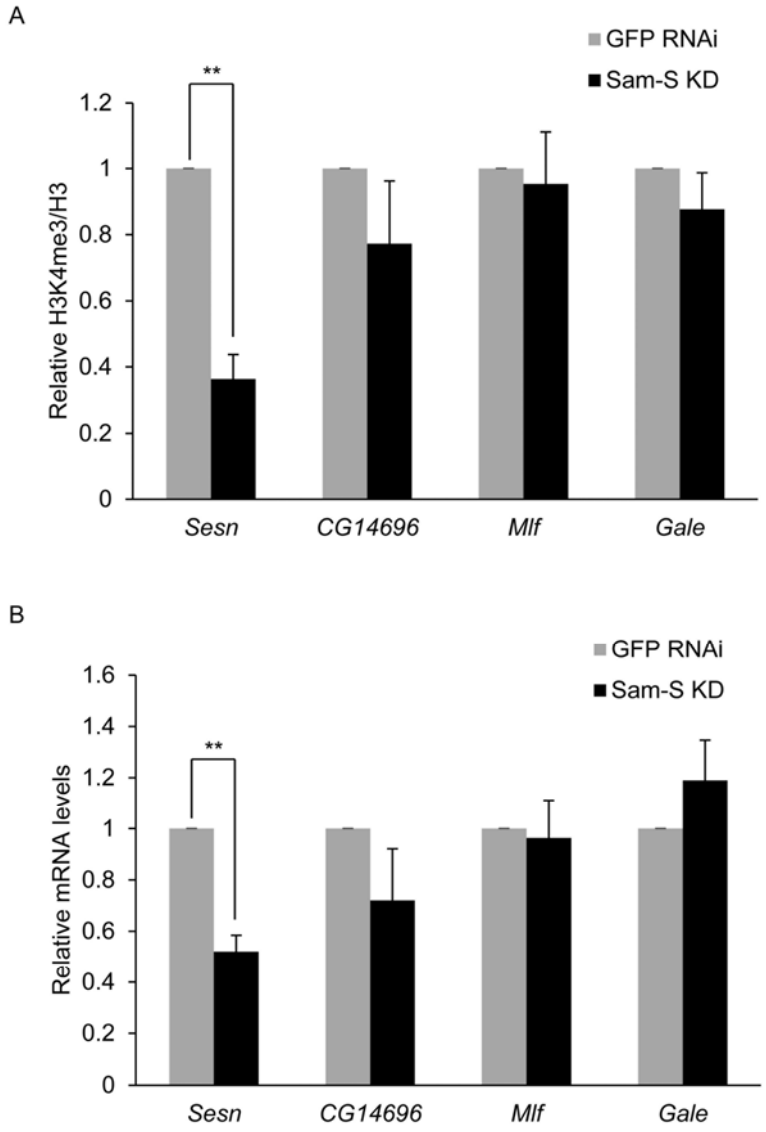

Fig. 2.10: Knockdown of *Sam-S* affects gene specific H3K4me3 levels and gene expression. (A) ChIP-qPCR analysis of H3K4me3 levels at selected genes in GFP RNAi control and *Sam-S* deficient cells. Real-time quantitative PCR analysis was performed using chromatin prepared from RNAi-treated S2 cells immunoprecipitated with antibody to H3K4me3 or H3. H3K4me3 levels were normalized to histone H3 at specific genes. Relative H3K4me3 signals were calculated by dividing normalized H3K4me3 levels in *Sam-S* deficient cells by the levels in GFP RNAi control. Results are the average of three biological replicates. Error bars represent standard error of the mean. Statistically significant results are indicated. (B) Expression of selected genes in GFP RNAi control and *Sam-S* deficient cells. *Taf1* was used to normalize expression levels. The relative mRNA was calculated by dividing normalized gene expression levels in *Sam-S* deficient cells by the levels in GFP RNAi control. Results are the average of three biological replicates. Error bars represent standard error of the mean. Statistically significant results are indicated. (**) $P < 0.01$.

Decreased global H3K4me3 levels resulting from reduced SAM-S or SET1 are restored to near control levels upon *lid* knockdown

Next, we wanted to explore the possible cooperation between enzymes involved in methionine metabolism and histone demethylases in regulating histone methylation. As described above, we focused on H3K4me3 mark. Consistent with published data (Ardehali et al., 2011; Hallson et al., 2012; Mohan et al., 2011), *Set1* influenced global H3K4me3 levels (Fig. 2.11). *Sam-S* was the only tested methionine metabolic gene affecting global H3K4me3 levels (Fig. 2.7), so we selected *Sam-S*, *Set1* as well as *lid* and *Kdm2* to investigate possible interactions in their contribution to H3K4me3 levels. We measured H3K4me3 levels by western blotting analysis in S2 cells with different combinations of the knockdown factors. Consistent with published data (Eissenberg et al., 2007; Lee et al., 2007; Lloret-Llinares et al., 2008; Secombe et al., 2007), reduced LID led to increased global H3K4me3 levels (Fig. 2.11). The role of KDM2 in histone methylation is still controversial (Kavi and Birchler, 2009; Lagarou et al., 2008; Li et al., 2010; Zheng et al., 2014). Our results showed that decreased KDM2 did not affect global H3K4me3 levels (Fig. 2.11), which suggests that KDM2 is not a major H3K4 demethylase. Additionally, although the data were not statistically significant, the H3K4me3 levels in double knockdown *lid* and *Kdm2* cells were intermediate between those of *lid* single knockdown and *Kdm2* single knockdown cells (Fig. 2.11). These results indicate that KDM2 may counteract the demethylase function of LID in S2 cells. Compared with lowered global H3K4me3 levels in *Sam-S* or *Set1* knockdown cells, reduction of LID, but not KDM2, in the context of reduced SAM-S or SET1, restored global H3K4me3 levels to near control levels (Fig. 2.11). These data further support our

conclusion that KDM2 is not a major H3K4 demethylase. Moreover, these results suggest that LID controls H3K4me3 levels in opposition to SAM-S or SET1. SET1 is a histone methyltransferase, thus it is not surprising that LID, as a histone demethylase, acts in opposition. SAM-S likely affects H3K4me3 levels by influencing the amount of the methyl donor SAM. Reduction of LID may allow more H3K4 to remain methylated. These data demonstrate the effect on histone methylation by a metabolic enzyme can be countered by the action of a chromatin modifier.

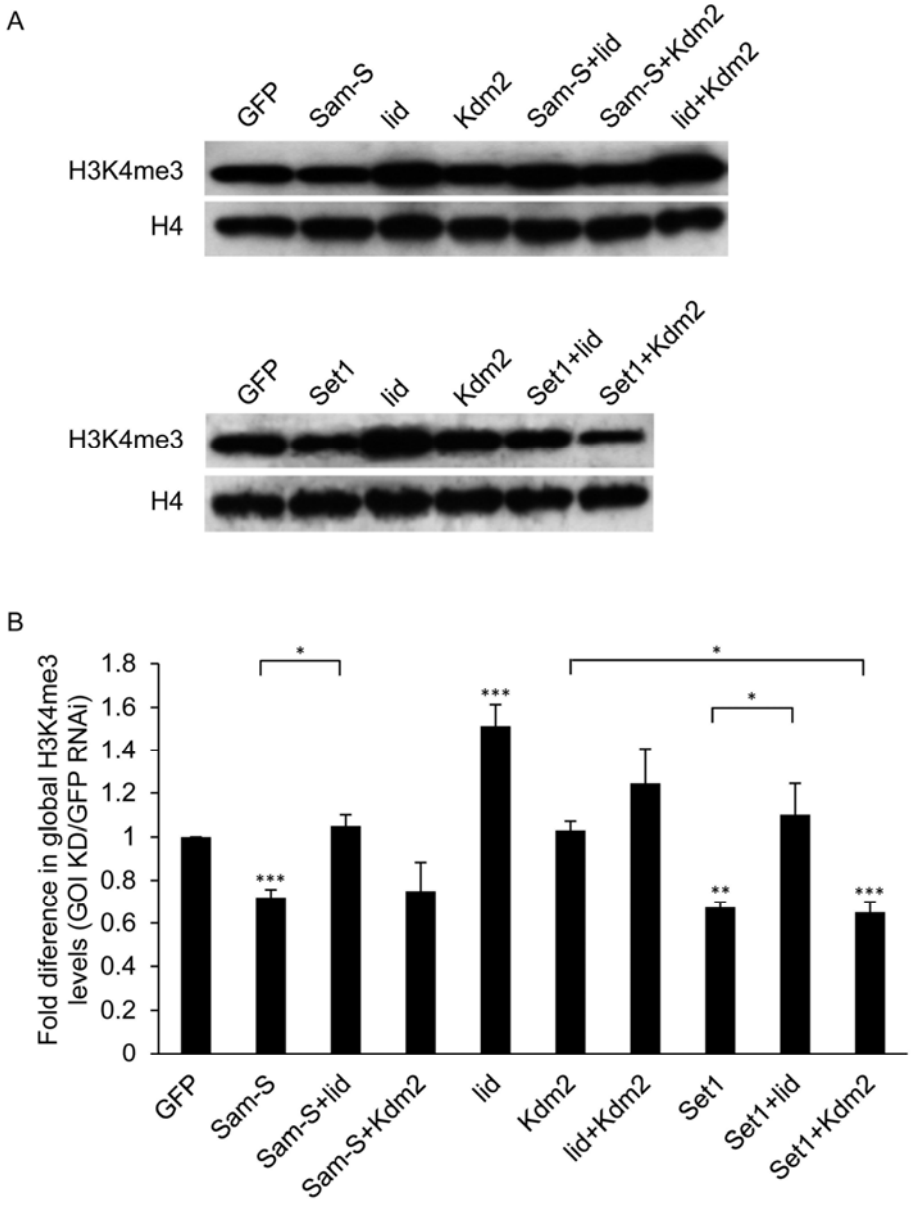

Fig. 2.11: Global H3K4me3 levels in S2 cells are regulated by the methionine metabolic enzyme SAM-S, histone demethylase LID and histone methyltransferase SET1. (A) Whole cell extracts from RNAi-treated cells were subjected to western blotting analysis for H3K4me3 or H4. (B) Western blots as shown in A were repeated with protein extracts prepared from at least three independent cultures and the results were quantified after normalization to histone H4. Error bars represent standard error of the mean. Statistically significant results comparing individual knockdown samples to the control are indicated on knockdown samples. P-values were also calculated between the double knockdown samples and each single knockdown sample for the two tested genes. Statistically significant results are indicated with the bars. (*) P <0.05, (**) P < 0.01, (***) P < 0.001. GFP, control cells treated with dsRNA against GFP. GOI KD, cells treated with dsRNA against the gene of interest.

DISCUSSION

In this study, we systematically analyzed two histone demethylases and the components of the methionine pathway including a single known histone methyltransferase in *Drosophila*. We investigated their role in the regulation of development, cell proliferation and histone methylation. We found that some enzymes involved in methionine metabolism and a demethylase affect viability and wing development in *Drosophila*. Further, all tested genes, except *Kdm2*, share similar roles in cell proliferation. Additionally, they cooperate to control histone methylation. Together, these data indicate the presence of a link between control of methionine metabolism and histone methylation to regulate multiple biological processes.

Reduction of SAM-S led to decreased global H3K4me3 and H3K9me2 in *Drosophila* S2 cells. H3K4me3 enrichment at a few tested genes was also affected by reduction of SAM-S, indicating the importance of SAM-S in regulation of gene specific histone methylation. Given that the level of methyl donor SAM is important for histone methylation (Brosnan and Brosnan, 2006), it is likely that SAM-S regulates histone methylation by controlling SAM levels. Additionally, SAM-S affects the amounts of metabolites in polyamine pathway (Larsson et al., 1996). Given that polyamine can bind to DNA and affect chromatin conformational status (Matthews, 1993), it is also possible that SAM-S affects histone methylation through general loss of polyamines. Interestingly, comparing our results with other published data (Li et al., 2011; Towbin et al., 2012), reduction of SAM-S did not affect all tested histone marks. SAM-S also does not influence the same histone mark in the same way among different species (Li et al., 2011; Towbin et al., 2012). Given the variety of the SAM binding affinity (K_m) between

histone methyltransferases (An et al., 2011; Chin et al., 2005; Horiuchi et al., 2013; Obianyo et al., 2008; Patnaik et al., 2004; Xiao et al., 2003), these differences are possibly due to variability of methyltransferase sensitivity to SAM levels (Katada et al., 2012). In this case, H3K4me3 and H3K9me2 specific methyltransferases are likely more sensitive to SAM levels compared to H3K4me2 specific methyltransferases. Alternatively, the levels of H3K4me2 methyltransferases, localized on chromatin at specific subdomains, may be different from the levels of H3K4me3 and H3K9me2 methyltransferases at those chromatin regions (Katada et al., 2012; Sassone-Corsi, 2013). We note that SAM-S showed the most significant role in histone methylation among all tested methionine metabolic genes. One possible explanation is that SAM-S directly controls SAM levels, while other key methionine metabolic genes likely indirectly influence SAM levels through affecting the concentration of intermediates in the pathway.

Of the three tested enzymes annotated to have methyltransferase activity, CG10903, CG9666 and MT2, whose histone methyltransferase activities are unknown, only CG9666 and MT2 affected histone methylation in S2 cells. This result suggests that these two enzymes may directly methylate histones. There is, however, another possibility. CG9666 has been predicted to be an N6-adenine DNA methyltransferase based on sequence and structural information on Flybase (http://flybase.org) (St Pierre et al., 2014). MT2 has possible CpG DNA methyltransferase activity (Tang et al., 2003). Links between CpG DNA methylation and histone methylation have been established in other organisms, including plants (Tariq and Paszkowski, 2004) and mammals (Rose and Klose, 2014). Histone methyltransferase enzymes may be targeted to particular

genes through recognition of methylated DNA. Thus, it is possible that CG9666 and MT2 regulate histone methylation via DNA methylation. The presence of CpG methylation in *Drosophila*, however, is the subject of current debate (Dunwell and Pfeifer, 2014). Low levels of this DNA modification have been detected by some methodologies (Capuano et al., 2014; Dunwell et al., 2013; Takayama et al., 2014) but not by others (Raddatz et al., 2013; Zemach et al., 2010). In addition, N6-methyladenine was recently detected in *Drosophila* (Zhang et al., 2015). The role of this DNA modification as an epigenetic mark, however, needs much further study (Heyn and Esteller, 2015). Determination of the substrates of these putative methyltransferases as well as the mechanisms through which they affect histone methylation will require further extensive biochemical analyses.

In our hands, LID, but not KDM2, removed H3K4me3. Interestingly, although the results were not statistically significant, the histone methylation levels in cells with double knockdown of *lid* and *Kdm2* were intermediate between the levels in *lid* single knockdown and *Kdm2* single knockdown cells. These observations suggest that decreased KDM2 may overcome the effect caused by reduction of LID. This assumption is consistent with the previously published (Gajan et al., 2016; Swaminathan et al., 2012) genetic studies from our laboratory, which showed that reduction of KDM2 or overexpression of LID can suppress the *Sin3A* knockdown curved wing phenotype in flies. One study, however, reported that *lid* or *Kdm2* mutants suppressed the $snr1^{E1}$ ectopic wing vein phenotype in *Drosophila*, although histone demethylase mutants *CG3654* and *CG8165* enhanced the $snr1^{E1}$ phenotype (Curtis et al., 2011). These data

indicate that LID and KDM2 can act in opposition in some specific cases, which is an interesting area for further investigation.

Reduction of all tested enzymes, but not KDM2, led to decreased cell number in wing imaginal discs and cultured cells. Alterations in a number of different pathways could lead to this observed decrease in cell proliferation. For some genes, the changes in histone methylation levels following RNAi knockdown could directly affect expression of important cell cycle associated genes. Additionally, it is possible that disruption of the methionine metabolic pathway influences global protein synthesis, which in turn impacts cell growth rate. This is a likely possibility for those enzymes that were not linked to changes in histone methylation. The decreased cell number could also be due to apoptosis, though we did not observe substantial numbers of dead cells upon RNAi knockdown in the S2 cell growth assay. Interestingly, for all genes affecting cell proliferation, with the exception of *Set1*, we noticed that the cell growth defects in the developing wing imaginal disc cells were much more pronounced compared to defects observed in cultured cells. It is possible that there is a stronger requirement for this pathway and these histone modifiers during development compared to cells proliferating in the culture dish. Alternatively, this difference could be the result of cell competition, which is based on the comparison of relative cell fitness between neighboring cells (Levayer and Moreno, 2013). The wild type cells grow faster than the RNAi knockdown cells, and thus the knockdown cells are eliminated during wing imaginal disc development.

RNAi knockdown of *Sam-S*, *Ahcy13* or *Cbs* resulted in lethality and cell proliferation defect in wing imaginal discs, but did not influence adult wing morphology.

There are several possible reasons to explain this difference between the observed phenotypes comparing whole animal development to wing specific development. The difference is possibly due to different RNAi efficiencies when distinct drivers are utilized. Another possibility is that methionine may be supplied non-cell autonomously to the RNAi knockdown wing disc cells, allowing development of a normal wing. Alternatively, these enzymes possibly play a more significant role in early stage embryogenesis relative to wing differentiation. Given that SAM-S regulated gene specific histone methylation and gene expression, it is possible that decreased histone methylation caused by *Sam-S* knockdown affects expression of genes which are critical for viability in embryogenesis, but not for differentiated wing development.

Reduction of CG10623 and MT2 affected cell proliferation in wing imaginal discs, but did not result in an abnormal wing. These contradictory results may be explained by cell competition, mentioned above (Levayer and Moreno, 2013). Due to the slower growth rate compared to wild type cells, *Mt2* or *CG10623* deficient cells may be eliminated during development, leading to normal wing morphology.

Among the six tested known or potential methyltransferases and demethylases, only *CG10903*, *Set1* and *lid* knockdown flies showed defects in both cell proliferation and development. In *Drosophila*, SET1 is the main H3K4 di- and tri-methyltransferase, while TRR and TRX are minor contributors for H3K4 methylation (Ardehali et al., 2011; Hallson et al., 2012; Mohan et al., 2011). Our results indicate that during embryonic and wing development, TRR and TRX are not able to functionally substitute for reduction of SET1. Among all tested genes, knockdown of *Set1* led to the smallest significant decrease in cell proliferation in S2 cells and wing imaginal discs. This finding raises the

possibility that SET1, TRR and TRX may be redundant in the regulation of cell proliferation in this specific cell type and wing developmental stage. Consistent with previous studies, we also demonstrate that LID is a major histone demethylase specific for H3K4me3 (Li et al., 2010). Therefore, SET1 and LID possibly influence cell proliferation and development via tight control of H3K4me3 levels, which in turn affects transcription of cell cycle associated genes and developmental genes. Whether TRR and TRX are able to counter the histone methylation effects due to reduction of LID, similar to the activity of SET1, is an area for future research. *CG10903* was found to have a significant role in cell proliferation and development. Expression of this gene, however, is quite low in S2 cells and during development (Graveley et al., 2011). While we do not have a definitive reason to explain how reduction of a gene with low RNA expression results in an observable phenotype, we note that other important developmental genes show the same pattern. For example, expression of *Pan* is low in S2 cells and during development (Graveley et al., 2011) and yet its reduction leads to heart development defects (Casad et al., 2012). Collectively, the results presented here indicate that methionine metabolism and histone methylation are critical for *Drosophila* development.

In conclusion, our findings demonstrate function and relationships of methionine metabolic enzymes and histone modifiers in regulating histone methylation. Our results reveal a role of these enzymes in influencing development and cell proliferation, which confirms the idea that metabolism and epigenetics can control key biological processes. Given that the changes of major metabolites and histone modifications are frequently observed in cancers (Katada et al., 2012), it is very important to understand the

interaction between nutrient pathways and epigenetics in regulation of biological processes. Because the metabolic pathways and histone modifying enzymes are conserved between flies and higher eukaryotes, *Drosophila* is a good model system to use to address these questions.

ACKNOWLEDGEMENTS

I wish to thank Valerie L. Barnes for performing all experiments in flies and verifying efficiency knockdown of targets in flies and cells, Sarah Gammouh and Archanna Radakrishnan for their assistance with scoring flies for the viability and wing phenotype experiments as well as Dr. Russell L. Finley, Jr. for providing the template DNA to make dsRNA against GFP.

CHAPTER 3 SIN3 DIRECTLY REGULATES METHIONINE METABOLIC GENE EXPRESSION TO AFFECT HISTONE METHYLATION

INTRODUCTION

Cellular function relies on the ability of the cell to sense and respond to the environment. Cellular response is mediated in part by epigenetic and metabolomic information (Kaelin and McKnight, 2013; Sassone-Corsi, 2013). Metabolic gene expression is under epigenetic control. Reduction of three histone modifiers, the H3K9 demethylase Jhdm2a, the H3K9/H3K56 deacetylase SIRT6 and the histone deacetylase HDAC1, leads to changes in metabolic gene transcription as well as metabolites in mouse and rat models (Gonneaud et al., 2015; Tateishi et al., 2009; Zhong et al., 2010). Because histone modifying enzymes utilize key metabolites, these metabolites could then feedback and impact epigenetic modifications. Indeed, several groups have demonstrated that histone methylation can be altered through changes in metabolism. For example, histone methylation is regulated by threonine metabolism in mouse embryonic stem cells (Shyh-Chang et al., 2013), by folate metabolism in yeast and human cells (Sadhu et al., 2013), and by methionine metabolism in yeast, fly, mouse and human cells (Liu et al., 2015; Mentch et al., 2015; Sadhu et al., 2013; Shiraki et al., 2014). Histone methylation and phosphorylation can also be modulated by changing glycolysis and serine metabolism in yeast (Li et al., 2015). While these studies collectively indicate that epigenetic control and metabolism are tightly connected, the mechanism for this cross-talk remains to be elucidated.

The SIN3 complex is one of the major histone modifying complexes present in cells. SIN3 is a conserved transcriptional scaffold protein, which interacts with the histone deacetylase (HDAC) RPD3 and other associated proteins (Grzenda et al., 2009;

Silverstein and Ekwall, 2005). In *Drosophila* and mammals, a histone demethylase is also part of a SIN3/RPD3 HDAC complex (Hayakawa and Nakayama, 2011). We previously reported a genetic interaction between *Drosophila Sin3A* and the genes encoding the histone demethylases KDM2 and dKDM5/LID (Gajan et al., 2016; Swaminathan et al., 2012). These biochemical and genetic data suggest that the SIN3 complex may regulate histone methylation in addition to histone acetylation. *Sin3A* is essential in *Drosophila* and mammals (Cowley et al., 2005; Dannenberg et al., 2005; David et al., 2008; Neufeld et al., 1998; Pennetta and Pauli, 1998). Deficiency of SIN3 leads to changes in expression of many genes involved in multiple biological processes, including cellular metabolism (Dannenberg et al., 2005; Gajan et al., 2016; Pile et al., 2003). SIN3 regulates genes involved in several metabolic pathways such as glycolysis, gluconeogenesis and the citric acid cycle and additionally, is associated with regulation of genes encoding proteins that process reactive oxygen species (ROS) and glutathione (Barnes et al., 2014; Barnes et al., 2010; Dannenberg et al., 2005; Gajan et al., 2016; Pile et al., 2003). The mechanism of how SIN3 regulates cellular metabolism, however, is not fully understood.

Methionine, an essential amino acid, is converted to the major methyl donor *S*-adenosylmethionine (SAM) by SAM synthetase (SAM-S) (Fig. 2.1). SAM is then converted to *S*-adenosylhomocysteine (SAH) and methylated substrates by methyltransferases. SAH is next hydrolyzed by adenosylhomocysteinase (AHCY) to homocysteine, which is in turn either converted to methionine through methionine synthase (MS) or to cystathionine by cystathionine-β-synthase (CBS). To date, according to Flybase (http://flybase.org) (St Pierre et al., 2014), *Sam-S* and *Cbs* are the

only known *Drosophila* genes encoding SAM synthetase (Larsson and Rasmuson-Lestander, 1994) and cystathionine-β-synthase, respectively. *Ahcy13* is the major adenosylhomocysteinase gene (Caggese et al., 1997). *CG10623* encodes a putative methionine synthase. The metabolites involved in methionine metabolism are critical for multiple pathways and biological processes (Locasale, 2013). For example, reduced methionine leads to decreased H3K4me3 in yeast and mammalian cells at least in part by modulating SAM levels (Mentch et al., 2015; Sadhu et al., 2013; Shiraki et al., 2014). Given that SIN3 may regulate histone methylation due to its biochemical or genetic association with the histone demethylases dKDM5/LID and KDM2 (Gajan et al., 2016; Moshkin et al., 2009; Spain et al., 2010; Swaminathan et al., 2012), we wanted to examine further the relationship between SIN3 and methionine metabolism in *Drosophila*.

In this work, we focused on the mechanism through which SIN3 regulates cellular metabolism. We provided evidence that SIN3 binds to the promoters of methionine metabolic genes and affects H3K4me3 and H3K9ac levels at the promoter regions of these genes to control their expression. We observed increased levels of SAM and global H3K4me3 when SIN3 was reduced. Collectively, these results reveal that SIN3 regulates the expression of methionine metabolic genes through controlling histone modification levels at the promoters of these genes, which in turn regulates cellular SAM concentration and global H3K4me3.

MATERIALS AND METHODS

Cell culture

The protocols for cell culture is previously described (Liu et al., 2015).

dsRNA production

The protocols for generation of constructs containing targeting sequences in pCRII-Topo vector and production of dsRNA are previously described (Liu et al., 2015; Pile et al., 2002).

RNA interference (RNAi)

The RNAi procedure is previously described (Liu et al., 2015; Pile et al., 2002). Western blotting analysis and reverse transcription PCR (RT-PCR) assays were routinely carried out for both single- and double-RNAi-treated cells to verify efficient knockdown of *Sin3A* and methionine metabolic genes, respectively.

Reverse transcription PCR assay (RT-PCR) and real-time quantitative RT-PCR assay (qRT-PCR)

The protocols for RNA extraction, cDNA preparation and qRT-PCR are previously described (Liu et al., 2015). *TBP-associated factor 1* (*Taf1*), using the following primer set 5’ to 3’ (forward primer) GTG GAG GAG CCA AGG GAG CC and (reverse primer) TCC CGC TCC TTG TGC GAA TG, was a loading control in RT-PCR. Primers used for other tested genes in the RT-PCR experiment are previously described (Liu et al., 2015). In qRT-PCR analysis, *Taf1* was used as a normalizer. All primers used in the qRT-PCR experiment are previously described (Liu et al., 2015). The gene expression changes are represented as the mean (± standard error of then mean (SEM)) of the fold changes observed in *Sin3A* knockdown cells compared to GFP RNAi control cells. qRT-PCR experiment utilized RNA isolated from three biological replicates for each cell type.

Metabolomics

Five biological replicates of RNAi-treated *Drosophila* S2 cells were harvested, flash frozen and sent to Metabolon Inc. (http://www.metabolon.com). Sample preparation and metabolomic analysis were conducted at Metabolon Inc. as previously described (Shin et al., 2014). The extracted samples were split into equal parts for analysis with ultra-performance liquid chromatography tandem mass-spectrometry (UPLC-MS/MS) and gas chromatography–mass spectrometry (GC/MS). The raw data are normalized to total protein concentration based on a Bradford assay. Statistically significant differences were determined using one-way ANOVA with post-hoc contrasts (*t*-tests).

Western blotting analysis

The western blotting analysis protocol is previously described (Liu et al., 2015; Pile et al., 2002). Primary antibodies included: SIN3 (1:2000; (Pile and Wassarman, 2000)), alpha-tubulin (1:1000, Cell signaling), H3K4me2 (1:5000; Millipore), H3K4me3 (1:2500; Active Motif), H3K9me2 (1:500; Millipore) and H4 (1:15,000; Abcam). Donkey anti-rabbit HRP-conjugated IgG (1:3000; GE Healthcare) was used as the secondary antibody. The antibody signals were detected using the clarity western ECL substrate (Bio-Rad) for H3K4me2 and H3K4me3 or ECL prime western blotting detection system (GE Healthcare) for SIN3, alpha-tubulin, H3K9me2 and H4. A minimum of three biological replicates was performed.

Chromatin immunoprecipitation and real-time quantitative PCR (ChIP-qPCR)

ChIP-qPCR procedure and antibodies are previously described (Liu et al., 2015). Primers used for qPCR are listed in Table 3.1. Three biological replicates were performed.

Table 3.1: Primers used for ChIP-qPCR analysis

Gene	Primer orientation	Primer sequence (oriented 5' to 3')
Sam-S	Forward	CCA CAC CTC CAC CGT CTA CT
	Reverse	CCT CTG TTC AAG TCG TGC AA
Ahcy13	Forward	CGA AGC CCA GCT ACA AAG TC
	Reverse	AAT AGA TGC AAT TCA CCC GC
CG10623	Forward	CGG AAA ACG TAC AGC AGT GA
	Reverse	GCA TTT GAC CAG AAT TGG CT
Cbs	Forward	CCC TTC CTG TTT CCA TCT GA
	Reverse	TGC GAA ATT GCG TGA GAT TA

Statistical analyses

All significance values, except metabolomics experiment, were calculated by the unpaired two sample Student‘s *t*-test from GraphPad Software.

RESULTS

SIN3 regulates expression of methionine metabolic genes and histone modifications at the promoters of these genes

Since SIN3 is a global transcriptional regulator (Grzenda et al., 2009; Silverstein and Ekwall, 2005) and affects the expression of genes involved in several metabolic pathways such as glycolysis, gluconeogenesis and the citric acid cycle (Barnes et al., 2010; Dannenberg et al., 2005; Gajan et al., 2016; Pile et al., 2003), we sought to determine if SIN3 regulates the transcription of methionine metabolic genes. Analysis of our recently published RNA-seq gene expression profiles of S2 and RNAi-mediated *Sin3A* knockdown cells (Gajan et al., 2016) indicates that reduction of SIN3 alters the expression of *Sam-S*, *Ahcy13*, *Cbs* and *CG10623* (Fig. 3.1A). To verify the RNA-seq data, we repeated the *Sin3A* knockdown experiment and analyzed mRNA levels by real-time qRT-PCR. The knockdown of *Sin3A* was validated by western blotting analysis (Fig. 3.1B). Consistent with the RNA-seq data, transcription of these genes was

significantly changed when SIN3 was reduced (Fig. 3.1C). These results demonstrate that SIN3 regulates the expression of methionine metabolic genes.

A

Gene	Relative expression (*Sin3A* KD / GFP RNAi)	P-value
Sam-S	2.02	0.00005
Ahcy13	1.44	0.00195
CG10623	2.14	0.00005
Cbs	0.55	0.00005

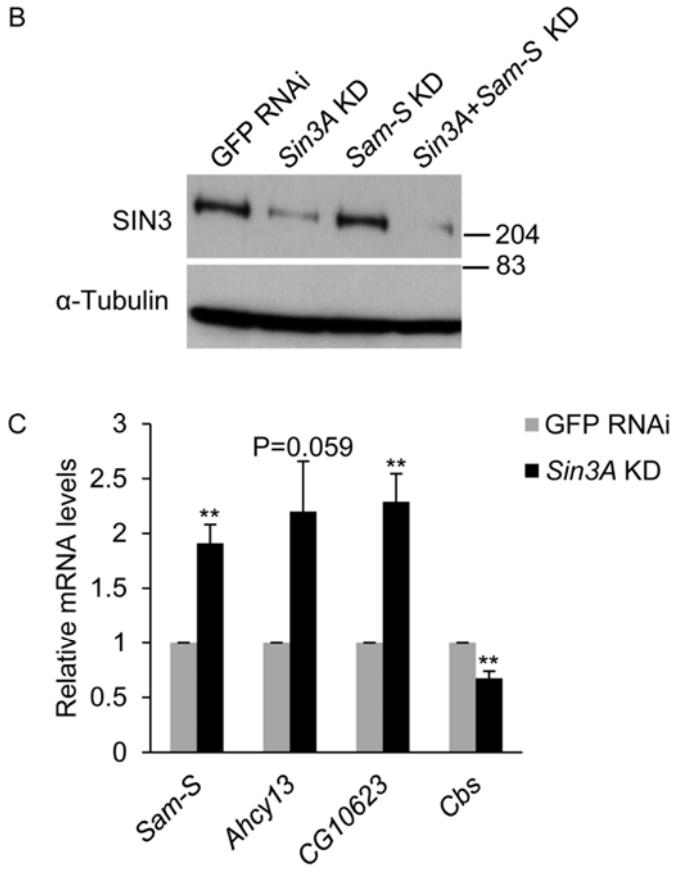

Fig. 3.1: Transcription of methionine metabolic genes is regulated by SIN3. (A) Expression of methionine metabolic genes as determined in an RNA-seq profile (Gajan et al., 2016). (B) Verification of *Sin3A* knockdown. Whole cell extracts from RNAi-treated cells were subjected to western blotting analysis using indicated antibodies. α-Tubulin acted as the loading control. Protein size markers are indicated on the right. (C) Real-time qRT-PCR analysis of transcription of methionine metabolic genes. The results are the average of three independent biological replicates. Error bars represent standard error of the mean. Statistically significant results comparing individual knockdown samples to the control are indicated on knockdown samples. (**) $P < 0.01$. GFP RNAi cells are the control cells. KD, knockdown.

Next, we wanted to investigate how SIN3 affects the expression of these genes. Investigation of our recent ChIP-seq analysis (Saha et al., 2016), indicates that SIN3 binds to the promoters of *Sam-S*, *Ahcy13*, *Cbs* and *CG10623* (Fig. 3.2A). Additionally, changing the level of SIN3 alters global and gene specific histone acetylation, especially the H3K9ac mark (Gajan et al., 2016; Spain et al., 2010). Proteomic studies indicate that SIN3 co-purifies with the H3K4me3 specific histone demethylase dKDM5/LID (Moshkin et al., 2009; Spain et al., 2010), suggesting that the SIN3 complex may affect histone methylation. Based on these previous findings, we hypothesized that SIN3 directly controls H3K9ac and H3K4me3 levels at the promoters of methionine metabolic genes to regulate their expression. To test this hypothesis, we performed ChIP-qPCR analysis. IgG was used as a non-specific control. Histone modification levels were normalized to histone H3 signal. Compared to IgG, strong enrichment of signals for tested histone antibodies was observed at all promoter regions sampled (Fig. 3.2B). Knockdown of *Sin3A* led to an increase of H3K9ac and H3K4me3 at *Sam-S, Ahcy13* and *CG10623*, whereas little to no change in H3K9ac was observed at *Cbs* (Fig. 3.2C). Consistent with published ChIP-seq analysis of H3K4me3 in S2 cells (Gan et al., 2010), we did not detect H3K4me3 at the promoter of *Cbs* in either the control or *Sin3A* knockdown condition (Fig. 3.2B). Given that H3K9ac and H3K4me3 are associated with active genes (Black et al., 2012; Black and Whetstine, 2011), their levels at the tested genes are consistent with our gene expression data (Fig. 3.1A, 3.1C and 3.2C). Together these findings suggest that SIN3 controls histone modifications at methionine metabolic genes to regulate their transcription.

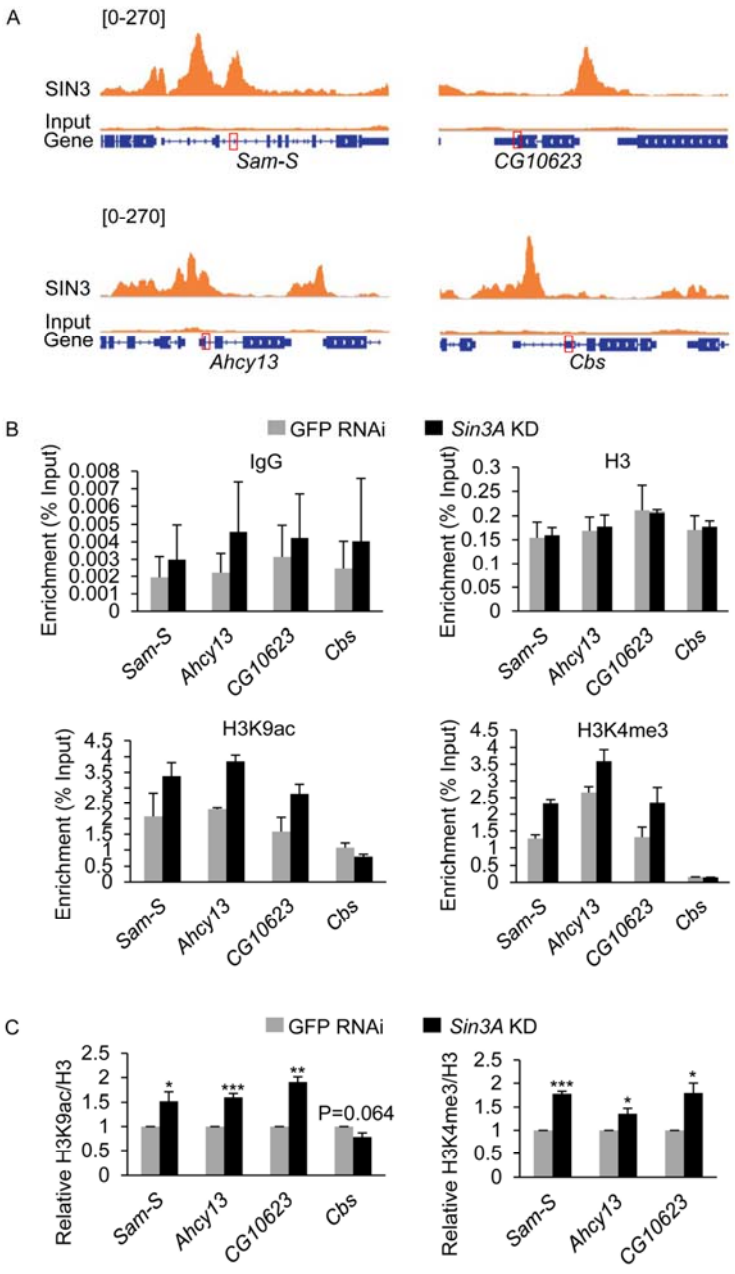

Fig. 3.2: H3K9ac and H3K4me3 levels at the promoters of methionine metabolic genes are regulated by SIN3. (A) SIN3 ChIP-seq signals at methionine metabolic genes. Red boxes label the regions sampled by ChIP-qPCR. (B) ChIP-qPCR analysis. The results are the average of two independent biological replicates. (C) Reduction of SIN3 leads to increased H3K9ac and H3K4me3 levels at the promoters of methionine metabolic genes. The results are the average of three independent biological replicates. Error bars represent standard error of the mean. Statistically significant results comparing individual knockdown samples to the control are indicated on knockdown samples. GFP RNAi cells are the control cells. (*) P <0.05, (**) P < 0.01, (***) P < 0.001. KD, knockdown.

SIN3 impacts the levels of SAM and global H3K4me3

The finding that the expression of methionine metabolic genes is regulated by SIN3 led us to examine if the levels of metabolites involved in methionine metabolism are also affected by SIN3. Through inspection of the methionine pathway, we noted that homocysteine has two major fates (Fig. 2.1). Since expression of *Sam-S*, *Ahcy13* and *CG10623* was up-regulated, while expression of *Cbs* was down-regulated in *Sin3A* knockdown cells compared to control cells (Fig. 3.1A and 3.1C), we hypothesized that homocysteine would be remethylated to methionine to generate SAM rather than be converted to cystathionine when SIN3 is reduced. If this hypothesis is correct, then more SAM should be observed in *Sin3A* knockdown cells relative to the control. To test our hypothesis, we used liquid chromatography-tandem mass spectroscopy and gas chromatography mass spectroscopy to generate a quantitative metabolomic profile. We found that SAM levels were significantly up-regulated in *Sin3A* knockdown cells compared to control cells, while other metabolites in the pathway showed little change (Fig. 3.3A). These results indicate that reduced SIN3 alters the expression of methionine metabolic genes to increase the amount of major methyl donor SAM.

A change in the cellular concentration of SAM has been demonstrated to result in altered histone methylation (Mentch et al., 2015; Sadhu et al., 2013; Shiraki et al., 2014). To examine if SIN3 affects global histone methylation, whole cell protein extracts from dsRNA-treated S2 cells were probed with antibodies specific for distinct histone methylation marks, as well as histone H4 as a loading control. Because SIN3 regulates gene specific H3K4me3 levels (Fig. 3.2C), we first tested this mark. Knockdown of *Sin3A* resulted in a small, but reproducible, increase in global H3K4me3 levels (Fig.

3.3B and 3.3C). H3K4me3 is more sensitive to cellular SAM concentration relative to other histone methylation marks (Mentch et al., 2015). We thus hypothesized that the effect of SIN3 on H3K4me3 would be greater as compared to other methylation marks. To test our hypothesis, we examined H3K4me2 and H3K9me2. We did not observe any significant changes in global H3K4me2 and H3K9me2 levels when SIN3 was reduced (Fig. 3.3B and 3.3C). Collectively, these data suggest that reduction of SIN3 leads to an increase in global H3K4me3 through increasing SAM levels.

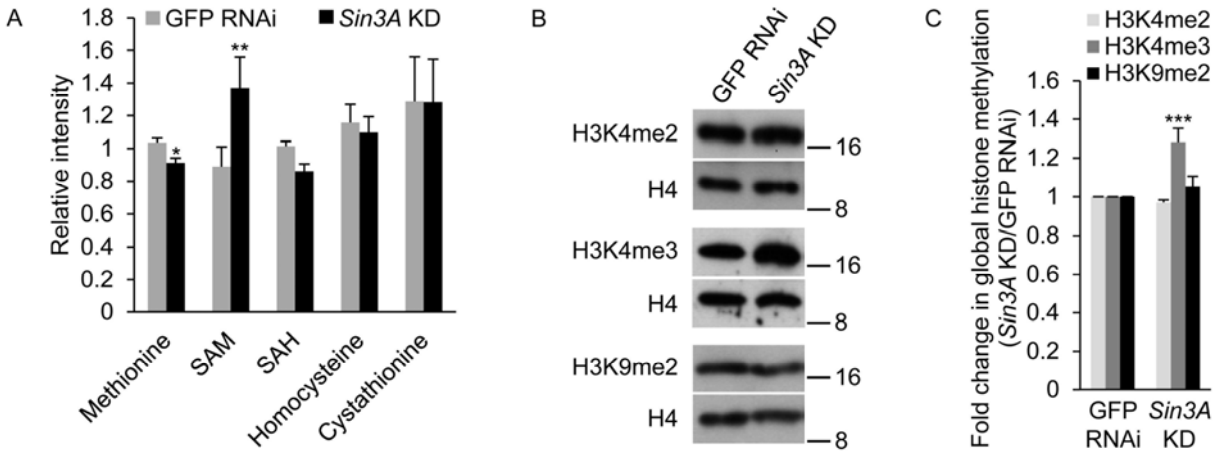

Fig. 3.3: Levels of SAM and global H3K4me3 are regulated by SIN3. (A) Effects of SIN3 on the cellular concentration of the metabolites involved in methionine metabolism. (B) Whole cell extracts from GFP RNAi control and *Sin3A* knockdown S2 cells were subjected to western blotting analysis using indicated antibodies. Protein size markers are indicated on the right. (C) Western blots as shown in (B) were repeated with protein extracts prepared from at least three independent cultures and the results were quantified after normalization to histone H4. Error bars represent standard error of the mean. Statistically significant results comparing individual knockdown samples to the control are indicated on knockdown samples. (*) P <0.05, (**) P < 0.01, (***) P < 0.001. KD, knockdown.

To further confirm the role of SIN3 in regulation of global H3K4me3, we chose two other genes, *Sam-S* and *Set1*, for this study. *Set1* is the main H3K4 di/tri methyltransferase in *Drosophila* (Ardehali et al., 2011; Hallson et al., 2012; Mohan et al., 2011). We used RNAi to knock down targets and efficiency was verified by Western

blotting and RT-PCR analysis (Fig. 3.1B, 3.4A and 3.4B). Consistent with published work (Ardehali et al., 2011; Hallson et al., 2012; Liu et al., 2015; Mohan et al., 2011), reduction of SAM-S or SET1 led to reduced global H3K4me3 levels in S2 cells (Fig. 3.4C and 3.4D). Interestingly, this decrease caused by reduced SAM-S or SET1 was restored to near control levels upon *Sin3A* knockdown (Fig. 3.4C and 3.4D), validating the findings that SIN3 affects global H3K4me3. *Set1* expression is not affected when SIN3 is reduced (Gajan et al., 2016), suggesting that the role of SIN3 in regulating H3K4me3 is not through the control of expression of the SET1 enzyme. Moreover, these data indicate that SIN3 is critical for the global H3K4me3 response to SAM limitation.

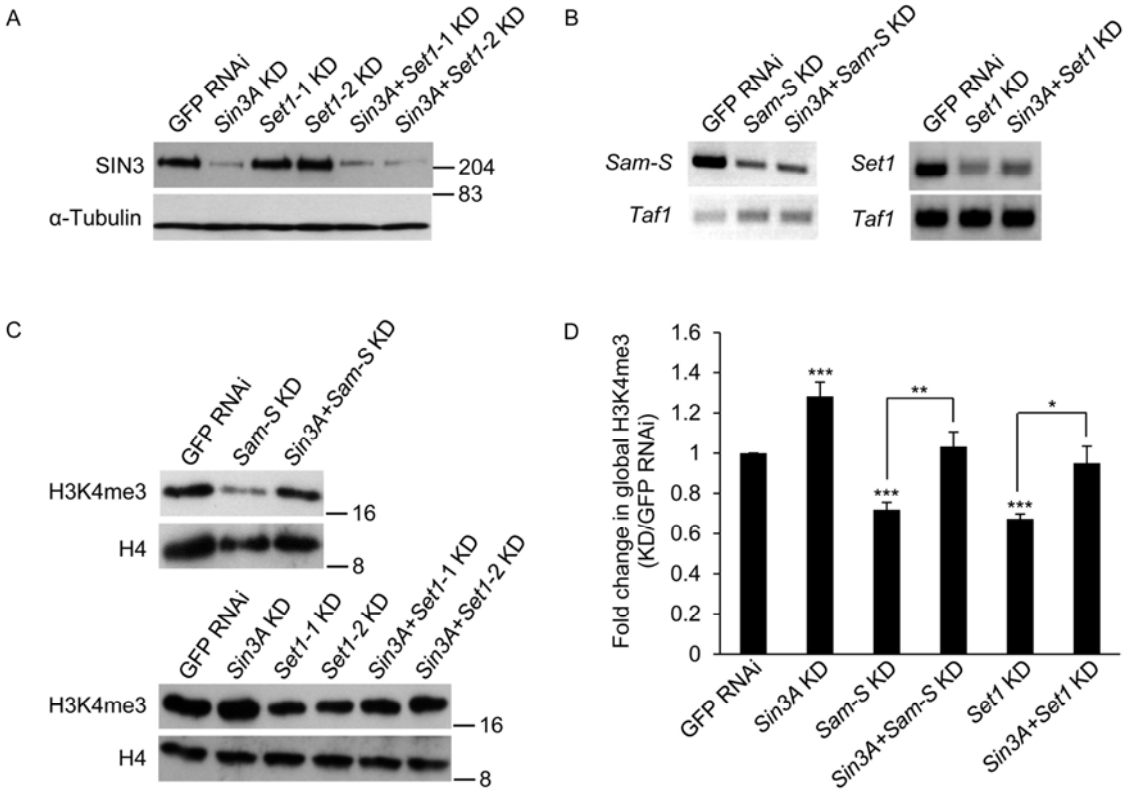

Fig. 3.4: Decreased global H3K4me3 levels caused by reduction of SAM-S or SET1 is restored to near control levels upon *Sin3A* knockdown. (A) Verification of *Sin3A* knockdown. Whole cell extracts from RNAi-treated cells were subjected to western blotting analysis using indicated antibodies. α-Tubulin acted as the loading control. Protein size markers are indicated on the right. (B) RT-PCR analysis of *Sam-S* and *Set1* transcript level. *Taf1* was used as a loading control. (C) Whole cell extracts from RNAi-treated cells were subjected to western blotting analysis using indicated antibodies. Protein size markers are indicated on the right. (D) Western blots as shown in (C) were repeated with protein extracts prepared from at least three independent cultures and the results were quantified after normalization to histone H4. *Set1*-1 KD and *Set1*-2 KD used two different dsRNA targeting different regions of *Set1* mRNA, but these regions overlap. Therefore, we used *Set1*-1 oligos for the rest of the study and referred it as *Set1* KD. Error bars represent standard error of the mean. Statistically significant results comparing individual knockdown samples to the control are indicated on knockdown samples. *P*-values were also calculated between the double knockdown samples and each single knockdown sample for the two tested genes, e.g. *Sin3A*+*Sam-S* KD to *Sin3A* KD or *Sin3A*+*Sam-S* KD to *Sam-S* KD. Statistically significant results are indicated with the bars. (*) P <0.05, (**) P < 0.01, (***) P < 0.001. GFP RNAi cells are the control cells. KD, knockdown.

DISCUSSION

In this study, we provide mechanistic insight into the relationship between an epigenetic regulator and metabolism. We first confirmed that SIN3 affects the expression of methionine metabolic genes. Next, we found that SIN3 influences histone acetylation and methylation at the promoters of these genes. Importantly, we observed that SIN3 regulates the levels of SAM and global histone methylation. Given that SIN3 is localized to methionine metabolic genes, these findings indicate that SIN3 directly regulates histone modifications at methionine metabolic genes to modulate their expression, which in turn impacts cellular SAM and global H3K4me3 levels. To our knowledge, this is the first demonstration of a regulatory role of SIN3 on methionine metabolism, and consequently on global H3K4me3.

It has been reported that changes in the amount of histone modifier enzymes affect metabolism (Gonneaud et al., 2015; Tateishi et al., 2009; Zhong et al., 2010). In this report, we demonstrate that altering SIN3, the scaffold protein for assembly of one of the two major cellular histone deacetylase complexes, affects the expression of metabolic genes to impact metabolism. The data support a model in which changing a scaffold protein will alter the assembly and/or recruitment of the functional histone modifying complex, which then impacts gene expression. SIN3 and methionine metabolism are conserved from yeast to mammals. The data of this report using the *Drosophila* model system are consistent with the reports on histone modifiers regulating metabolism in yeast and mammals, which strongly suggests that this process is evolutionarily conserved across different species.

Our work indicates that SIN3 impacts both global and gene specific H3K4me3. These results are consistent with the previous finding that reduction of both mammalian SIN3A and SIN3B leads to increased H3K4me3 at a specific group of genes in differentiated C2C12 myotubes (van Oevelen et al., 2008). Given that H3K4me3 is associated with active genes (Black et al., 2012; Black and Whetstine, 2011), the regulatory role of SIN3 on histone methylation may contribute to the mechanism of how SIN3 affects transcription, which in turn regulates biological processes. Previous studies have found that methionine metabolism is sufficient to determine histone methylation at least in part by modulating SAM levels (Mentch et al., 2015; Sadhu et al., 2013; Shiraki et al., 2014). Our data indicate that SIN3 impacts H3K4me3 through affecting the expression of the genes encoding enzymes in this pathway, which ultimately controls the levels of key metabolites. Given that the H3K4me3 specific demethylase dKDM5/LID interacts with SIN3 (Moshkin et al., 2009; Spain et al., 2010), it is possible that dKDM5/LID also contributes to the effect of SIN3 on H3K4me3, which is an interesting area for further research.

ACKNOWLEDGEMENTS

I wish to thank Dr. Russell L. Finley, Jr. for providing the template DNA to make dsRNA against GFP.

CHAPTER 4 IDENTIFICATION OF METABOLIC PATHWAYS AFFECTED BY SIN3

INTRODUCTION

The SIN3 complex is one of the major histone modifying complexes present in cells. SIN3 is a conserved transcriptional scaffold protein associated with the histone deacetylase RPD3 (Grzenda et al., 2009; Silverstein and Ekwall, 2005). *Sin3A*, as an essential gene in *Drosophila* and mammals, plays an important role in regulating transcription, cell proliferation and development (Barnes et al., 2014; Cowley et al., 2005; Dannenberg et al., 2005; David et al., 2008; Gajan et al., 2016; Neufeld et al., 1998; Pennetta and Pauli, 1998; Pile et al., 2002; Pile et al., 2003; Sharma et al., 2008; Swaminathan and Pile, 2010; van Oevelen et al., 2008). Consistent with the functions of SIN3, genome-wide transcriptome analyses reveal that genes involved in stress response, cell cycle, development and metabolism are regulated by SIN3 (Gajan et al., 2016; Pile et al., 2003). In Chapter 3, we demonstrate that reduction of SIN3 affects the expression of methionine metabolic genes. In fact, SIN3-regulated metabolic genes also include genes involved in glycolysis, gluconeogenesis, the citric acid cycle as well as fatty acid, glutathione and pyrimidine metabolism (Barnes et al., 2014; Gajan et al., 2016; Pile et al., 2003). Although these studies indicate the presence of a connection between SIN3 and metabolism, a systematical metabolome analysis for SIN3 has not been performed.

Our work described in Chapter 3 demonstrates that *Sin3A* genetically interacts with *S*-adenosylmethionine synthetase (*Sam-S*). Furthermore, we provide evidence that decreased H3K4me3 caused by reduced SAM-S is restored to near control levels upon *Sin3A* knockdown. These data indicate that there is an interaction between SIN3 and

SAM-S in regulation of histone methylation. The relationship between SIN3 and SAM-S in affecting gene expression and metabolism, however, remains unknown.

In *Drosophila*, there is only one known *Sam-S* gene and it is essential (Larsson and Rasmuson-Lestander, 1998; Liu et al., 2015). Three types of mammalian SAM-S, named MATI, MATII and MATIII, are encoded by three methionine adenosyltransferase genes *MAT1A*, *MAT2A* and *MAT2B* (Kotb et al., 1997). Liver-expressed *MAT1A* encodes a catalytic subunit α1 that can form either a homotetramer that is called MATI or a homodimer called MATIII. *MAT2A* is ubiquitously expressed and encodes another catalytic subunit, α2. α2 binds to a regulatory subunit β, which is encoded by *MAT2B,* to form an active complex called MATII (Kotb et al., 1997). Although it is a metabolic enzyme, yeast and mammalian SAM-S has been demonstrated to be present in nuclei and to localize to chromatin (Katoh et al., 2011; Li et al., 2015; Reytor et al., 2009). Furthermore, SAM-S has been demonstrated to affect transcription. Genes involved in cell proliferation, cell differentiation, signaling pathways and the immune response were misregulated when MAT1A was depleted in mice (Lu et al., 2001). In yeast, SAM-S was recently demonstrated to associate with other metabolic enzymes to form the SESAME complex, which regulates gene expression through affecting histone modification by sensing glycolysis and glucose-derived serine metabolism (Li et al., 2015).

In this work, to determine the physiologic outcome of the *Sin3A* and *Sam-S* gene regulatory network, we performed a genome-wide transcriptome analysis and generated a metabolomic profile in cells with altered SIN3 and SAM-S levels. We performed the RNA-seq analysis in *Sam-S* knockdown and *Sin3A*+*Sam-S* knockdown *Drosophila* cultured S2 cells, as well as mass spectroscopy in *Sin3A* knockdown, *Sam-S*

knockdown and *Sin3A+Sam-S* knockdown cells. Additionally, to explore how the interaction between SIN3 and SAM-S in regulation of histone methylation links to cellular metabolism, we carried out Pearson correlation analysis. We found that glycolysis is a major pathway correlated with global H3K4me3 levels regulated by reduction of SIN3 and/or SAM-S.

MATERIALS AND METHODS

Cell culture

The protocols for cell culture is previously described (Liu et al., 2015).

dsRNA production

The protocols for generation of constructs containing targeting sequences in pCRII-Topo vector and production of dsRNA are previously described (Liu et al., 2015; Pile et al., 2002).

RNA interference (RNAi)

The RNAi procedure is previously described (Liu et al., 2015; Pile et al., 2002). Western blotting and reverse transcription PCR (RT-PCR) analyses were routinely carried out for both single- and double-RNAi-treated cells to verify efficient knockdown of *Sin3A* and *Sam-S*, respectively.

Western blotting analysis

The western blotting analysis protocol is previously described (Liu et al., 2015; Pile et al., 2002). Primary antibodies included SIN3 (1:2000, (Pile and Wassarman, 2000)) and α-Tubulin (1:1000, Cell signaling). Donkey anti-rabbit HRP-conjugated IgG (1:3000, GE Healthcare) was used as the secondary antibody. The antibody signals were detected using the ECL prime western blotting detection system (GE Healthcare).

Reverse transcription PCR assay (RT-PCR) and real-time quantitative RT-PCR assay (qRT-PCR)

The protocol for RNA extraction and cDNA preparation is described in (Liu et al., 2015). For RT-PCR, *TBP-associated factor 1* (*Taf1*), using the following primer set 5' to 3' (forward primer) GTG GAG GAG CCA AGG GAG CC and (reverse primer) TCC CGC TCC TTG TGC GAA TG, was a loading control. The qRT-PCR procedure and the primers used in qRT-PCR are described previously (Liu et al., 2015). *Taf1* was used to normalize RNA levels. The gene expression changes are represented as the mean (± standard error of the mean (SEM)) of the fold changes observed in knockdown samples compared to GFP RNAi control cells. qRT-PCR results are the average for three biological replicates.

Gene expression analysis by RNA-seq

Three biological replicates of RNAi-treated *Drosophila* S2 cells were harvested, frozen and sent to the Applied Genomics Technology Center, Wayne State University. The RNA-seq experiment and bioinformatic analysis were performed as previously described (Gajan et al., 2016). The significantly differentially expressed genes are listed in Supplementary Data 1. Gene ontology (GO) and KEGG pathway analyses were performed using DAVID (Huang da et al., 2009). We pooled related gene ontology categories with *P*-value <0.05 into a single broader category as previously described (Saha et al., 2016). Detailed information regarding GO and KEGG pathway analyses is shown in Supplementary Data 2.

Metabolomics

Five biological replicates of RNAi-treated *Drosophila* S2 cells were harvested, flash frozen and sent to Metabolon Inc. (http://www.metabolon.com). Sample preparation and metabolomic analysis were conducted at Metabolon Inc. as previously described (Shin et al., 2014). The extracted samples were split into equal parts for analysis with ultra-performance liquid chromatography tandem mass-spectrometry (UPLC-MS/MS) and gas chromatography–mass spectrometry (GC/MS). The raw data are normalized to total protein concentration based on a Bradford assay. Statistical significant differences were determined using one-way ANOVA with post-hoc contrasts (*t*-tests). The partial least squares discriminant analysis (PLS-DA) was performed using the Excel add-in Multibase package (Numerical Dynamics, Japan), which is based on a classical PLS regression. The metabolomic profile is provided as Supplementary Data 3.

Correlation analysis

The Pearson correlation analysis was performed in ArrayStudio (OmicSoft) using data for global H3K4me3 levels, which were used as a 'bin' for each sample in the group to correlate H3K4me3 levels with detected biochemicals.

Chromatin immunoprecipitation and real-time quantitative PCR (ChIP-qPCR)

The ChIP-qPCR procedure is previously described (Liu et al., 2015). For immunoprecipitation, IgG acted as a non-specific control and histone H3 was used to normalize histone modification levels. 2.5 µl IgG, 3 µl H3K9ac (Millipore), 3 µl H3K4me3 (Active Motif) or 4 µl H3 C-terminus (Abcam) antibody was used. Primers used for qPCR are listed in Table 4.1. Three biological replicates were performed. All significance values were calculated by the unpaired two sample Student's *t* test from

GraphPad Software (http://www.graphpad.com/quickcalcs/ttest1/).

Table 4.1: Primers used for ChIP-qPCR analysis

Gene	Primer orientation	Primer sequence (oriented 5' to 3')
Gapdh-1	Forward	GGA AAA GGA AAA AGC GGC
	Reverse	GCG GCC AAA TCC GTT AAT
Pfk	Forward	CAG AAT CCT CAG ATT TTC GAC C
	Reverse	GGC TAA ATC CGC CCA AGA
Pyk	Forward	GCG CGC CAC AAG TAA AAT
	Reverse	GCT GCA TTA TTT CCG ATG G

RESULTS

RNA-seq analysis identifies common and distinct genes regulated by SIN3 and SAM-S

In Chapter 3, we show that the decrease in the global H3K4me3 level caused by reduction of SAM-S is returned to near control level upon *Sin3A* knockdown (Fig. 3.4C and 3.4D), which indicates that SIN3 and SAM-S act in opposition with regard to regulation of global histone methylation. To determine the possible underlying transcriptional network regulated by SIN3 and SAM-S, we performed an RNA-seq experiment to identify genome-wide changes in gene expression upon RNA interference (RNAi) mediated reduction of SIN3 or SAM-S or both in *Drosophila* S2 cells. S2 cells treated with dsRNA targeting GFP acted as the control. Knockdown of *Sin3A* and *Sam-S* was verified by western blotting analysis and RT-qPCR, respectively (Fig. 3.1B, 3.4B and 4.1). Three biological replicates were prepared for the RNA-seq study. The reproducibility of the data was confirmed by performing a Pearson's correlation analysis (Fig. 4.2). The RNA-seq data obtained from *Sin3A* knockdown S2 cells have been recently published (Gajan et al., 2016).

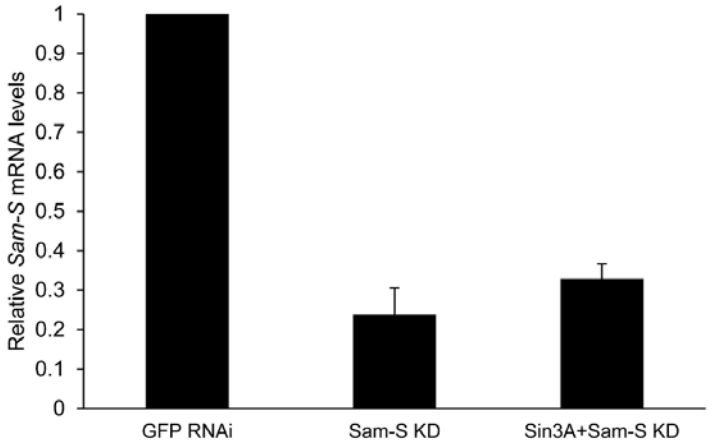

Fig. 4.1: Real time qPCR analysis verifies knockdown of *Sam-S* for RNA-seq samples. Real time qRT-PCR analysis of total RNA extracts from RNAi-treated S2 cells. All experimental samples were compared to GFP dsRNA treated control. *Taf1* was used to normalize expression levels. The results are the average of three biological replicates. Error bars represent standard error of the mean. (*) P <0.05, (**) P < 0.01, (***) P < 0.001. KD, knockdown.

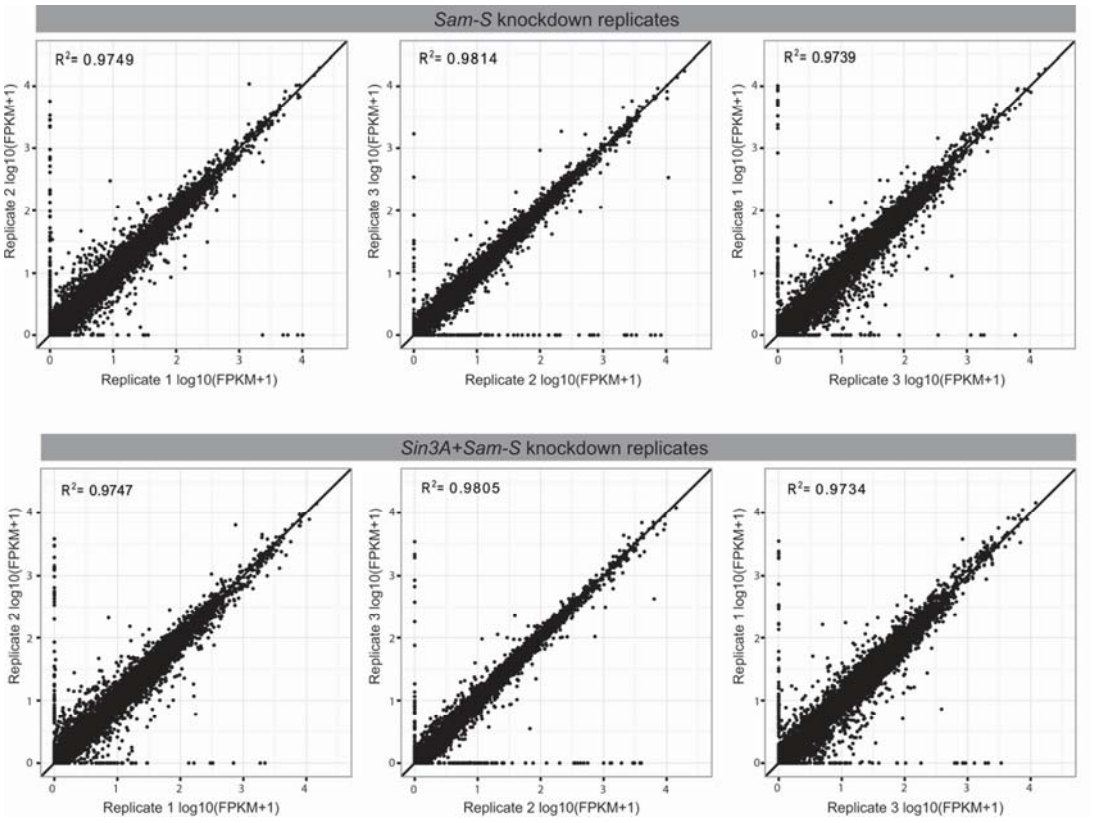

Fig. 4.2: Biological replicates of the RNA-seq data correlate significantly. Scatter plots represent the correlation between biological replicates of the RNA-seq experiment. KD, knockdown.

Differential expression analysis was performed by comparing knockdown samples to control. To identify significantly regulated genes using the RNA-seq data sets, we selected genes having more than or equal to 1.5-fold change expression with an FDR cutoff of 0.05 (Fig. 4.3 and Supplementary Data 1). Of the 18 genes regulated by SAM-S, 11 (61%) genes were upregulated and 7 (39%) genes were downregulated in the *Sam-S* knockdown cells (Fig. 4.3A). Since reduction of SAM-S leads to decreased global H3K4me3 (Liu et al., 2015), a histone mark associated with active genes (Black et al., 2012; Black and Whetstine, 2011), we predicted that the expression of a large number of genes may be changed upon knockdown of *Sam-S*. In fact, only 18 genes were regulated by SAM-S. There are several possible reasons accounting for the minimal gene expression impact due to SAM-S reduction. First, it may be due to incompletely depleted SAM-S. Given that *Sam-S* is a highly expressed gene (Gajan et al., 2016), it is possible that the remaining SAM-S following RNAi knockdown is enough to maintain function. Second, although global H3K4me3, a mark associated with active genes, was decreased in the *Sam-S* knockdown cells, this change may not reach a threshold necessary to affect the expression of many genes. In this respect, it was reported that 63 genes were misregulated in *MAT1A* knockout mice compared to wild type, even though global DNA methylation was changed (Lu et al., 2001). As we recently reported (Fig. 4.3B and in Saha et al. 2016), in the *Sin3A* single knockdown cells, 263 (43%) genes were upregulated and 349 (57%) genes were downregulated. Interestingly, although SAM-S knockdown alone did not alter the expression of many genes, the number of genes that are affected by dual knockdown is significantly higher than that of even *Sin3A* knockdown alone. Of the 734 genes misregulated upon dual

knockdown of *Sin3A* and *Sam-S*, 258 (35%) genes were upregulated and 476 (65%) genes were downregulated (Fig. 4.3C). The increased number of regulated genes in the *Sin3A+Sam-S* knockdown compared to each single knockdown suggests that there is an additive role of these proteins in regulation of transcription.

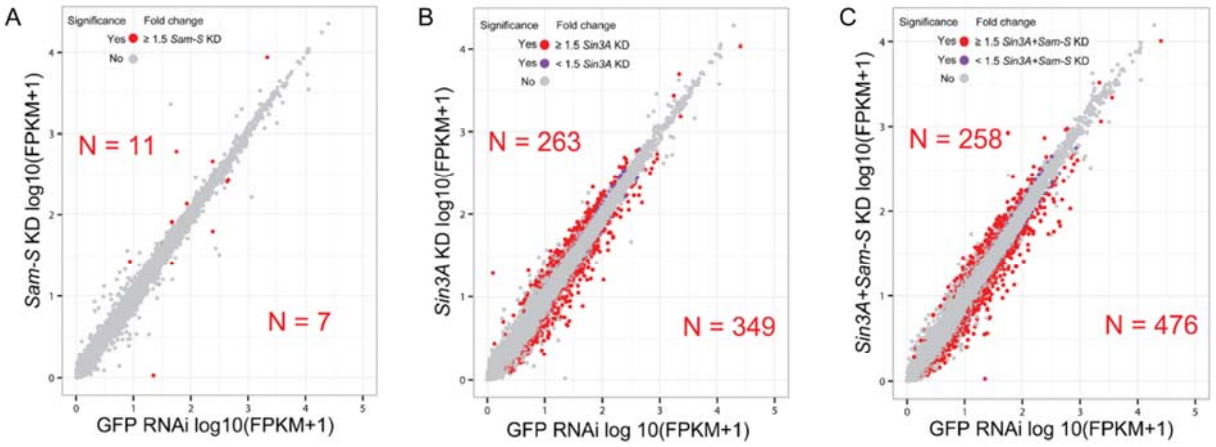

Fig. 4.3: Reduction of SIN3 and SAM-S affects cellular gene expression profiles. Scatter plots indicate the changes of gene expression in the *Sam-S* knockdown cells (A), the Sin3A knockdown cells (B) as previously reported (Saha et al. 2016), and the *Sin3A+Sam-S* knockdown cells (C) compared to the GFP RNAi control cells. Red spots, significantly regulated genes having more than or equal to 1.5-fold change expression; purple spots, significantly regulated genes having less than 1.5-fold change expression; gray spots, non-significantly regulated genes. KD, knockdown.

There were some shared targets between different knockdown samples (Fig. 4.4A). All of these common targets, except *Sam-S* and *E(spl)mbeta-HLH*, were changed in the same direction between any two tested conditions (Fig. 4.4B). *Sam-S* was downregulated in the *Sam-S* knockdown and the *Sin3A+Sam-S* knockdown cells due to RNAi, while it was upregulated in the *Sin3A* knockdown cells. *E(spl)mbeta-HLH*, as one of the downstream target genes of the Notch signaling pathway, is dispensable for adult midgut homeostasis in *Drosophila* (Lu and Li, 2015). *E(spl)mbeta-HLH* was upregulated in the *Sam-S* knockdown, while downregulated in the *Sin3A* knockdown cells.

A

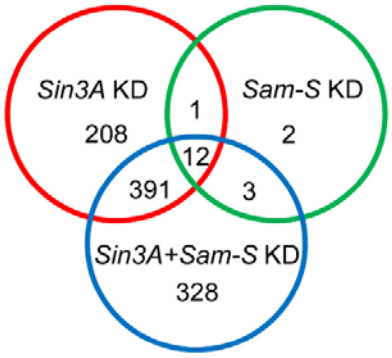

C

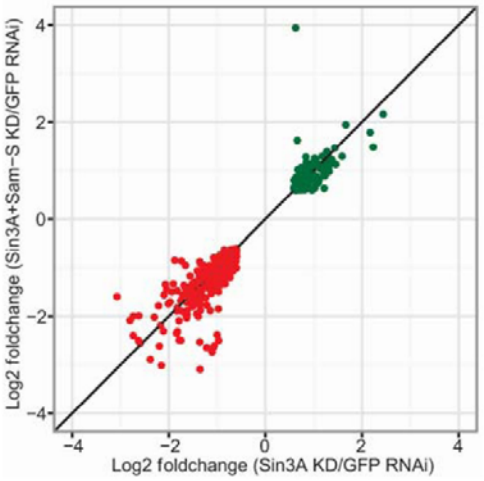

B

Category	*Sam-S* KD	*Sin3A* KD	Number of genes	Gene
1	Up	Up	7	
2	Down	Down	4	
3	Up	Down	1	*E(spl)mbeta-HLH*
4	Down	Up	1	*Sam-S*

Category	*Sam-S* KD	*Sin3A+Sam-S* KD	Number of genes
1	Up	Up	8
2	Down	Down	7
3	Up	Down	0
4	Down	Up	0

Category	*Sin3A* KD	*Sin3A+Sam-S* KD	Number of genes	Gene
1	Up	Up	132	
2	Down	Down	270	
3	Up	Down	1	*Sam-S*
4	Down	Up	0	

Fig. 4.4: Genes regulated by SIN3 and SAM-S as determined by RNA-seq. (A) Venn diagram showing shared and unique genes regulated by SIN3 and SAM-S. (B) Categorization of the genes that were dysregulated between knockdown samples. (C) Comparison of shared genes regulated by SIN3 alone as well as by both SIN3 and SAM-S in the same direction. Green spots, upregulated genes; red spots, downregulated genes. KD, knockdown.

Since there were 402 genes regulated by SIN3 as well as by both SIN3 and SAM-S and the change in expression following knockdown was in the same direction, we further analyzed these shared genes. Compared to genes that are higher in expression in the knockdown samples, more genes that are downregulated are common targets. The 132 genes that were upregulated in the *Sin3A* knockdown and the *Sin3A+Sam-S* knockdown cells showed a similar degree of induced expression under both conditions relative to control. On the other hand, the downregulated 270 genes showed a smaller level of loss of expression in the *Sin3A* knockdown as observed in the *Sin3A+Sam-S* knockdown cells (Fig. 4.4C). The different degree of expression changes for shared genes between the *Sin3A+Sam-S* knockdown and the *Sin3A* knockdown cells suggests a function for SAM-S in regulating transcription for these targets.

To verify the RNA-seq data, we utilized the RNAi knockdown samples prepared for metabolomic study, which will be described below, to analyze mRNA levels by real-time qRT-PCR. All tested genes showed similar expression trends between the real-time qRT-PCR results and RNA-seq data (Fig. 4.5).

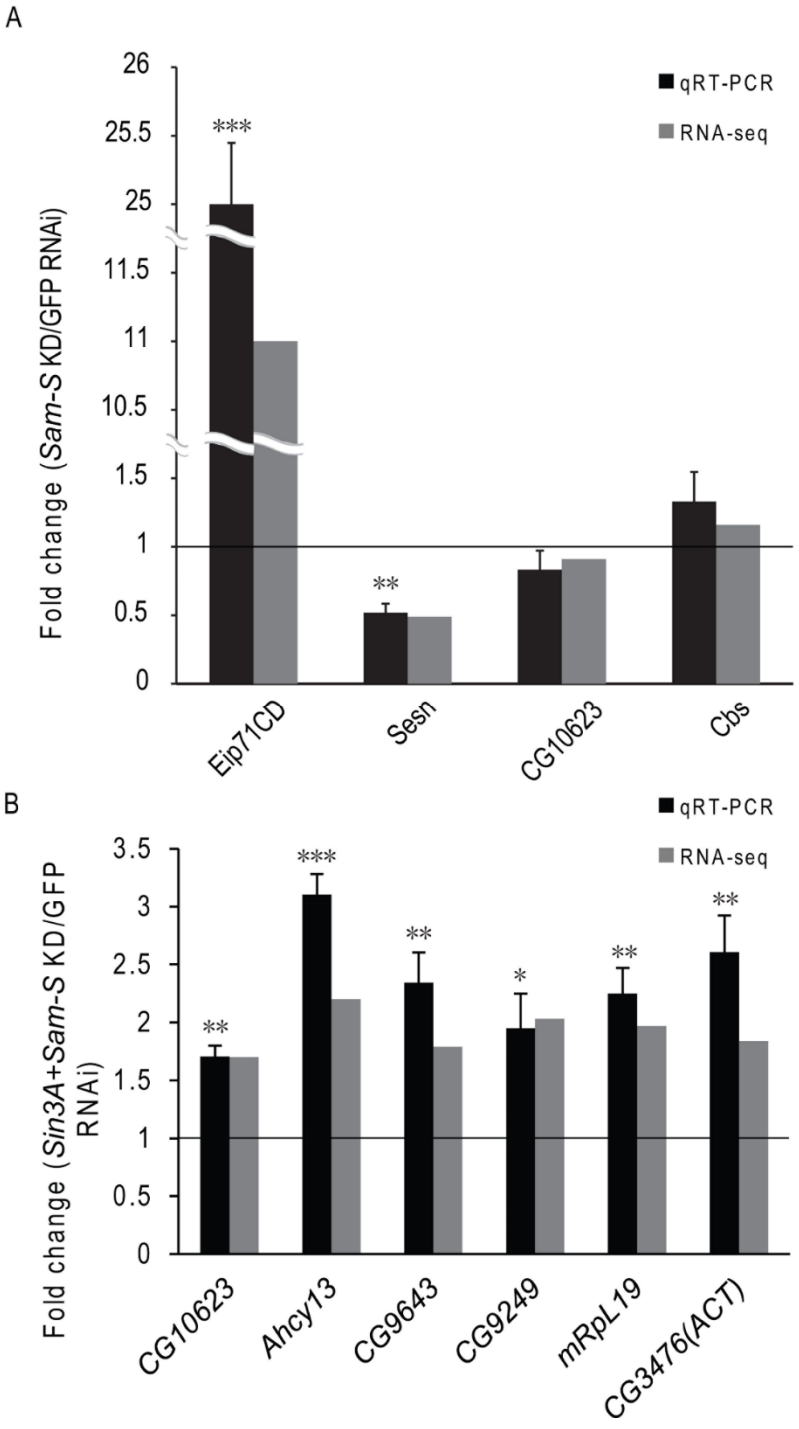

Figure 4.5: Real time qPCR analysis validates the RNAseq data. Real time qRT-PCR analysis of total RNA extracts from S2 cells treated with dsRNA targeting *Sam-S* (A) or both *Sin3A* and *Sam-S* (B). All experimental samples were compared to GFP dsRNA treated control. *Taf1* was used to normalize expression levels. The results are the average of three biological replicates. Error bars represent standard error of the mean. (*) P <0.05, (**) P < 0.01, (***) P < 0.001. KD, knockdown.

Next, we sought to determine the biological processes and the pathways regulated by SIN3 and SAM-S. We performed gene ontology (GO) and KEGG pathway analyses on the significantly regulated genes identified by RNA-seq using the DAVID gene annotation module (Huang da et al., 2009). Although the RNA-seq data in the *Sin3A* knockdown S2 cells were analyzed in two previous publications, the authors of Gajan et al., 2016 used a slightly different fold change cutoff relative to this study to identify targets that were then used for GO and KEGG pathway analyses. Additionally, only direct targets, those bound by SIN3, were analyzed for GO analysis in Saha et al., 2016. Therefore, we re-performed GO and KEGG pathway analyses for SIN3-regulated genes in this study.

Since only 18 genes were misregulated in the *Sam-S* knockdown compared to the control cells, sulfur amino acid metabolic process was the only significantly enriched biological process regulated by SAM-S and there was no significantly enriched pathway regulated by SAM-S (Fig. 4.6A and Supplementary Data 2). Many similar biological processes and pathways were regulated by SIN3 alone and by both SIN3 and SAM-S (Fig. 4.6B, 4.6C and Supplementary Data 2). These shared biological processes include stress response, cell cycle, oxidation reduction, morphogenesis, cell differentiation, development, signaling transduction and metabolism. The common pathways cover fatty acid and pyrimidine metabolism. Interestingly, there were several distinct processes and pathways affected in the *Sin3A* knockdown or the *Sin3A+Sam-S* knockdown cells (Fig. 4.6B, 4.6C and Supplementary Data 2). Consistent with the previous analysis (Gajan et al., 2016), cell junction assembly process as well as fructose and mannose metabolism were specific to SIN3-regulated genes. Transport

process was unique to the genes regulated upon dual knockdown of *Sin3A* and *Sam-S.* Comparatively, a small set of spindle assembly genes, involved in cell cycle processes, were affected in the *Sin3A* knockdown cells, while a large number of cell cycle genes were observed to change in expression in the *Sin3A+Sam-S* knockdown cells. Several cell cycle related pathways, such as DNA replication, mismatch repair and purine metabolism, were specific to genes regulated upon dual knockdown of *Sin3A* and *Sam-S.* These distinct functional categories of regulated genes indicate different roles of these proteins in regulation of biological processes and pathways.

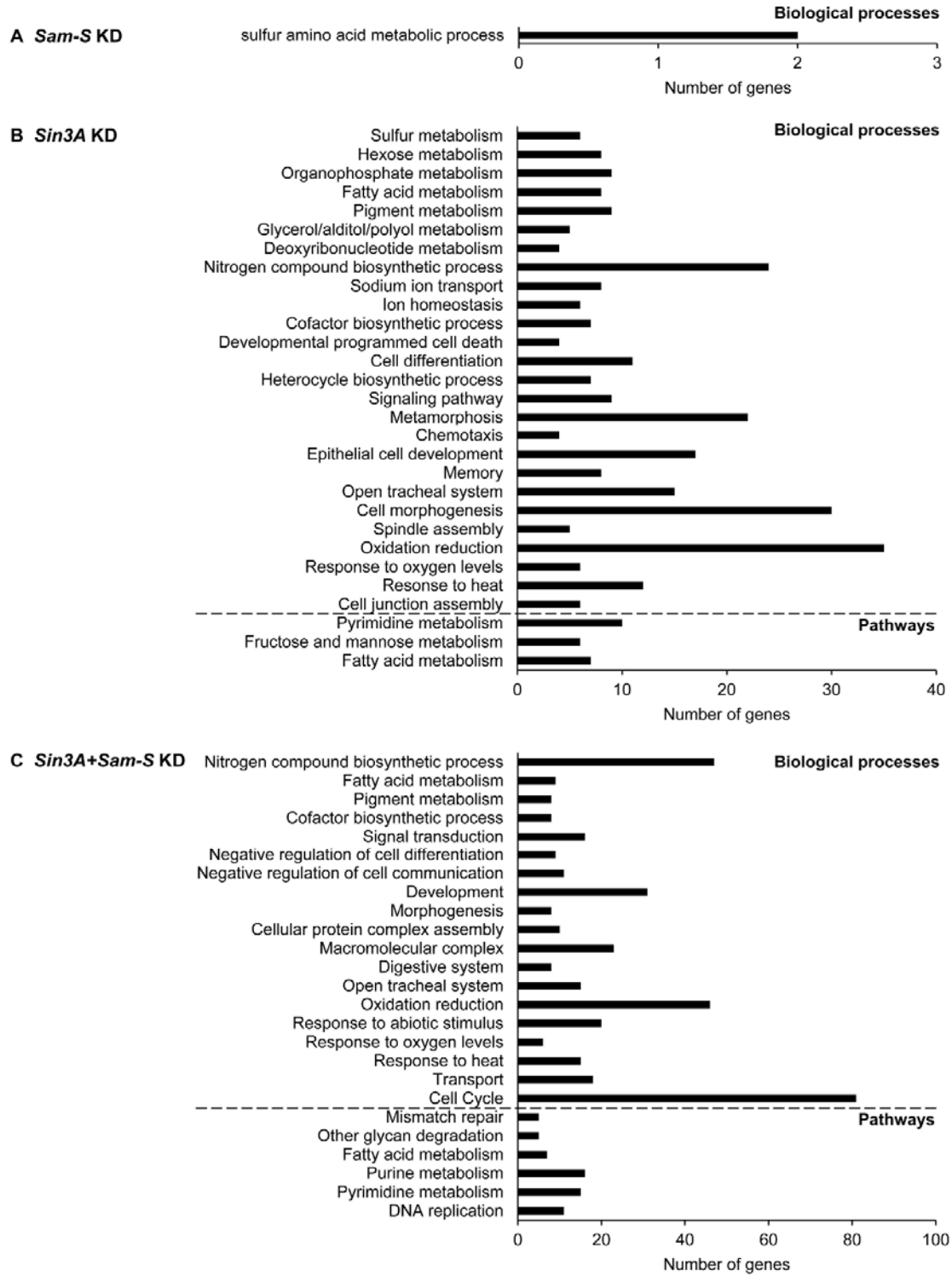

Fig. 4.6: Gene ontology and KEGG pathways analyses of the genes regulated by SIN3 and SAM-S as determined by RNA-seq. Gene ontology analysis is listed above the dashed line, while KEGG pathway analysis is below the dashed line. P<0.05. KD, knockdown.

Metabolomic study identifies metabolites regulated by SIN3 and SAM-S

To gain an understanding of the metabolic pathways regulated by SIN3 and SAM-S, we conducted a thorough metabolic study. We used ultra-performance liquid chromatography tandem mass-spectrometry (UPLC-MS/MS) and gas chromatography–mass spectrometry (GC/MS) to generate a quantitative metabolomic profile for five biological replicates of GFP RNAi control, *Sin3A* knockdown, *Sam-S* knockdown and *Sin3A+Sam-S* knockdown S2 cells. The RNAi efficiency was routinely validated by western blotting analysis and RT-PCR (Fig. 3.1B and 3.4B).

We performed a partial least squares discriminant analysis (PLS-DA) of the metabolomic data and found that each sample had a unique metabolic profile (Fig. 4.7). At a statistical significance of *p*-value≤0.05, 248 metabolites were altered in the *Sin3A* knockdown sample relative to the control, 53 in the *Sam-S* knockdown and 207 in the *Sin3A+Sam-S* knockdown cells. These metabolic data clearly indicate that altering the levels of SIN3 or SAM-S leads to a change in the cellular metabolic profile. The finding that knockdown of *Sin3A* results in a more profound change to the cellular metabolome as compared to the *Sam-S* knockdown sample strongly suggests that SIN3 regulates multiple metabolic pathways, not only methionine metabolism, which has been described in Chapter 3.

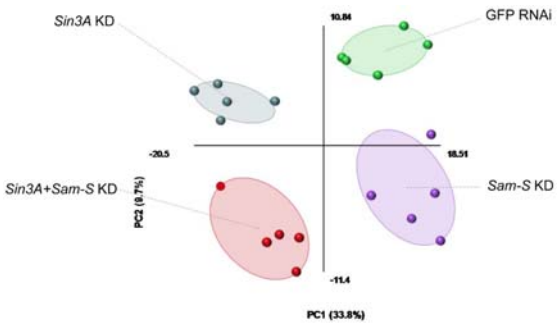

Fig. 4.7: PLS-DA analysis for the metabolic data. KD, knockdown.

We detected a number of glycolytic metabolites that were affected by reduction of SIN3 (Fig. 4.8A and 4.9A). Metabolites from glycolysis I, including glucose, glucose-6-phosphate, fructose-6-phosphate and fructose-1,6-biphosphate, were significantly downregulated in the *Sin3A* knockdown cells compared to control cells (Fig. 4.9A). While metabolites from glycolysis II, including 3-phosphoglycerate and pyruvate, were significantly upregulated in the *Sin3A* knockdown cells (Fig. 4.9A). These data suggest that reduction of SIN3 leads to increased glycolytic function. There are two possible explanations for the different changes between glycolytic I and II metabolites when SIN3 was reduced. It was reported that increased O-GlcNAcylation leads to increased glucose flux and inhibition of O-GlcNAcylation results in decreased glycolysis flux (Ferrer et al., 2014). It is possible that the significant changes in glucosamine-6-phosphate (Glc-6-P), N-acetylglucosamine-6-phosphate (N-AcetylGlc-6-P) and N-acetylglucosamine-1-phosphate (N-AcetylGlc-1-P) concentration observed in the *Sin3A* knockdown cells compared to the control leads to altered O-GlcNAcylation, which in turn results in a decreased pool of the metabolites involved in glycolysis I (Fig. 4.8A and 4.9B). Second, the increased pyruvate concentration may be due to TCA dysfunction. In addition, we observed that glycolytic metabolites were altered in the opposite direction in the *Sam-S* knockdown sample relative to the *Sin3A* knockdown sample (Fig. 4.9A). In the *Sam-S* knockdown sample, decreased pyruvate and increased sedoheptulose-7-phosphate (sedoheptulose-7-P) levels suggest increased input into the pentose phosphate pathway (Fig. 4.8A, 4.9A and 4.9B). Moreover, the levels of these glycolytic metabolites in cells with dual knockdown of *Sin3A* and *Sam-S* were intermediate between the levels in the *Sin3A* single knockdown and the *Sam-S* single knockdown

cells (Fig. 4.9A). Given that decreased global H3K4me3 levels caused by reduction of SAM-S are restored to near control levels upon *Sin3A* knockdown (Fig. 3.4C and 3.4D), it is possible that there is a link between glycolysis and histone methylation in the tested knockdown samples.

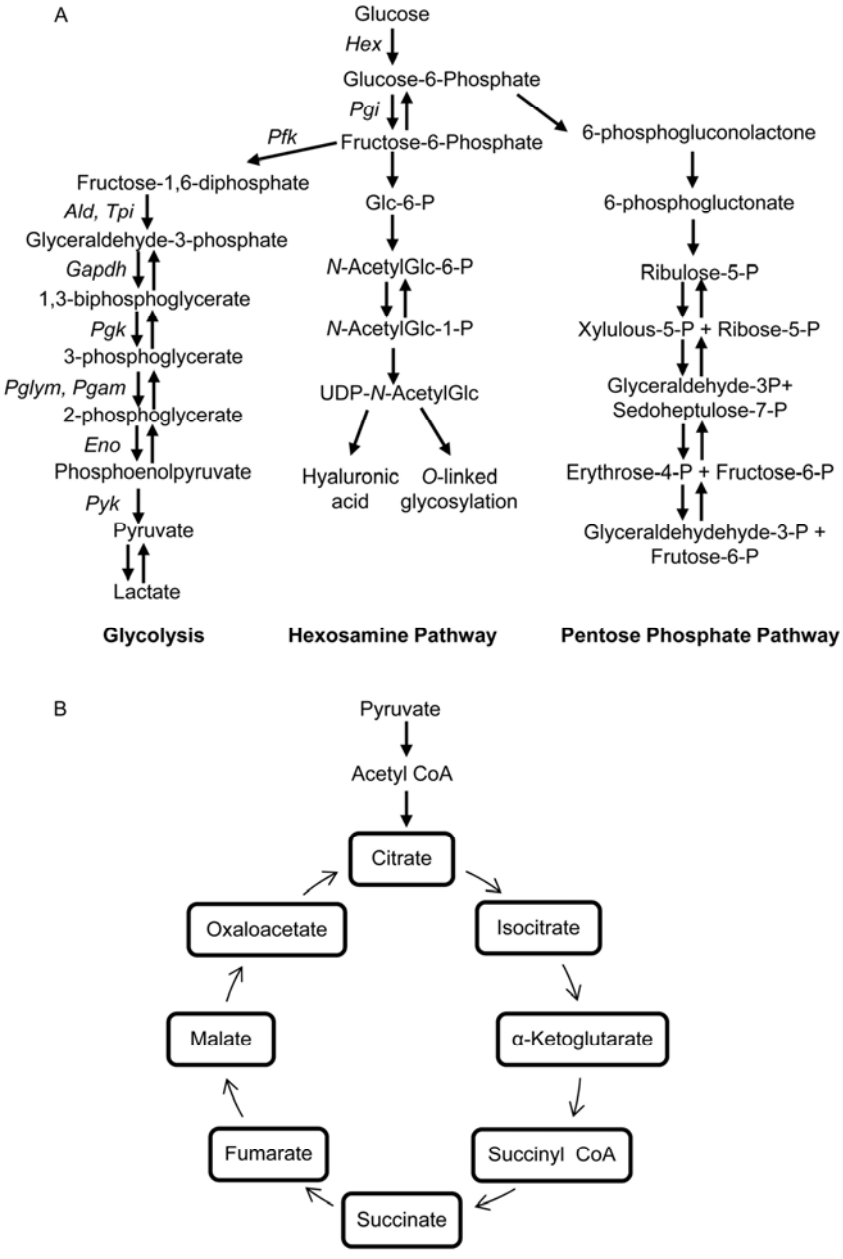

Fig. 4.8: Schematic of the metabolic pathways. Schematic of the glycolytic, hexosamine and pentose phosphate pathways (A) (Sutton-McDowall et al., 2010) and the TCA cycle (B).

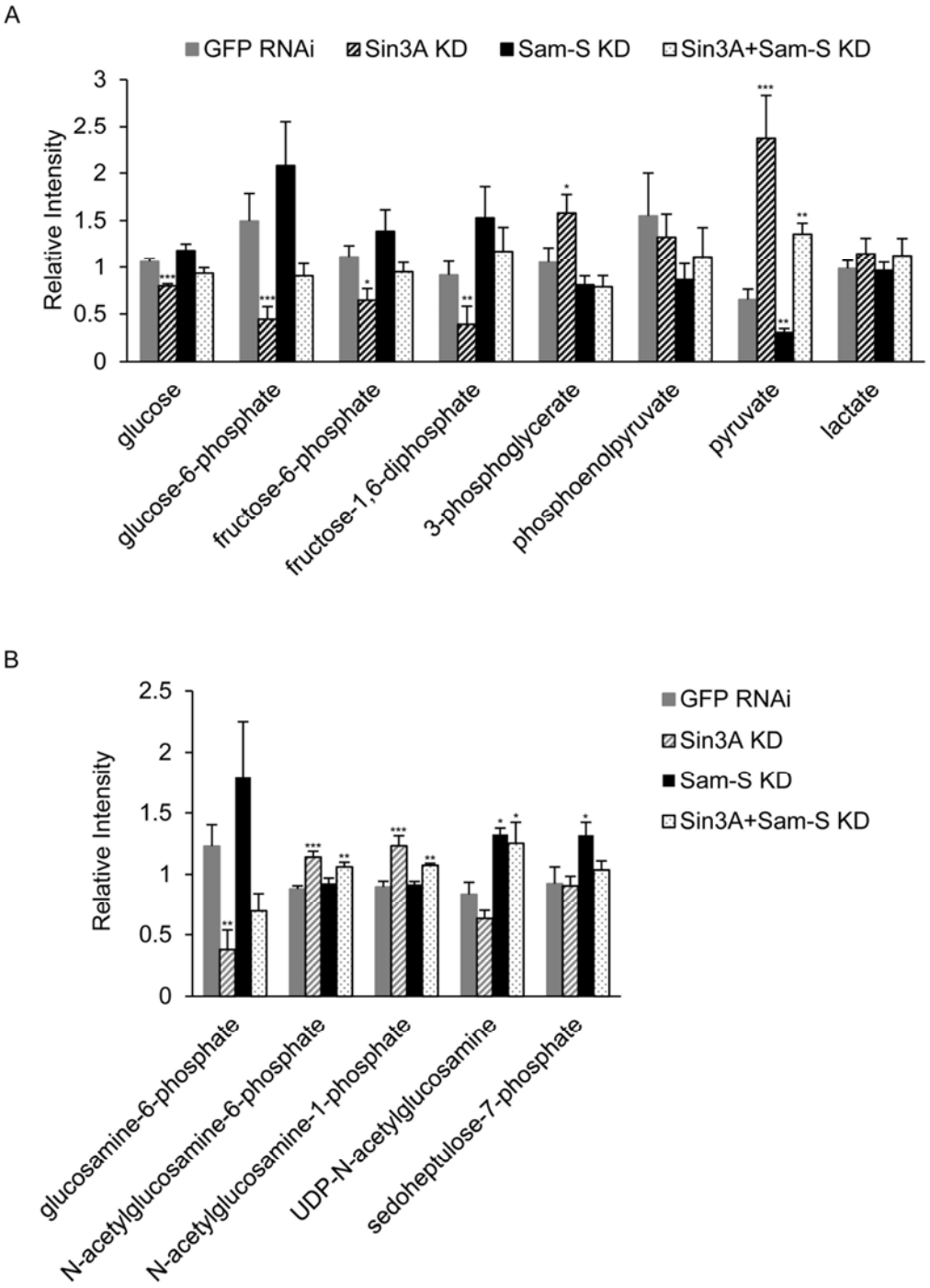

Fig. 4.9: Effects of SIN3 and SAM-S on the glycolytic, hexosamine and pentose phosphate pathways. The levels of the metabolites involved in the glycolytic (A), hexosamine and pentose phosphate pathways (B) in RNAi-treated cells. Error bars represent standard error of the mean. Statistically significant results comparing individual knockdown samples to the control are indicated on knockdown. (*) $P<0.05$, (**) $P < 0.01$, (***) $P < 0.001$. KD, knockdown.

Nearly every metabolite associated with TCA cycle, with the exception of oxaloacetate and succinyl-CoA, was detected in our metabolomics study (Fig. 4.8B and 4.10). Consistent with the observation of aberrant mitochondrial function caused by reduction of SIN3 (Barnes et al., 2010), all observed intermediates involved in TCA cycle, except α-ketoglutarate, were decreased in the *Sin3A* knockdown and the *Sin3A+Sam-S* knockdown cells relative to the control. Compared to the control, the cellular concentration of the metabolites in the TCA cycle in the *Sam-S* knockdown cells was not affected. These data suggest that SIN3, but not SAM-S, affects the TCA cycle. The similar trends in altered glycolytic metabolite level observed comparing the *Sin3A* knockdown and the *Sin3A+Sam-S* knockdown cells indicate that there is no feedback between SIN3 and SAM-S in regulation of this pathway. Given that pyruvate was significantly increased, while lactate was not changed in the *Sin3A* knockdown and the *Sin3A+Sam-S* knockdown cells (Fig. 4.9A), it is likely that the observed accumulation of pyruvate is due to a decrease in the flux through the TCA cycle under these conditions. Collectively, these findings indicate that decreased SIN3 results in reduced TCA cycle flux and increased glycolysis.

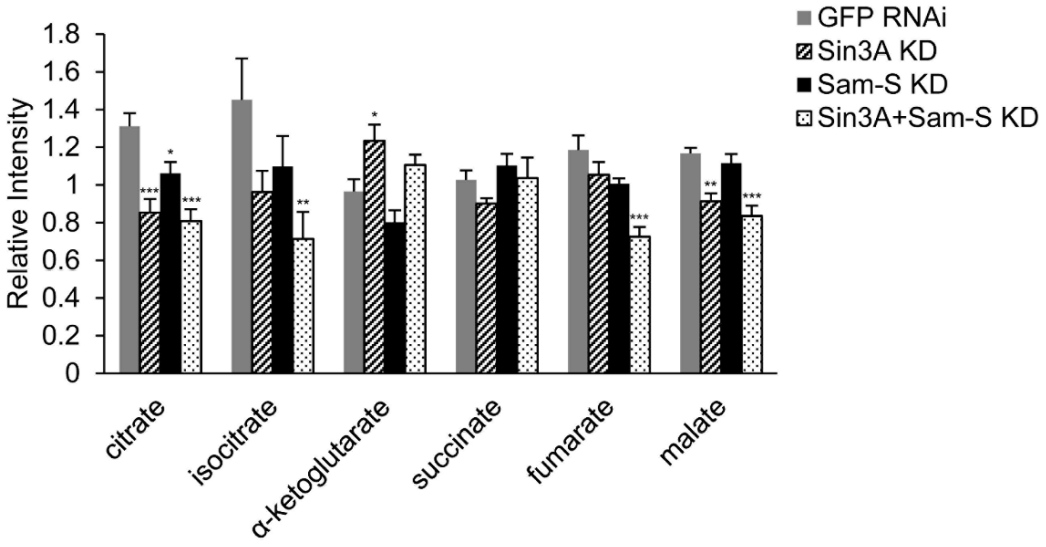

Fig. 4.10: Effects of SIN3 and SAM-S on the TCA cycle. Error bars represent standard error of the mean. Statistically significant results comparing individual knockdown samples to the control are indicated on knockdown samples. (*) P<0.05, (**) P < 0.01, (***) P < 0.001. KD, knockdown.

The effects of SIN3 and SAM-S on methionine metabolism

In Chapter 2, we demonstrate that reduced SAM-S leads to decreased global H3K4me3. In Chapter 3, we determine that SIN3 alters the expression of methionine metabolic genes to influence SAM levels, which in turn impact global H3K4me3. To further explore how SIN3 and SAM-S regulate this histone mark, we analyzed the expression of metabolic genes and the concentration of the metabolites involved in the methionine pathway using the RNA-seq and the metabolomics data in the *Sin3A* knockdown, *Sam-S* knockdown and *Sin3A+Sam-S* knockdown S2 cells. To verify the RNA-seq data, we used RNA isolated from the RNAi knockdown samples prepared for metabolomic study to measure mRNA levels by real-time qRT-PCR. Both RNA-seq and qRT-PCR results reveal that *Sam-S* was the only gene in the methionine metabolic pathway showing altered expression when SAM-S was reduced (Fig. 4.11A). Reduction of SAM-S resulted in decreased SAM levels and no changes for other metabolites

involved in methionine metabolism (Fig. 4.11B). These data indicate that SAM-S affects SAM levels to influence global H3K4me3. The expression of tested methionine metabolic genes showed similar trends comparing the *Sin3A+Sam-S* knockdown and the *Sin3A* knockdown cells (Fig. 4.11A). Not surprisingly, SAM was low in the dual knockdown sample as the cells were missing the key synthesis enzyme (Fig. 4.11B). Homocysteine and cystathionine were downregulated when both SIN3 and SAM-S were reduced and methionine was not altered in any significant way (Fig. 4.11B). We note that there is a discrepancy between the cellular SAM concentration and histone H3K4me3 levels in the different conditions. While SAM levels were low in both the *Sam-S* and *Sin3A+Sam-S* knockdown cells, global H3K4me3 levels were only impacted in the *Sam-3* knockdown sample relative to the control (Fig. 3.4C, 3.4D and 4.11B). There is one possibility to explain this apparent discrepancy. When SAM-S alone is reduced, cells can only generate a small amount of SAM, which is not enough to maintain normal H3K4me levels. SAM is consumed for histone methylation, which in turn leads to a decreased pool of SAM in the *Sam-S* knockdown cells. In contrast, in the *Sin3A+Sam-S* knockdown cells, reduction of *Sin3A* alters gene expression patterns in such a way that the effects of decreased *Sam-S* expression were compensated by the changes in the expression of other methionine metabolic genes. This compensation could allow production of SAM to be used for histone methylation. Therefore, we predict that cells with dual knockdown of *Sin3A* and *Sam-S* produce a certain level of SAM, which is higher than the concentration of SAM in the *Sam-S* knockdown but lower than the control cells. In the *Sin3A+Sam-S* knockdown cells, this limited amount of SAM is used to maintain H3K4me3, ultimately resulting in a decreased pool of observed SAM.

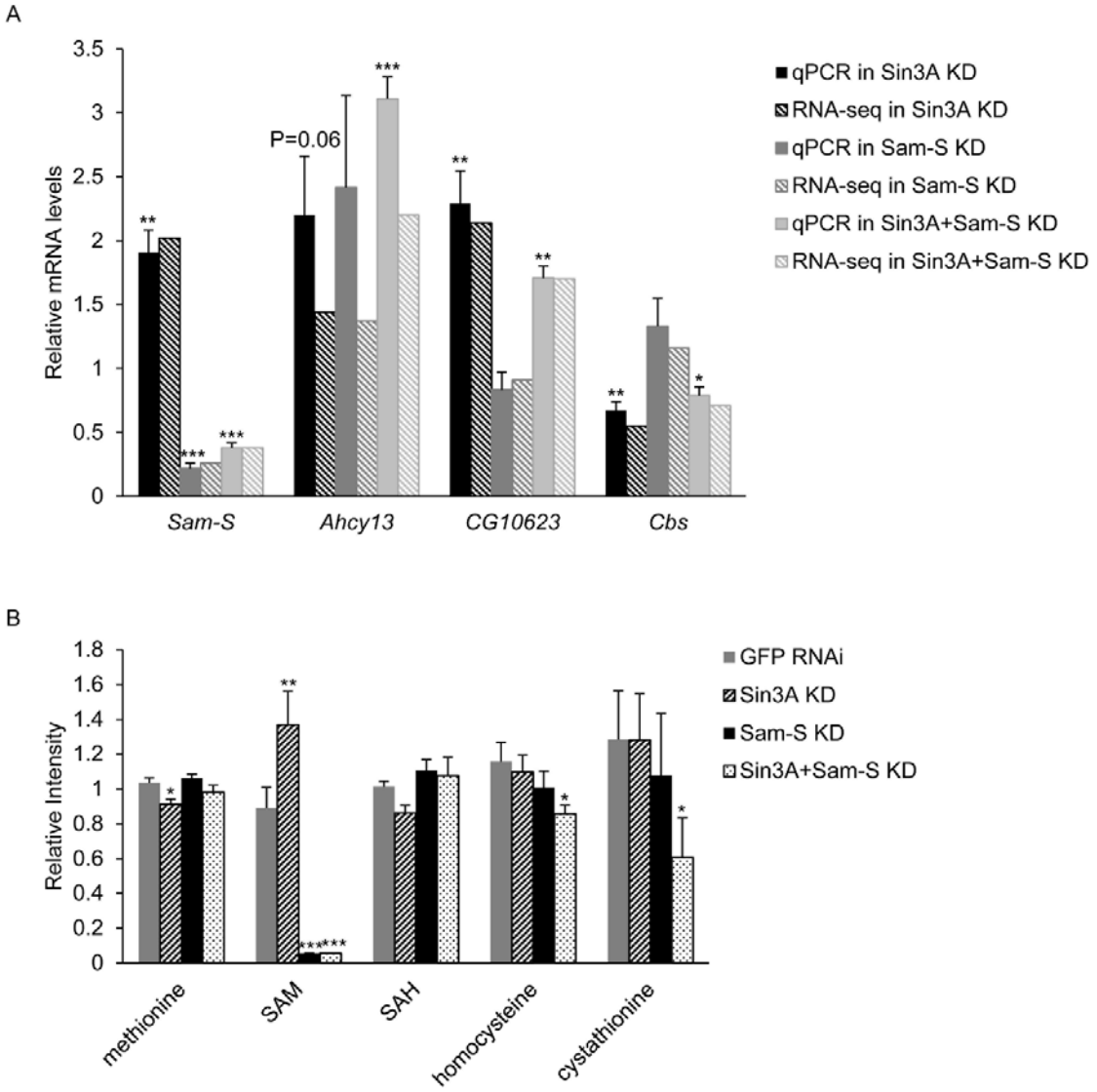

Fig. 4.11: Effects of SIN3 and SAM-S on methionine metabolism. The effects of SIN3 and SAM-S on the expression of genes (A) and the concentration of metabolites (B) involved in methionine metabolism. Error bars represent standard error of the mean. Statistically significant results comparing individual knockdown samples to the control are indicated on knockdown samples. (*) P <0.05, (**) P < 0.01, (***) P < 0.001. KD, knockdown.

Glycolysis is correlated with global H3K4me3 levels upon knockdown of *Sin3A* and *Sam-S*

We next used the metabolic profiles along with the relative global H3K4me3 levels in GFP RNAi control, *Sin3A* knockdown, *Sam-S* knockdown and *Sin3A+Sam-S* knockdown S2 cells to perform a Pearson correlation analysis. The list of metabolites whose concentrations changed significantly with changes in H3K4me3 due to the experimental condition was generated. Interestingly, we found that glycolysis is a major pathway correlated with global H3K4me3 levels upon reduction of SIN3 and/or SAM-S. In all tested knockdown samples, the amount of glucose, glucose-6-phosphate, fructose-6-phosphate and fructose-1,6-biphosphate were negatively correlated with global H3K4me3 levels, while the levels of 3-phosphoglycerate and pyruvate were positively correlated (Fig. 4.12). The correlation was statistically significant. The mechanism of how glycolysis is linked to global H3K4me3 upon reduction of SIN3 and/or SAM-S is largely unknown, which is an interesting area for further investigation.

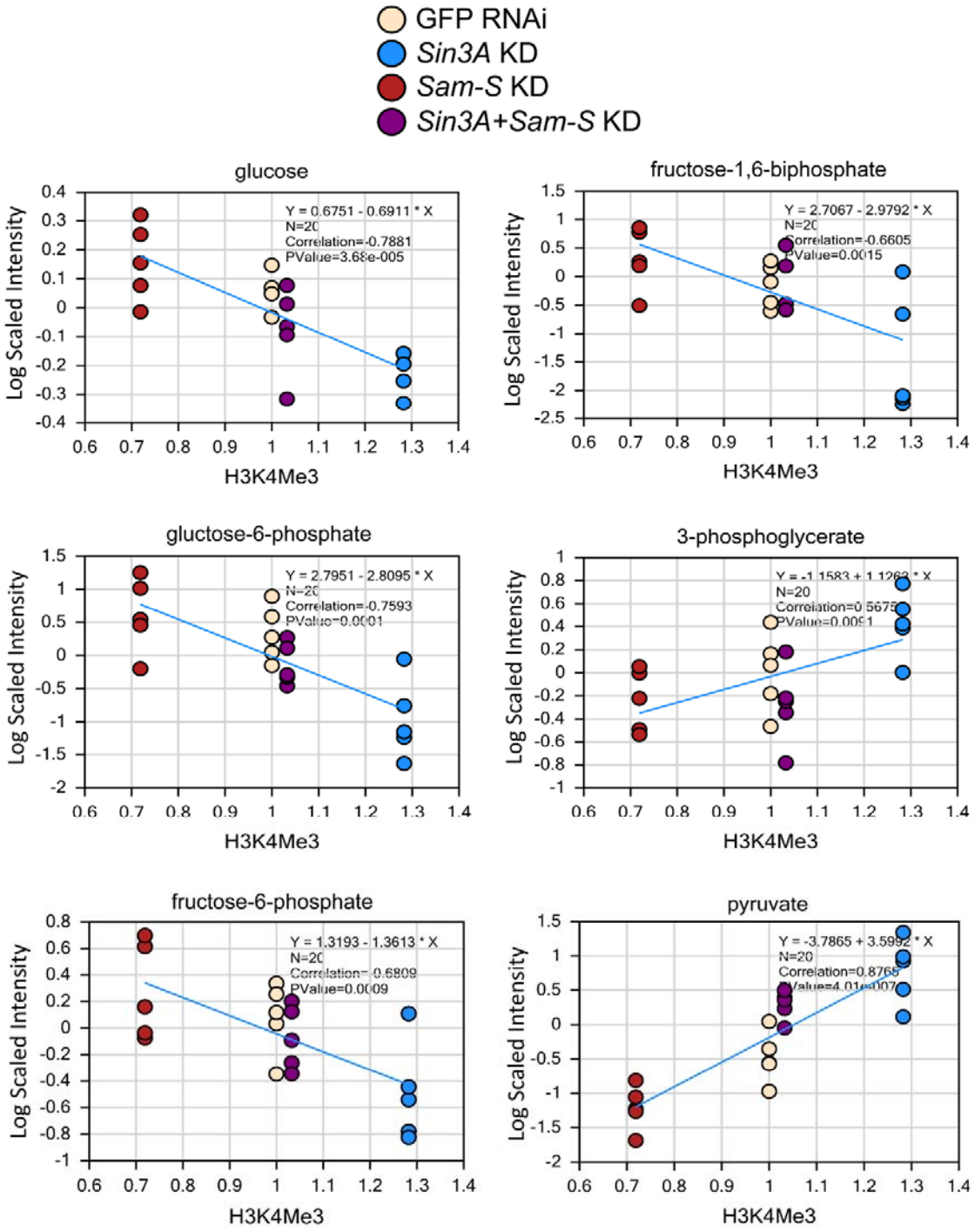

Fig. 4.12: The concentration of the metabolites in glycolysis is correlated with the global H3K4me3 levels upon reduction of SIN3 and/or SAM-S. Pearson correlation analysis between metabolite levels and global H3K4me3 levels. KD, knockdown.

The H3K9ac levels at the promoters of glycolytic genes are impacted by SIN3

Inspection of the glycolytic pathway indicates that not only are metabolites in the pathway affected (Fig. 4.9A), but the expression of several genes, such as *Pfk*, *Gapdh1*, and *Pyk*, that encode enzymes in the pathway is increased in the *Sin3A* RNAi knockdown samples (Barnes et al., 2010). Inspection of our recently obtained ChIP-seq data set (Saha et al., 2016) indicates that each of these genes is bound by SIN3 (Fig. 4.8A and 4.13). Given that SIN3 regulates H3K9ac and H3K4me3 levels at the promoters of methionine metabolic genes (Fig. 3.2C), we hypothesized that SIN3 likely has a similar effect on these histone marks at glycolytic genes. To test this hypothesis, we performed ChIP-qPCR analysis in the GFP RNAi control and the *Sin3A* knockdown cells. Reduction of SIN3 protein was confirmed by western blotting analysis (Fig. 3.1B). IgG was used as a non-specific control. H3K9ac and H3K4me3 levels were normalized to the histone H3 signal. Typically, compared to IgG, a more than 60 fold enrichment of H3, 200 fold enrichment of H3K9ac and 264 fold enrichment of H3K4me3 were observed at all regions sampled (Fig. 4.14). Knockdown of *Sin3A* led to an increase of H3K9ac but surprisingly, no change of H3K4me3 at *Pfk*, *Gapdh-1* and *Pyk* (Fig. 4.15). It is interesting that increased H3K4me3 levels were observed at the promoters of the methionine metabolic genes, but not at the glycolytic genes, when SIN3 was reduced (Fig. 3.2C and Fig. 4.15B). There are several explanations for this difference. First, although H3K4me3 at the tested promoter regions of the glycolytic genes was not changed, it is possible that this mark is changed at other regions of the promoters. Second, SIN3 may specifically affect H3K4me3 levels at the promoters of a group of genes, however, the mechanism for this specificity remains to be determined. Given

that H3K9ac is associated with active genes (Black et al., 2012; Black and Whetstine, 2011), H3K9ac levels at the tested genes were in accord with the gene expression level. Taken together, these data indicate that SIN3 directly regulates glycolytic genes through control of H3K9ac at their promoters and the change in expression of these key enzymes leads to the alterations in the intermediates in the glycolytic pathway.

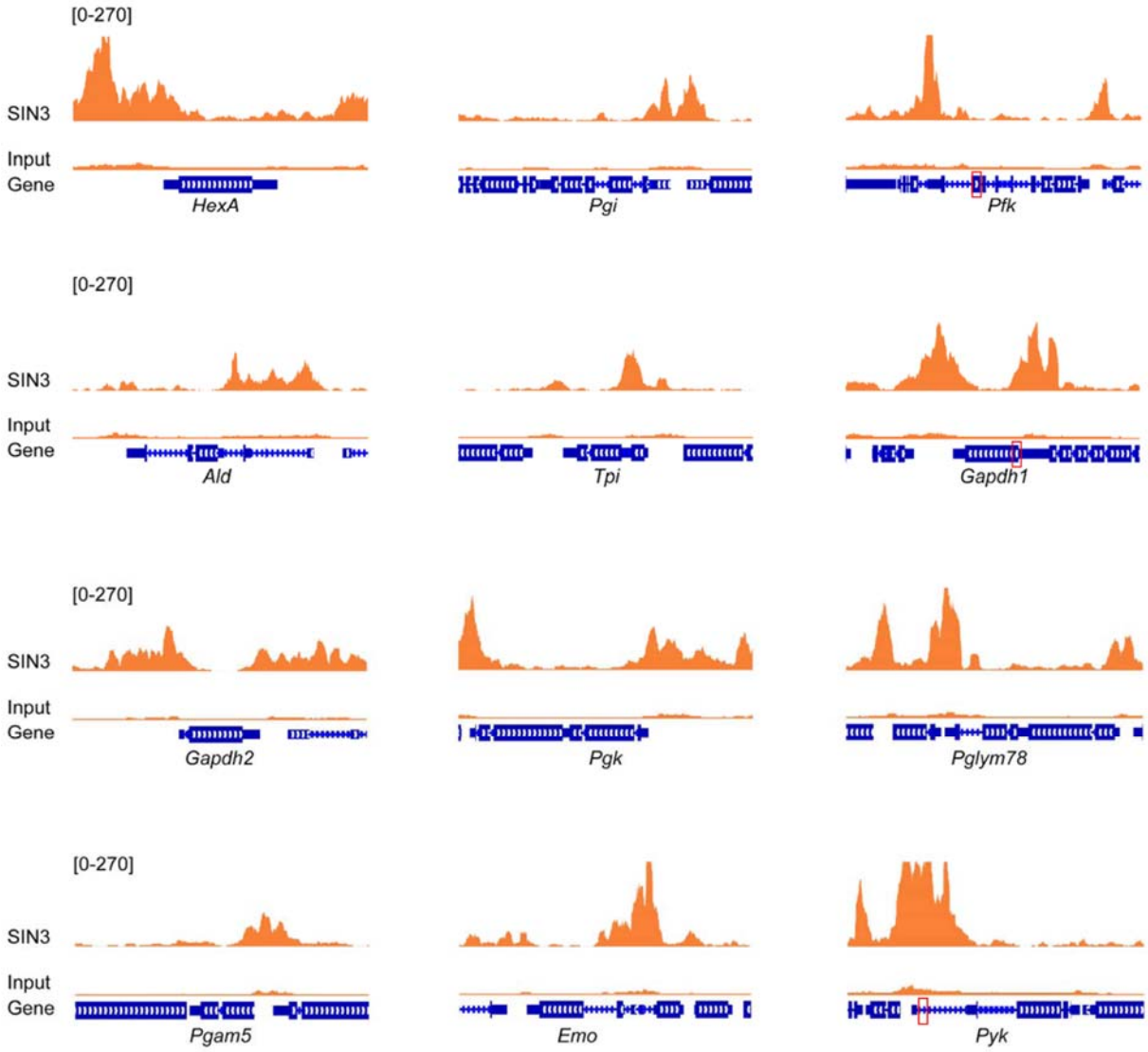

Fig. 4.13: SIN3 binds to the promoters of glycolytic genes. SIN3 ChIP-seq signals at glycolytic genes. Red boxes label the regions sampled by ChIP-qPCR.

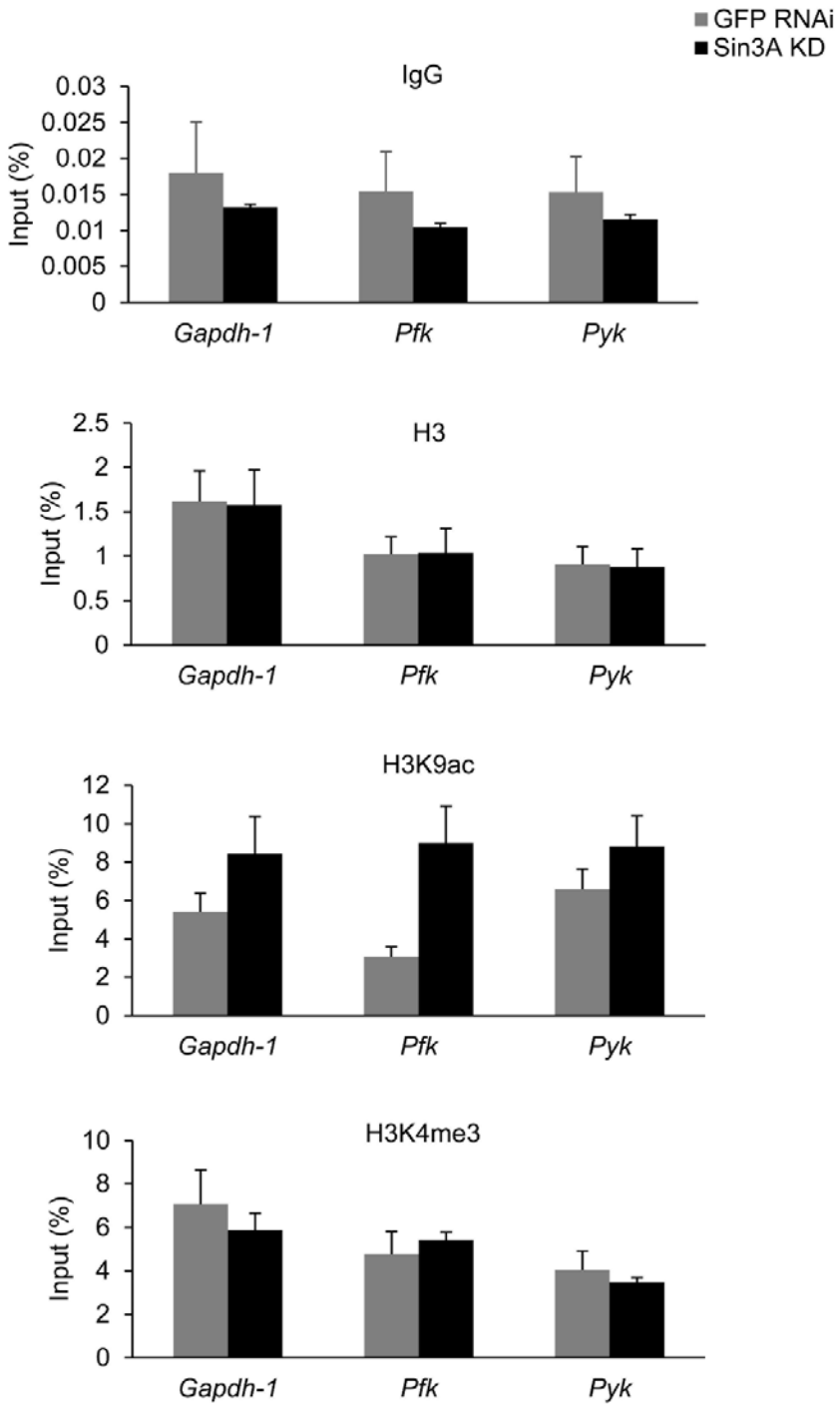

Fig. 4.14: Input levels of IgG, H3, H3K9ac and H3K4me3 at the promoters of glycolytic genes. ChIP-qPCR analysis was performed using DNA prepared from chromatin pulled down by IgG, H3, H3K9ac or H3K4me3 antibody in the GFP RNAi control and the *Sin3A* deficient S2 cells. Results are the average of three biological replicates. Error bars represent standard error of the mean. KD, knockdown.

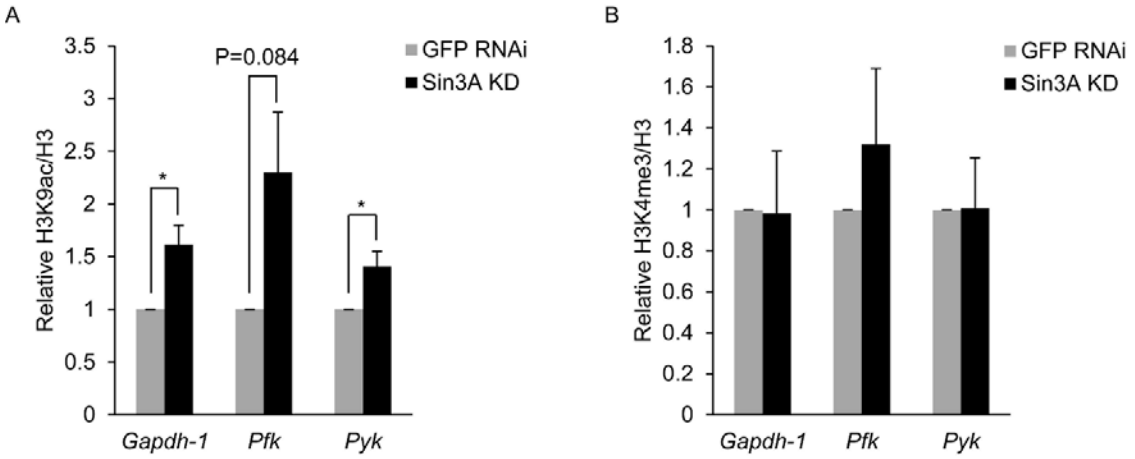

Fig. 4.15: Effect of SIN3 on histone modifications at the promoters of glycolytic genes. Enrichment of H3K9ac (A) and H3K4me3 (B) at the promoters of glycolytic genes in the GFP RNAi control and the *Sin3A* deficient S2 cells. Results are the average of three biological replicates. Error bars represent standard error of the mean. Statistically significant results are indicated. (*) P <0.05. KD, knockdown.

DISCUSSION

In this work, we identified the genes and the metabolites regulated by SIN3 and SAM-S. The data suggest that these proteins have some common and some distinct effects on transcription and metabolism. Given that SAM-S affects histone methylation and that SIN3 regulates histone methylation and acetylation, it is possible that SIN3 and SAM-S influence the expression of shared and unique genes through altering gene specific histone modifications. The altered gene expression patterns then in turn impact common and distinct biological processes.

Reduction of SAM-S leads to decreased global H3K4me3 levels (Fig. 2.7, 3.4C and 3.4D) and reduced H3K4me3 levels at the promoters of some specific genes (Fig. 2.10A). It is likely that the global decrease of H3K4me3 caused by incompletely depleted SAM-S cannot reach the necessary threshold to impact the expression of many genes. Since H3K4me3 is a histone mark associated with active genes (Black et al., 2012; Black and Whetstine, 2011), the observed difference between global and

gene specific H3K4me3 levels may lead to the result that only a few genes changed in expression when SAM-S was reduced. It is possible that SIN3 regulates the expression of a large group of genes through altering H3K4me3 and H3K9ac, which is supported by the findings that SIN3 affected these histone marks at the promoters of methionine metabolic genes and their transcription (Fig. 3.1A, 3.1C and 3.2C). In the *Sin3A+Sam-S* knockdown cells, a relatively large number of genes were misregulated compared to each single knockdown sample (Fig. 4.3 and Supplementary Data 1). The global H3K4me3 levels in the *Sin3A+Sam-S* knockdown cells, however, were similar to the control (Fig. 3.4C and 3.4D). In addition, the degree of change in expression for the genes shared between the *Sin3A+Sam-S* knockdown and the *Sin3A* knockdown cells were different (Fig. 4.4C). There are several possibilities to explain how transcription is regulated in the *Sin3A+Sam-S* knockdown cells. First, H3K9ac is probably affected in the *Sin3A+Sam-S* knockdown cells. Second, other histone methylation marks may be influenced when SIN3 and SAM-S are reduced. Third, although SAM-S alone does not affect expression levels of most genes, it may sensitive the genome in some way to make genes more dependent on regulation by SIN3. Fourth, SAM-S has been demonstrated to localize on the chromatin and recruit regulatory proteins, to affect gene expression (Katoh et al., 2011; Li et al., 2015; Reytor et al., 2009). The mechanism of how SAM-S is recruited to the chromatin, however, is not fully understood. It is possible that reduction of SIN3 alters chromatin structure by changing histone acetylation, which in turn affects the binding of incompletely depleted SAM-S on the chromatin and the result is a change in gene expression.

We found that glycolysis is a major pathway correlated with global H3K4me3

upon reduction of SIN3 and/or SAM-S (Fig. 4.12), but the mechanism remains unknown. A recent study reported that SESAME, a complex containing serine metabolic enzymes, SAM-S, acetyl-CoA synthetase and pyruvate kinase PYK1, affects H3K4me3 through sensing glycolysis in yeast (Li et al., 2015). Disruption of glycolysis resulted in decreased H3K4me3 and increased cellular glucose led to increased H3K4me3 (Li et al., 2015). In addition, the SESAME complex auto-regulates the expression of *Pyk1* (Li et al., 2015). It is possible that the SESAME complex is also present in *Drosophila* and it may contribute to the noted association between glycolysis and global H3K4me3 revealed in our study. We speculate that reduction of SAM-S leads to a decrease in the amount of the SESAME complex, which in turn affects *Pyk1* expression and then glycolysis. In this study, we provided evidence that flux through glycolysis was increased when SIN3 was reduced (Fig. 4.9A). Therefore, it is likely that glycolysis is balanced between the action of the SESAME complex and the SIN3 complex. To test all of these possibilities, more extensive experiments are required.

ACKNOWLEDGEMENTS

I wish to thank Ambikai Gajan for help with RNA-seq sample preparation, Nirmalya Saha for support with analysis of RNA-seq data as well as Dr. Russell L. Finley, Jr. for providing the template DNA to make dsRNA against GFP. Additionally, I really appreciate the help from the members of the Applied Genomics Technology Center, School of Medicine, Wayne State University for their assistance in the RNA-seq experiment. Daniel Lott extracted RNA and checked RNA quality. Alya'a Samaak prepared the cDNA library and performed the next-generation sequencing. Dr. Adele Kruger performed the quality control analysis for the RNA-seq data.

CHAPTER 5 FUTURE DIRECTIONS

Our study has demonstrated that SIN3 directly regulates genes encoding enzymes that process metabolites. This work has contributed to our understanding of the role of SIN3 in regulating metabolism. However, outstanding questions remain, which are discussed below.

Does LID contribute to the effect of SIN3 on regulating H3K4me3?

Our work indicates that SIN3 impacts H3K4me3 levels through affecting methionine metabolism. Given that the H3K4me3 specific demethylase LID interacts with SIN3 (Moshkin et al., 2009; Spain et al., 2010), it is possible that LID contributes to the role of SIN3 in regulation of H3K4me3. We hypothesize that reduction of SIN3 leads to decreased LID binding or LID activity, which in turn results in increased H3K4me3. To test this hypothesis, Ambikai Gajan measured LID binding by ChIP-qPCR when SIN3 was reduced through RNAi in *Drosophila* S2 cells (Gajan, 2015). Cells treated with dsRNA to target GFP were used as the control. The results showed that reduction of SIN3 increased LID enrichment at tested genes that were bound by LID under normal condition, compared to control cells (Gajan, 2015). However, increased LID binding was also observed at a negative control gene, so the data are inconclusive. We plan to repeat this experiment to determine if the increase in LID binding is due to an experimental artifact caused by sample variability or due to reduced SIN3. We also want to to use a demethylase (Jumonji-type) activity assay kit (Promega) to measure LID demethylase activity when *Sin3A* is knocked down. Together, these data will help us understand whether and how LID contributes to the role of SIN3 in regulation of H3K4me3.

Which SIN3 complex components are required to affect metabolism?

This study demonstrates that reduced SIN3 leads to changes in metabolism. It is unclear if this effect is caused by the scaffold protein SIN3 alone or through altering the function of the SIN3 complex as a whole, due to changes in the SIN3 level. To test the contribution of the SIN3 complex in mediation of the metabolic response to SAM limitation, we will monitor global H3K4me3 levels, expression of genes encoding methionine metabolic enzymes, histone modifications at these promoters and the levels of key intermediates in the methionine pathway in S2 cells with single knockdown of each SIN3 complex component, as well as double knockdown of individual component and *Sam-S*. Control cells will be treated with dsRNA to GFP. If a component is important for the response to reduction of SAM-S, then we predict that cells with dual knockdown of the component and *Sam-S* will lose this response, and methylation levels will be similar to those observed in *Sin3A+Sam-S* knockdown cells. These results will determine if and how the SIN3 complex mediates a response to changes in the concentration of SAM, the major cellular methyl donor in the cell.

How does SIN3 bind to metabolic genes?

Neither SIN3 nor components of the SIN3 complex have been found to bind to a specific DNA consensus element at target promoters (Silverstein and Ekwall, 2005). Rather, SIN3 and other complex components interact with sequence specific DNA binding transcription factors that likely function to recruit the complex to specific gene promoter regions. SIN3 is localized to metabolic genes and regulates their expression (Fig. 3.3 and 3.5A), the mechanism behind the recruitment of SIN3 at metabolic genes, however, is still unclear. To identify which transcription factors are necessary for SIN3

binding at metabolic genes, we will start with a candidate factor approach. We can use modENCODE ChIP-seq data to look for transcription factors that bind to promoters of genes encoding enzymes in the methionine and/or glycolytic pathway. After generating a list of candidate transcription factors, we will reduce the level of each candidate factor in S2 cells by RNAi. qRT-PCR and ChIP-qPCR analyses will be performed to measure SIN3 binding and expression of metabolic gene targets in presence or absence of each candidate recruitment factor. Control samples will be cells treated with dsRNA to target GFP. If the expression of the metabolic gene is altered and SIN3 binding is reduced in the RNAi cells relative to the control sample, these results will indicate that the transcription factor is important for SIN3 chromatin binding and regulatory control of the metabolic gene target.

To further investigate how transcription factors help SIN3 bind to chromatin, we will determine which components of the SIN3 complex interact with transcription factors by co-immunoprecipitation. These data will also help us better understand which components are important for regulation of metabolism.

Does SIN3 binding change under conditions that alter cellular metabolic status?

Our work indicates that SIN3 regulates methionine metabolism and glycolysis. We next want to explore if SIN3 senses a change in metabolic status of the cell. We will determine if SIN3 binding varies with changes in metabolic status. To measure SIN3 chromatin recruitment, we will perform ChIP-qPCR at methionine metabolic genes or glycolytic genes in S2 cells with reduced SAM levels by *Sam-S* RNAi knockdown or with 2-Deoxy-D-glucose (2DG) to inhibit glycolytic flux, respectively. If the enrichment of SIN3 is altered under the experimental conditions relative to the control, these data will

suggest that the way in which SIN3 affects histone modifications at these genes is through its differential recruitment. If SIN3 levels are equivalent in the experimental conditions relative to control, these data would suggest that the activity of the complex, rather than recruitment, is somehow impacted in response to a change in metabolic status. If SIN3 binding changes under *Sam-S* knockdown or inhibition glycolysis, these findings would strongly support the idea that SIN3 is a direct target of a signaling response to cellular metabolic change. To further investigate how SIN3 binding is altered when metabolic status is changed, we will monitor the interaction between transcription factors and the SIN3 complex components in cells with the treatments described above.

Is the SIN3 complex posttranslational modified and is the modification changed when cellular metabolic status is altered?

It was reported that in response to the hormone glucagon, HDACs are dephosphorylated and then the dephosphorylated HDACs deacetylate FOXO, which in turn influences metabolism (Mihaylova et al., 2011; Wang et al., 2011). These findings raise the possibility that the SIN3 complex can be posttranslationally modified under various environmental conditions and the modification status is altered under changing metabolic conditions. To examine possible modifications, we will immunoprecipitate the SIN3 complex from control S2 cells as well as *Sam-S* knockdown cells and cells in which glycolysis is inhibited. The immunoprecipitated proteins will then be analyzed by mass-spectrometry to look for modified amino acid residues. If we determine that specific amino acid residues are modified and that the modification status is dynamic and dependent on cellular metabolic status, we will next test if that amino acid residue

and that modification are required for the SIN3 complex to mediate the cellular response. We will perform site directed mutagenesis on the SIN3 complex protein in S2 cells and determine if the gene expression response of metabolic genes has been lost. We will use CRISPR/Cas9 genome editing to alter the endogenous gene in S2 cells using published methods (Bassett et al., 2013). Results of these experiments will provide information regarding amino acid modification of SIN3 complex components in different cellular conditions. Additionally, these results have the potential to indicate that the SIN3 complex serves as a direct sensor to mediate a response to metabolic change.

How does glycolysis link to global H3K4me3 upon reduction of SIN3 and SAM-S?

This study reveals that glycolysis is correlated with H3K4me3 mediated by SIN3 and SAM-S. The mechanism, however, remains unknown. It was reported that, in yeast, glucose regulates H3K4me3 through SESAME, a complex containing serine metabolic enzymes, SAM-S, acetyl-CoA synthetase and pyruvate kinase Pyk1 (Li et al., 2015). Therefore, it is possible that SESAME complex is also present in *Drosophila* and it contributes to the control of glycolysis and through controlling H3K4me3 at glycolytic genes. To determine if there is a SESAME complex in *Drosophila*, we will analyze proteins that co-purify with Pyk followed by mass spectrometry, which is previously described (Li et al., 2015).

The answers to these questions are expected to help us understand whether SIN3 is a direct sensor of cellular metabolic status, how SIN3 impacts metabolism and if SIN3 influences H3K4me3 via LID in addition to methionine metabolism. These data will lead us to a better understanding of the function and significance of SIN3.

REFERENCES

Albertini, E., Koziel, R., Durr, A., Neuhaus, M., and Jansen-Durr, P. (2012). Cystathionine beta synthase modulates senescence of human endothelial cells. Aging *4*, 664-673.

Allfrey, V.G., Faulkner, R., and Mirsky, A.E. (1964). Acetylation and Methylation of Histones and Their Possible Role in the Regulation of Rna Synthesis. Proc Natl Acad Sci U S A *51*, 786-794.

An, S., Yeo, K.J., Jeon, Y.H., and Song, J.J. (2011). Crystal structure of the human histone methyltransferase ASH1L catalytic domain and its implications for the regulatory mechanism. The Journal of biological chemistry *286*, 8369-8374.

Ardehali, M.B., Mei, A., Zobeck, K.L., Caron, M., Lis, J.T., and Kusch, T. (2011). Drosophila Set1 is the major histone H3 lysine 4 trimethyltransferase with role in transcription. The EMBO journal *30*, 2817-2828.

Ayer, D.E., Lawrence, Q.A., and Eisenman, R.N. (1995). Mad-Max transcriptional repression is mediated by ternary complex formation with mammalian homologs of yeast repressor Sin3. Cell *80*, 767-776.

Bannister, A.J., and Kouzarides, T. (2011). Regulation of chromatin by histone modifications. Cell research *21*, 381-395.

Bannister, A.J., Zegerman, P., Partridge, J.F., Miska, E.A., Thomas, J.O., Allshire, R.C., and Kouzarides, T. (2001). Selective recognition of methylated lysine 9 on histone H3 by the HP1 chromo domain. Nature *410*, 120-124.

Barnes, V.L., Bhat, A., Unnikrishnan, A., Heydari, A.R., Arking, R., and Pile, L.A. (2014). SIN3 is critical for stress resistance and modulates adult lifespan. Aging *6*, 645-660.

Barnes, V.L., Strunk, B.S., Lee, I., Huttemann, M., and Pile, L.A. (2010). Loss of the SIN3 transcriptional corepressor results in aberrant mitochondrial function. BMC biochemistry *11*, 26.

Bender, J., and Fink, G.R. (1995). Epigenetic control of an endogenous gene family is revealed by a novel blue fluorescent mutant of Arabidopsis. Cell *83*, 725-734.

Bernstein, B.E., Humphrey, E.L., Erlich, R.L., Schneider, R., Bouman, P., Liu, J.S., Kouzarides, T., and Schreiber, S.L. (2002). Methylation of histone H3 Lys 4 in coding regions of active genes. Proceedings of the National Academy of Sciences of the United States of America *99*, 8695-8700.

Black, J.C., Van Rechem, C., and Whetstine, J.R. (2012). Histone lysine methylation dynamics: establishment, regulation, and biological impact. Molecular cell *48*, 491-507.

Black, J.C., and Whetstine, J.R. (2011). Chromatin landscape: methylation beyond transcription. Epigenetics : official journal of the DNA Methylation Society *6*, 9-15.

Bledau, A.S., Schmidt, K., Neumann, K., Hill, U., Ciotta, G., Gupta, A., Torres, D.C., Fu, J., Kranz, A., Stewart, A.F., *et al.* (2014). The H3K4 methyltransferase Setd1a is first required at the epiblast stage, whereas Setd1b becomes essential after gastrulation. Development *141*, 1022-1035.

Briggs, S.D., Bryk, M., Strahl, B.D., Cheung, W.L., Davie, J.K., Dent, S.Y., Winston, F., and Allis, C.D. (2001). Histone H3 lysine 4 methylation is mediated by Set1 and

required for cell growth and rDNA silencing in Saccharomyces cerevisiae. Genes & development *15*, 3286-3295.

Brosnan, J.T., and Brosnan, M.E. (2006). The sulfur-containing amino acids: an overview. The Journal of nutrition *136*, 1636S-1640S.

Brownell, J.E., Zhou, J., Ranalli, T., Kobayashi, R., Edmondson, D.G., Roth, S.Y., and Allis, C.D. (1996). Tetrahymena histone acetyltransferase A: a homolog to yeast Gcn5p linking histone acetylation to gene activation. Cell *84*, 843-851.

Caggese, C., Ragone, G., Barsanti, P., Moschetti, R., Messina, A., Massari, S., and Caizzi, R. (1997). The S-adenosyl-L-homocysteine hydrolase of Drosophila melanogaster: identification, deduced amino acid sequence and cytological localization of the structural gene. Molecular & general genetics : MGG *253*, 492-498.

Cantoni, G.L. (1952). The Nature of the Active Methyl Donor Formed Enzymatically from L-Methionine and Adenosinetriphosphate. J Am Chem Soc *74*, 2.

Capuano, F., Mulleder, M., Kok, R., Blom, H.J., and Ralser, M. (2014). Cytosine DNA methylation is found in Drosophila melanogaster but absent in Saccharomyces cerevisiae, Schizosaccharomyces pombe, and other yeast species. Analytical chemistry *86*, 3697-3702.

Casad, M.E., Yu, L., Daniels, J.P., Wolf, M.J., and Rockman, H.A. (2012). Deletion of Siah-interacting protein gene in Drosophila causes cardiomyopathy. Molecular genetics and genomics : MGG *287*, 351-360.

Chen, M.W., Hua, K.T., Kao, H.J., Chi, C.C., Wei, L.H., Johansson, G., Shiah, S.G., Chen, P.S., Jeng, Y.M., Cheng, T.Y.*, et al.* (2010). H3K9 histone

methyltransferase G9a promotes lung cancer invasion and metastasis by silencing the cell adhesion molecule Ep-CAM. Cancer research *70*, 7830-7840.

Cherbas, L., Hu, X., Zhimulev, I., Belyaeva, E., and Cherbas, P. (2003). EcR isoforms in Drosophila: testing tissue-specific requirements by targeted blockade and rescue. Development *130*, 271-284.

Chin, H.G., Pradhan, M., Esteve, P.O., Patnaik, D., Evans, T.C., Jr., and Pradhan, S. (2005). Sequence specificity and role of proximal amino acids of the histone H3 tail on catalysis of murine G9A lysine 9 histone H3 methyltransferase. Biochemistry *44*, 12998-13006.

Cluntun, A.A., Huang, H., Dai, L., Liu, X., Zhao, Y., and Locasale, J.W. (2015). The rate of glycolysis quantitatively mediates specific histone acetylation sites. Cancer Metab *3*, 10.

Cote, J., Quinn, J., Workman, J.L., and Peterson, C.L. (1994). Stimulation of GAL4 derivative binding to nucleosomal DNA by the yeast SWI/SNF complex. Science *265*, 53-60.

Cowley, S.M., Iritani, B.M., Mendrysa, S.M., Xu, T., Cheng, P.F., Yada, J., Liggitt, H.D., and Eisenman, R.N. (2005). The mSin3A chromatin-modifying complex is essential for embryogenesis and T-cell development. Molecular and cellular biology *25*, 6990-7004.

Curtis, B.J., Zraly, C.B., Marenda, D.R., and Dingwall, A.K. (2011). Histone lysine demethylases function as co-repressors of SWI/SNF remodeling activities during Drosophila wing development. Developmental biology *350*, 534-547.

Dannenberg, J.H., David, G., Zhong, S., van der Torre, J., Wong, W.H., and Depinho, R.A. (2005). mSin3A corepressor regulates diverse transcriptional networks governing normal and neoplastic growth and survival. Genes & development *19*, 1581-1595.

Davey, C.A., Sargent, D.F., Luger, K., Maeder, A.W., and Richmond, T.J. (2002). Solvent mediated interactions in the structure of the nucleosome core particle at 1.9 a resolution. Journal of molecular biology *319*, 1097-1113.

David, G., Grandinetti, K.B., Finnerty, P.M., Simpson, N., Chu, G.C., and Depinho, R.A. (2008). Specific requirement of the chromatin modifier mSin3B in cell cycle exit and cellular differentiation. Proceedings of the National Academy of Sciences of the United States of America *105*, 4168-4172.

Dawson, M.A., and Kouzarides, T. (2012). Cancer epigenetics: from mechanism to therapy. Cell *150*, 12-27.

DeBerardinis, R.J., and Thompson, C.B. (2012). Cellular metabolism and disease: what do metabolic outliers teach us? Cell *148*, 1132-1144.

Dhalluin, C., Carlson, J.E., Zeng, L., He, C., Aggarwal, A.K., and Zhou, M.M. (1999). Structure and ligand of a histone acetyltransferase bromodomain. Nature *399*, 491-496.

Dou, Y., and Gorovsky, M.A. (2000). Phosphorylation of linker histone H1 regulates gene expression in vivo by creating a charge patch. Molecular cell *6*, 225-231.

Duffy, J.B. (2002). GAL4 system in Drosophila: a fly geneticist's Swiss army knife. Genesis *34*, 1-15.

Dunwell, T.L., McGuffin, L.J., Dunwell, J.M., and Pfeifer, G.P. (2013). The mysterious presence of a 5-methylcytosine oxidase in the Drosophila genome: possible explanations. Cell cycle *12*, 3357-3365.

Dunwell, T.L., and Pfeifer, G.P. (2014). Drosophila genomic methylation: new evidence and new questions. Epigenomics *6*, 459-461.

Eissenberg, J.C., Lee, M.G., Schneider, J., Ilvarsonn, A., Shiekhattar, R., and Shilatifard, A. (2007). The trithorax-group gene in Drosophila little imaginal discs encodes a trimethylated histone H3 Lys4 demethylase. Nature structural & molecular biology *14*, 344-346.

Esse, R., Imbard, A., Florindo, C., Gupta, S., Quinlivan, E.P., Davids, M., Teerlink, T., Tavares de Almeida, I., Kruger, W.D., Blom, H.J.*, et al.* (2014). Protein arginine hypomethylation in a mouse model of cystathionine beta-synthase deficiency. FASEB journal : official publication of the Federation of American Societies for Experimental Biology *28*, 2686-2695.

Ferrer, C.M., Lynch, T.P., Sodi, V.L., Falcone, J.N., Schwab, L.P., Peacock, D.L., Vocadlo, D.J., Seagroves, T.N., and Reginato, M.J. (2014). O-GlcNAcylation regulates cancer metabolism and survival stress signaling via regulation of the HIF-1 pathway. Molecular cell *54*, 820-831.

Finch, J.T., Lutter, L.C., Rhodes, D., Brown, R.S., Rushton, B., Levitt, M., and Klug, A. (1977). Structure of nucleosome core particles of chromatin. Nature *269*, 29-36.

Gajan, A. (2015). Analyzing the interactions of KDM5/LID and Sin3 in drosophila melanogaster, pp. 184 p.

Gajan, A., Barnes, V.L., Liu, M., Saha, N., and Pile, L.A. (2016). The histone demethylase dKDM5/LID interacts with the SIN3 histone deacetylase complex and shares functional similarities with SIN3. Epigenetics & chromatin *9*, 4.

Gan, Q., Schones, D.E., Ho Eun, S., Wei, G., Cui, K., Zhao, K., and Chen, X. (2010). Monovalent and unpoised status of most genes in undifferentiated cell-enriched Drosophila testis. Genome biology *11*, R42.

Gerke, J., Bayram, O., and Braus, G.H. (2012). Fungal S-adenosylmethionine synthetase and the control of development and secondary metabolism in Aspergillus nidulans. Fungal genetics and biology : FG & B *49*, 443-454.

Gildea, J.J., Lopez, R., and Shearn, A. (2000). A screen for new trithorax group genes identified little imaginal discs, the Drosophila melanogaster homologue of human retinoblastoma binding protein 2. Genetics *156*, 645-663.

Gonneaud, A., Turgeon, N., Boisvert, F.M., Boudreau, F., and Asselin, C. (2015). Loss of histone deacetylase Hdac1 disrupts metabolic processes in intestinal epithelial cells. FEBS letters *589*, 2776-2783.

Gorisch, S.M., Wachsmuth, M., Toth, K.F., Lichter, P., and Rippe, K. (2005). Histone acetylation increases chromatin accessibility. Journal of cell science *118*, 5825-5834.

Graveley, B.R., Brooks, A.N., Carlson, J.W., Duff, M.O., Landolin, J.M., Yang, L., Artieri, C.G., van Baren, M.J., Boley, N., Booth, B.W.*, et al.* (2011). The developmental transcriptome of Drosophila melanogaster. Nature *471*, 473-479.

Grzenda, A., Lomberk, G., Zhang, J.S., and Urrutia, R. (2009). Sin3: master scaffold and transcriptional corepressor. Biochimica et biophysica acta *1789*, 443-450.

Hallson, G., Hollebakken, R.E., Li, T., Syrzycka, M., Kim, I., Cotsworth, S., Fitzpatrick, K.A., Sinclair, D.A., and Honda, B.M. (2012). dSet1 is the main H3K4 di- and tri-methyltransferase throughout Drosophila development. Genetics *190*, 91-100.

Han, M., and Grunstein, M. (1988). Nucleosome loss activates yeast downstream promoters in vivo. Cell *55*, 1137-1145.

Hayakawa, T., and Nakayama, J. (2011). Physiological roles of class I HDAC complex and histone demethylase. Journal of biomedicine & biotechnology *2011*, 129383.

Hayakawa, T., Ohtani, Y., Hayakawa, N., Shinmyozu, K., Saito, M., Ishikawa, F., and Nakayama, J. (2007). RBP2 is an MRG15 complex component and down-regulates intragenic histone H3 lysine 4 methylation. Genes to cells : devoted to molecular & cellular mechanisms *12*, 811-826.

Hermes, M., Osswald, H., Riehle, R., Piesch, C., and Kloor, D. (2008). S-Adenosylhomocysteine hydrolase overexpression in HEK-293 cells: effect on intracellular adenosine levels, cell viability, and DNA methylation. Cellular physiology and biochemistry : international journal of experimental cellular physiology, biochemistry, and pharmacology *22*, 223-236.

Herranz, H., and Milan, M. (2008). Signalling molecules, growth regulators and cell cycle control in Drosophila. Cell cycle *7*, 3335-3337.

Heyn, H., and Esteller, M. (2015). An Adenine Code for DNA: A Second Life for N6-Methyladenine. Cell *161*, 710-713.

Hong, L., Schroth, G.P., Matthews, H.R., Yau, P., and Bradbury, E.M. (1993). Studies of the DNA binding properties of histone H4 amino terminus. Thermal denaturation

studies reveal that acetylation markedly reduces the binding constant of the H4 "tail" to DNA. The Journal of biological chemistry *268*, 305-314.

Horiuchi, K.Y., Eason, M.M., Ferry, J.J., Planck, J.L., Walsh, C.P., Smith, R.F., Howitz, K.T., and Ma, H. (2013). Assay development for histone methyltransferases. Assay and drug development technologies *11*, 227-236.

Hu, Y., Sopko, R., Foos, M., Kelley, C., Flockhart, I., Ammeux, N., Wang, X., Perkins, L., Perrimon, N., and Mohr, S.E. (2013). FlyPrimerBank: an online database for Drosophila melanogaster gene expression analysis and knockdown evaluation of RNAi reagents. G3 *3*, 1607-1616.

Huang da, W., Sherman, B.T., and Lempicki, R.A. (2009). Systematic and integrative analysis of large gene lists using DAVID bioinformatics resources. Nat Protoc *4*, 44-57.

Jacobsen, S.E., and Meyerowitz, E.M. (1997). Hypermethylated SUPERMAN epigenetic alleles in arabidopsis. Science *277*, 1100-1103.

Jasper, H., Benes, V., Atzberger, A., Sauer, S., Ansorge, W., and Bohmann, D. (2002). A genomic switch at the transition from cell proliferation to terminal differentiation in the Drosophila eye. Developmental cell *3*, 511-521.

Kabil, H., Kabil, O., Banerjee, R., Harshman, L.G., and Pletcher, S.D. (2011). Increased transsulfuration mediates longevity and dietary restriction in Drosophila. Proceedings of the National Academy of Sciences of the United States of America *108*, 16831-16836.

Kaelin, W.G., Jr., and McKnight, S.L. (2013). Influence of metabolism on epigenetics and disease. Cell *153*, 56-69.

Kakimoto, Y., and Akazawa, S. (1970). Isolation and identification of N-G,N-G- and N-G,N'-G-dimethyl-arginine, N-epsilon-mono-, di-, and trimethyllysine, and glucosylgalactosyl- and galactosyl-delta-hydroxylysine from human urine. The Journal of biological chemistry *245*, 5751-5758.

Katada, S., Imhof, A., and Sassone-Corsi, P. (2012). Connecting threads: epigenetics and metabolism. Cell *148*, 24-28.

Katoh, Y., Ikura, T., Hoshikawa, Y., Tashiro, S., Ito, T., Ohta, M., Kera, Y., Noda, T., and Igarashi, K. (2011). Methionine adenosyltransferase II serves as a transcriptional corepressor of Maf oncoprotein. Molecular cell *41*, 554-566.

Kavi, H.H., and Birchler, J.A. (2009). Drosophila KDM2 is a H3K4me3 demethylase regulating nucleolar organization. BMC research notes *2*, 217.

Kleff, S., Andrulis, E.D., Anderson, C.W., and Sternglanz, R. (1995). Identification of a gene encoding a yeast histone H4 acetyltransferase. The Journal of biological chemistry *270*, 24674-24677.

Korkes, S., Del Campillo, A., Gunsalas, I.C., and Ochoa, S. (1951). Enzymatic synthesis of citric acid. IV. Pyruvate as acetyl donor. The Journal of biological chemistry *193*, 721-735.

Kornberg, R.D. (1974). Chromatin structure: a repeating unit of histones and DNA. Science *184*, 868-871.

Kotb, M., Mudd, S.H., Mato, J.M., Geller, A.M., Kredich, N.M., Chou, J.Y., and Cantoni, G.L. (1997). Consensus nomenclature for the mammalian methionine adenosyltransferase genes and gene products. Trends in genetics : TIG *13*, 51-52.

Krajewski, W.A., and Becker, P.B. (1998). Reconstitution of hyperacetylated, DNase I-sensitive chromatin characterized by high conformational flexibility of nucleosomal DNA. Proceedings of the National Academy of Sciences of the United States of America *95*, 1540-1545.

Kurdistani, S.K., Tavazoie, S., and Grunstein, M. (2004). Mapping global histone acetylation patterns to gene expression. Cell *117*, 721-733.

Kwon, H., Imbalzano, A.N., Khavari, P.A., Kingston, R.E., and Green, M.R. (1994). Nucleosome disruption and enhancement of activator binding by a human SW1/SNF complex. Nature *370*, 477-481.

Lachner, M., O'Carroll, D., Rea, S., Mechtler, K., and Jenuwein, T. (2001). Methylation of histone H3 lysine 9 creates a binding site for HP1 proteins. Nature *410*, 116-120.

Lagarou, A., Mohd-Sarip, A., Moshkin, Y.M., Chalkley, G.E., Bezstarosti, K., Demmers, J.A., and Verrijzer, C.P. (2008). dKDM2 couples histone H2A ubiquitylation to histone H3 demethylation during Polycomb group silencing. Genes & development *22*, 2799-2810.

Larsson, J., and Rasmuson-Lestander, A. (1994). Molecular cloning of the S-adenosylmethionine synthetase gene in Drosophila melanogaster. FEBS letters *342*, 329-333.

Larsson, J., and Rasmuson-Lestander, A. (1998). Somatic and germline clone analysis in mutants of the S-adenosylmethionine synthetase encoding gene in Drosophila melanogaster. FEBS letters *427*, 119-123.

Larsson, J., Zhang, J., and Rasmuson-Lestander, A. (1996). Mutations in the Drosophila melanogaster gene encoding S-adenosylmethionine synthetase [corrected] suppress position-effect variegation. Genetics *143*, 887-896.

Lee, J.H., Budanov, A.V., Park, E.J., Birse, R., Kim, T.E., Perkins, G.A., Ocorr, K., Ellisman, M.H., Bodmer, R., Bier, E.*, et al.* (2010). Sestrin as a feedback inhibitor of TOR that prevents age-related pathologies. Science *327*, 1223-1228.

Lee, N., Zhang, J., Klose, R.J., Erdjument-Bromage, H., Tempst, P., Jones, R.S., and Zhang, Y. (2007). The trithorax-group protein Lid is a histone H3 trimethyl-Lys4 demethylase. Nature structural & molecular biology *14*, 341-343.

Lee, Y.S., and Carthew, R.W. (2003). Making a better RNAi vector for Drosophila: use of intron spacers. Methods *30*, 322-329.

Levayer, R., and Moreno, E. (2013). Mechanisms of cell competition: themes and variations. The Journal of cell biology *200*, 689-698.

Li, L., Greer, C., Eisenman, R.N., and Secombe, J. (2010). Essential functions of the histone demethylase lid. PLoS genetics *6*, e1001221.

Li, S., Swanson, S.K., Gogol, M., Florens, L., Washburn, M.P., Workman, J.L., and Suganuma, T. (2015). Serine and SAM Responsive Complex SESAME Regulates Histone Modification Crosstalk by Sensing Cellular Metabolism. Molecular cell *60*, 408-421.

Li, W., Han, Y., Tao, F., and Chong, K. (2011). Knockdown of SAMS genes encoding S-adenosyl-l-methionine synthetases causes methylation alterations of DNAs and histones and leads to late flowering in rice. Journal of plant physiology *168*, 1837-1843.

Lin, M.J., Tang, L.Y., Reddy, M.N., and Shen, C.K. (2005). DNA methyltransferase gene dDnmt2 and longevity of Drosophila. The Journal of biological chemistry *280*, 861-864.

Liu, M., Barnes, V.L., and Pile, L.A. (2015). Disruption of Methionine Metabolism in Drosophila melanogaster Impacts Histone Methylation and Results in Loss of Viability. G3 *6*, 121-132.

Lloret-Llinares, M., Carre, C., Vaquero, A., de Olano, N., and Azorin, F. (2008). Characterization of Drosophila melanogaster JmjC+N histone demethylases. Nucleic acids research *36*, 2852-2863.

Locasale, J.W. (2013). Serine, glycine and one-carbon units: cancer metabolism in full circle. Nature reviews Cancer *13*, 572-583.

Lu, S.C., Alvarez, L., Huang, Z.Z., Chen, L., An, W., Corrales, F.J., Avila, M.A., Kanel, G., and Mato, J.M. (2001). Methionine adenosyltransferase 1A knockout mice are predisposed to liver injury and exhibit increased expression of genes involved in proliferation. Proceedings of the National Academy of Sciences of the United States of America *98*, 5560-5565.

Lu, Y., and Li, Z. (2015). Notch signaling downstream target E(spl)mbeta is dispensable for adult midgut homeostasis in Drosophila. Gene *560*, 89-95.

Luger, K., Mader, A.W., Richmond, R.K., Sargent, D.F., and Richmond, T.J. (1997). Crystal structure of the nucleosome core particle at 2.8 A resolution. Nature *389*, 251-260.

Lynen, F., Reichert, E., and Rueff, L. (1951). Ann Chem, *574*.

Martinez-Pastor, B., Cosentino, C., and Mostoslavsky, R. (2013). A tale of metabolites: the cross-talk between chromatin and energy metabolism. Cancer discovery *3*, 497-501.

Matthews, H.R. (1993). Polyamines, chromatin structure and transcription. BioEssays : news and reviews in molecular, cellular and developmental biology *15*, 561-566.

Mentch, S.J., Mehrmohamadi, M., Huang, L., Liu, X., Gupta, D., Mattocks, D., Gomez Padilla, P., Ables, G., Bamman, M.M., Thalacker-Mercer, A.E.*, et al.* (2015). Histone Methylation Dynamics and Gene Regulation Occur through the Sensing of One-Carbon Metabolism. Cell metabolism *22*, 861-873.

Mihaylova, M.M., Vasquez, D.S., Ravnskjaer, K., Denechaud, P.D., Yu, R.T., Alvarez, J.G., Downes, M., Evans, R.M., Montminy, M., and Shaw, R.J. (2011). Class IIa histone deacetylases are hormone-activated regulators of FOXO and mammalian glucose homeostasis. Cell *145*, 607-621.

Miller, M.W., Duhl, D.M., Winkes, B.M., Arredondo-Vega, F., Saxon, P.J., Wolff, G.L., Epstein, C.J., Hershfield, M.S., and Barsh, G.S. (1994). The mouse lethal nonagouti (a(x)) mutation deletes the S-adenosylhomocysteine hydrolase (Ahcy) gene. The EMBO journal *13*, 1806-1816.

Mohan, M., Herz, H.M., Smith, E.R., Zhang, Y., Jackson, J., Washburn, M.P., Florens, L., Eissenberg, J.C., and Shilatifard, A. (2011). The COMPASS family of H3K4 methylases in Drosophila. Molecular and cellular biology *31*, 4310-4318.

Moshkin, Y.M., Kan, T.W., Goodfellow, H., Bezstarosti, K., Maeda, R.K., Pilyugin, M., Karch, F., Bray, S.J., Demmers, J.A., and Verrijzer, C.P. (2009). Histone chaperones ASF1 and NAP1 differentially modulate removal of active histone

marks by LID-RPD3 complexes during NOTCH silencing. Molecular cell *35*, 782-793.

Moussaieff, A., Rouleau, M., Kitsberg, D., Cohen, M., Levy, G., Barasch, D., Nemirovski, A., Shen-Orr, S., Laevsky, I., Amit, M., *et al.* (2015). Glycolysis-mediated changes in acetyl-CoA and histone acetylation control the early differentiation of embryonic stem cells. Cell Metab *21*, 392-402.

Mudd, S.H., and Cantoni, G.L. (1958). Activation of methionine for transmethylation. III. The methionine-activating enzyme of Bakers' yeast. The Journal of biological chemistry *231*, 481-492.

Nakayama, J., Rice, J.C., Strahl, B.D., Allis, C.D., and Grewal, S.I. (2001). Role of histone H3 lysine 9 methylation in epigenetic control of heterochromatin assembly. Science *292*, 110-113.

Neufeld, T.P., Tang, A.H., and Rubin, G.M. (1998). A genetic screen to identify components of the sina signaling pathway in Drosophila eye development. Genetics *148*, 277-286.

Neumuller, R.A., Richter, C., Fischer, A., Novatchkova, M., Neumuller, K.G., and Knoblich, J.A. (2011). Genome-wide analysis of self-renewal in Drosophila neural stem cells by transgenic RNAi. Cell stem cell *8*, 580-593.

Newman, E.B., Budman, L.I., Chan, E.C., Greene, R.C., Lin, R.T., Woldringh, C.L., and D'Ari, R. (1998). Lack of S-adenosylmethionine results in a cell division defect in Escherichia coli. Journal of bacteriology *180*, 3614-3619.

Obianyo, O., Osborne, T.C., and Thompson, P.R. (2008). Kinetic mechanism of protein arginine methyltransferase 1. Biochemistry *47*, 10420-10427.

Patnaik, D., Chin, H.G., Esteve, P.O., Benner, J., Jacobsen, S.E., and Pradhan, S. (2004). Substrate specificity and kinetic mechanism of mammalian G9a histone H3 methyltransferase. The Journal of biological chemistry *279*, 53248-53258.

Pennetta, G., and Pauli, D. (1998). The Drosophila Sin3 gene encodes a widely distributed transcription factor essential for embryonic viability. Development genes and evolution *208*, 531-536.

Phillips, D.M. (1963). The presence of acetyl groups of histones. Biochem J *87*, 258-263.

Pile, L.A., Schlag, E.M., and Wassarman, D.A. (2002). The SIN3/RPD3 deacetylase complex is essential for G(2) phase cell cycle progression and regulation of SMRTER corepressor levels. Molecular and cellular biology *22*, 4965-4976.

Pile, L.A., Spellman, P.T., Katzenberger, R.J., and Wassarman, D.A. (2003). The SIN3 deacetylase complex represses genes encoding mitochondrial proteins: implications for the regulation of energy metabolism. The Journal of biological chemistry *278*, 37840-37848.

Pile, L.A., and Wassarman, D.A. (2000). Chromosomal localization links the SIN3-RPD3 complex to the regulation of chromatin condensation, histone acetylation and gene expression. The EMBO journal *19*, 6131-6140.

Raddatz, G., Guzzardo, P.M., Olova, N., Fantappie, M.R., Rampp, M., Schaefer, M., Reik, W., Hannon, G.J., and Lyko, F. (2013). Dnmt2-dependent methylomes lack defined DNA methylation patterns. Proceedings of the National Academy of Sciences of the United States of America *110*, 8627-8631.

Rea, S., Eisenhaber, F., O'Carroll, D., Strahl, B.D., Sun, Z.W., Schmid, M., Opravil, S., Mechtler, K., Ponting, C.P., Allis, C.D.*, et al.* (2000). Regulation of chromatin structure by site-specific histone H3 methyltransferases. Nature *406*, 593-599.

Reytor, E., Perez-Miguelsanz, J., Alvarez, L., Perez-Sala, D., and Pajares, M.A. (2009). Conformational signals in the C-terminal domain of methionine adenosyltransferase I/III determine its nucleocytoplasmic distribution. FASEB journal : official publication of the Federation of American Societies for Experimental Biology *23*, 3347-3360.

Roh, T.Y., Cuddapah, S., Cui, K., and Zhao, K. (2006). The genomic landscape of histone modifications in human T cells. Proceedings of the National Academy of Sciences of the United States of America *103*, 15782-15787.

Rose, N.R., and Klose, R.J. (2014). Understanding the relationship between DNA methylation and histone lysine methylation. Biochimica et biophysica acta *1839*, 1362-1372.

Sadhu, M.J., Guan, Q., Li, F., Sales-Lee, J., Iavarone, A.T., Hammond, M.C., Cande, W.Z., and Rine, J. (2013). Nutritional control of epigenetic processes in yeast and human cells. Genetics *195*, 831-844.

Saha, N., Liu, M., Gajan, A., and Pile, L.A. (2016). Genome-wide studies reveal novel and distinct biological pathways regulated by SIN3 isoforms. BMC genomics *17*, 111.

Sanders, R.D., Sefton, J.M., Moberg, K.H., and Fridovich-Keil, J.L. (2010). UDP-galactose 4' epimerase (GALE) is essential for development of Drosophila melanogaster. Disease models & mechanisms *3*, 628-638.

Sassone-Corsi, P. (2013). Physiology. When metabolism and epigenetics converge. Science *339*, 148-150.

Schaefer, M., Pollex, T., Hanna, K., Tuorto, F., Meusburger, M., Helm, M., and Lyko, F. (2010). RNA methylation by Dnmt2 protects transfer RNAs against stress-induced cleavage. Genes & development *24*, 1590-1595.

Schmidt, E.E., Pelz, O., Buhlmann, S., Kerr, G., Horn, T., and Boutros, M. (2013). GenomeRNAi: a database for cell-based and in vivo RNAi phenotypes, 2013 update. Nucleic acids research *41*, D1021-1026.

Schubeler, D., MacAlpine, D.M., Scalzo, D., Wirbelauer, C., Kooperberg, C., van Leeuwen, F., Gottschling, D.E., O'Neill, L.P., Turner, B.M., Delrow, J.*, et al.* (2004). The histone modification pattern of active genes revealed through genome-wide chromatin analysis of a higher eukaryote. Genes & development *18*, 1263-1271.

Secombe, J., Li, L., Carlos, L., and Eisenman, R.N. (2007). The Trithorax group protein Lid is a trimethyl histone H3K4 demethylase required for dMyc-induced cell growth. Genes & development *21*, 537-551.

Sharma, V., Swaminathan, A., Bao, R., and Pile, L.A. (2008). Drosophila SIN3 is required at multiple stages of development. Developmental dynamics : an official publication of the American Association of Anatomists *237*, 3040-3050.

Shi, Y., Lan, F., Matson, C., Mulligan, P., Whetstine, J.R., Cole, P.A., Casero, R.A., and Shi, Y. (2004). Histone demethylation mediated by the nuclear amine oxidase homolog LSD1. Cell *119*, 941-953.

Shilatifard, A. (2012). The COMPASS family of histone H3K4 methylases: mechanisms of regulation in development and disease pathogenesis. Annual review of biochemistry *81*, 65-95.

Shin, S.Y., Fauman, E.B., Petersen, A.K., Krumsiek, J., Santos, R., Huang, J., Arnold, M., Erte, I., Forgetta, V., Yang, T.P.*, et al.* (2014). An atlas of genetic influences on human blood metabolites. Nature genetics *46*, 543-550.

Shiraki, N., Shiraki, Y., Tsuyama, T., Obata, F., Miura, M., Nagae, G., Aburatani, H., Kume, K., Endo, F., and Kume, S. (2014). Methionine metabolism regulates maintenance and differentiation of human pluripotent stem cells. Cell metabolism *19*, 780-794.

Shyh-Chang, N., Locasale, J.W., Lyssiotis, C.A., Zheng, Y., Teo, R.Y., Ratanasirintrawoot, S., Zhang, J., Onder, T., Unternaehrer, J.J., Zhu, H.*, et al.* (2013). Influence of threonine metabolism on S-adenosylmethionine and histone methylation. Science *339*, 222-226.

Silverstein, R.A., and Ekwall, K. (2005). Sin3: a flexible regulator of global gene expression and genome stability. Current genetics *47*, 1-17.

Spain, M.M., Caruso, J.A., Swaminathan, A., and Pile, L.A. (2010). Drosophila SIN3 isoforms interact with distinct proteins and have unique biological functions. The Journal of biological chemistry *285*, 27457-27467.

St Pierre, S.E., Ponting, L., Stefancsik, R., McQuilton, P., and FlyBase, C. (2014). FlyBase 102--advanced approaches to interrogating FlyBase. Nucleic acids research *42*, D780-788.

Sutton-McDowall, M.L., Gilchrist, R.B., and Thompson, J.G. (2010). The pivotal role of glucose metabolism in determining oocyte developmental competence. Reproduction *139*, 685-695.

Swaminathan, A., Barnes, V.L., Fox, S., Gammouh, S., and Pile, L.A. (2012). Identification of genetic suppressors of the Sin3A knockdown wing phenotype. PloS one *7*, e49563.

Swaminathan, A., and Pile, L.A. (2010). Regulation of cell proliferation and wing development by Drosophila SIN3 and String. Mechanisms of development *127*, 96-106.

Swanson, D.A., Liu, M.L., Baker, P.J., Garrett, L., Stitzel, M., Wu, J., Harris, M., Banerjee, R., Shane, B., and Brody, L.C. (2001). Targeted disruption of the methionine synthase gene in mice. Molecular and cellular biology *21*, 1058-1065.

Takahashi, H., McCaffery, J.M., Irizarry, R.A., and Boeke, J.D. (2006). Nucleocytosolic acetyl-coenzyme a synthetase is required for histone acetylation and global transcription. Mol Cell *23*, 207-217.

Takayama, S., Dhahbi, J., Roberts, A., Mao, G., Heo, S.J., Pachter, L., Martin, D.I., and Boffelli, D. (2014). Genome methylation in D. melanogaster is found at specific short motifs and is independent of DNMT2 activity. Genome research *24*, 821-830.

Tang, L.Y., Reddy, M.N., Rasheva, V., Lee, T.L., Lin, M.J., Hung, M.S., and Shen, C.K. (2003). The eukaryotic DNMT2 genes encode a new class of cytosine-5 DNA methyltransferases. The Journal of biological chemistry *278*, 33613-33616.

Tariq, M., and Paszkowski, J. (2004). DNA and histone methylation in plants. Trends in genetics : TIG *20*, 244-251.

Tateishi, K., Okada, Y., Kallin, E.M., and Zhang, Y. (2009). Role of Jhdm2a in regulating metabolic gene expression and obesity resistance. Nature *458*, 757-761.

Taunton, J., Hassig, C.A., and Schreiber, S.L. (1996). A mammalian histone deacetylase related to the yeast transcriptional regulator Rpd3p. Science *272*, 408-411.

Tehlivets, O., Malanovic, N., Visram, M., Pavkov-Keller, T., and Keller, W. (2013). S-adenosyl-L-homocysteine hydrolase and methylation disorders: yeast as a model system. Biochimica et biophysica acta *1832*, 204-215.

Teperino, R., Schoonjans, K., and Auwerx, J. (2010). Histone methyl transferases and demethylases; can they link metabolism and transcription? Cell Metab *12*, 321-327.

Towbin, B.D., Gonzalez-Aguilera, C., Sack, R., Gaidatzis, D., Kalck, V., Meister, P., Askjaer, P., and Gasser, S.M. (2012). Step-wise methylation of histone H3K9 positions heterochromatin at the nuclear periphery. Cell *150*, 934-947.

Tsukiyama, T., and Wu, C. (1995). Purification and properties of an ATP-dependent nucleosome remodeling factor. Cell *83*, 1011-1020.

van Oevelen, C., Wang, J., Asp, P., Yan, Q., Kaelin, W.G., Jr., Kluger, Y., and Dynlacht, B.D. (2008). A role for mammalian Sin3 in permanent gene silencing. Molecular cell *32*, 359-370.

Wang, B., Moya, N., Niessen, S., Hoover, H., Mihaylova, M.M., Shaw, R.J., Yates, J.R., 3rd, Fischer, W.H., Thomas, J.B., and Montminy, M. (2011). A hormone-dependent module regulating energy balance. Cell *145*, 596-606.

Warburg, O. (1956). On the origin of cancer cells. Science *123*, 309-314.

Watanabe, M., Osada, J., Aratani, Y., Kluckman, K., Reddick, R., Malinow, M.R., and Maeda, N. (1995). Mice deficient in cystathionine beta-synthase: animal models for mild and severe homocyst(e)inemia. Proceedings of the National Academy of Sciences of the United States of America *92*, 1585-1589.

Wellen, K.E., Hatzivassiliou, G., Sachdeva, U.M., Bui, T.V., Cross, J.R., and Thompson, C.B. (2009). ATP-citrate lyase links cellular metabolism to histone acetylation. Science *324*, 1076-1080.

Xiao, B., Jing, C., Wilson, J.R., Walker, P.A., Vasisht, N., Kelly, G., Howell, S., Taylor, I.A., Blackburn, G.M., and Gamblin, S.J. (2003). Structure and catalytic mechanism of the human histone methyltransferase SET7/9. Nature *421*, 652-656.

Zemach, A., McDaniel, I.E., Silva, P., and Zilberman, D. (2010). Genome-wide evolutionary analysis of eukaryotic DNA methylation. Science *328*, 916-919.

Zhang, G., Huang, H., Liu, D., Cheng, Y., Liu, X., Zhang, W., Yin, R., Zhang, D., Zhang, P., Liu, J., *et al.* (2015). N6-methyladenine DNA modification in Drosophila. Cell *161*, 893-906.

Zheng, Y., Hsu, F.N., Xu, W., Xie, X.J., Ren, X., Gao, X., Ni, J.Q., and Ji, J.Y. (2014). A developmental genetic analysis of the lysine demethylase KDM2 mutations in Drosophila melanogaster. Mechanisms of development *133*, 36-53.

Zhong, L., D'Urso, A., Toiber, D., Sebastian, C., Henry, R.E., Vadysirisack, D.D., Guimaraes, A., Marinelli, B., Wikstrom, J.D., Nir, T.*, et al.* (2010). The histone deacetylase Sirt6 regulates glucose homeostasis via Hif1alpha. Cell *140*, 280-293.

ABSTRACT

AN ANALYSIS OF THE INTERACTION BETWEEN SIN3 AND METHIONINE METABOLISM IN *DROSOPHILA*

by

MENGYING LIU

August 2016

Advisor: Dr. Lori A. Pile

Major: Biological Sciences

Degree: Doctor of Philosophy

Chromatin modification and cellular metabolism are tightly connected. The mechanism for this cross-talk, however, remains incompletely understood. SIN3 controls histone acetylation through association with the histone deacetylase RPD3. In this study, my major goal is to explore the mechanism of how SIN3 regulates cellular metabolism.

Methionine metabolism generates the major methyl donor *S*-adenosylmethionine (SAM) for histone methylation. In collaboration with others, I report that reduced levels of some enzymes involved in methionine metabolism and histone demethylases lead to lethality, as well as wing development and cell proliferation defects in *Drosophila melanogaster*. Additionally, disruption of methionine metabolism can directly affect histone methylation levels. Reduction of little imaginal discs (LID) histone demethylase, but not lysine-specific demethylase 2 (KDM2) demethylase, is able to counter the effects on histone methylation due to reduction of SAM synthetase (SAM-S). Taken together, these results reveal an essential role of key enzymes that control methionine metabolism and histone methylation.

Next, we demonstrate the genetic interaction between *Sin3A* and methionine metabolic genes. We find that SIN3 binds to methionine metabolic genes, affects histone modifications at the promoter regions of these genes and regulates their expression. We provide evidence that alteration of SIN3 level influences the amount of SAM and global H3K4me3. Furthermore, reduction of SIN3 can restore decreased global H3K4me3 caused by knockdown of either SAM-S or the histone methyltransfase SET1 to near control levels. Collectively, these results indicate that SIN3 directly regulates expression of methionine metabolic genes to control SAM levels, which in turn affect global H3K4me3.

To further identify specific genes and cellular metabolic pathways requiring the activity of SIN3, we performed RNA-seq and metabolomics analysis when SIN3 and/or SAM-S is reduced. Moreover, we did correlation analysis between global H3K4me3 levels and the metabolic profiles to generate a list of metabolites whose concentration change significantly with the alteration in H3K4me3. We find glycolysis is a major pathway correlated with global H3K4me3 upon reduction of SIN3 and/or SAM-S. We demonstrate that SIN3 binds to glycolytic genes, affects H3K9ac, not H3K4me3, at the promoter regions of these genes and regulates their expression. Altogether, these results suggest that SIN3 directly regulates transcription of glycolytic genes to affect glycolysis, which is associated with H3K4me3 due to unknown mechanism.

Overall, our study reveals that SIN3 is an important epigenetic regulator connecting cellular metabolism and histone modification.

Supplementary files are included:

- Supplementary Data 1_ML – Excel spreadsheet containing detailed RNAseq

differential expression analysis

- Supplementary Data 2_ML – Excel spreadsheet containing detailed gene ontology and KEGG pathway analyses
- Supplementary Data 3_ML – Excel spreadsheet containing detailed metabolomic analysis

AUTOBIOGRAPHICAL STATEMENT

MENGYING LIU

EDUCATION:

2010-2016 PhD in Biology, Wayne State University, Detroit, USA
2006-2009 MS in Microbiology, Huazhong Agricultural University, Wuhan, China
2002-2006 BS in National Training Base for Life Science Talents, Huazhong Agricultural University, Wuhan, China

PUBLICATIONS:

Liu, M. and Pile, L.A. SIN3 directly regulates methionine metabolic gene expression to affect histone methylation. *In preparation*

Saha, N., **Liu, M.**, Gajan, A., and Pile, L.A. (2016). Genome-wide studies reveal novel and distinct biological pathways regulated by SIN3 isoforms. BMC genomics *17*, 111.

Gajan, A., Barnes, V.L., **Liu, M**., Saha, N., and Pile, L.A. (2016). The histone demethylase dKDM5/LID interacts with the SIN3 histone deacetylase complex and shares functional similarities with SIN3. Epigenetics & chromatin *9*, 4.

Liu, M., Barnes, V.L., and Pile, L.A. (2015). Disruption of Methionine Metabolism in *Drosophila melanogaster* Impacts Histone Methylation and Results in Loss of Viability. G3 *6*, 121-132.

HONORS AND AWARDS:

2015: **Second Place Poster Award** – Karmanos Molecular Therapeutics Program Annual Research Symposium

Outstanding Graduate Research Assistant Award – Dept. of Biological Sciences – Wayne State University

2013: **Best Student Poster Presentation** – 13th International Congress of Invertebrate Reproduction and Development conference

2012: **Outstanding Graduate Teaching Assistant Award** – Dept. of Biological Sciences – Wayne State University